Hamiltonian Approach to $1+1$ dimensional Yang–Mills theory in Coulomb gauge

H. Reinhardt, W. Schleifenbaum

Institut für Theoretische Physik
Universität Tübingen
D-72076 Tübingen, Germany

Abstract

We study the Hamiltonian approach to $1+1$ dimensional Yang–Mills theory in Coulomb gauge, considering both the pure Coulomb gauge and the gauge where in addition the remaining constant gauge field is restricted to the Cartan algebra. We evaluate the corresponding Faddeev–Popov determinants, resolve Gauss' law and derive the Hamiltonians, which differ in both gauges due to additional zero modes of the Faddeev–Popov kernel in the pure Coulomb gauge. By Gauss' law the zero modes of the Faddeev–Popov kernel constrain the physical wave functionals to zero colour charge states. We solve the Schrödinger equation in the pure Coulomb gauge and determine the vacuum wave functional. The gluon and ghost propagators and the static colour Coulomb potential are calculated in the first Gribov region as well as in the fundamental modular region, and Gribov copy effects are studied. We explicitly demonstrate that the Dyson–Schwinger equations do not specify the Gribov region while the propagators and vertices do depend on the Gribov region chosen. In this sense, the Dyson–Schwinger equations alone do not provide the full non-abelian quantum gauge theory, but subsidiary conditions must be required. Implications of Gribov copy effects for lattice calculations of the infrared behaviour of gauge-fixed propagators are discussed. We compute the ghost-gluon vertex and provide a sensible truncation of Dyson–Schwinger equations. Approximations of the variational approach to the $3+1$ dimensional theory are checked by comparison to the $1+1$ dimensional case.

Key words:

Email address: hugo.reinhardt@uni-tuebingen.de (H. Reinhardt, W. Schleifenbaum).

1 Introduction

In recent years there has been a renewed interest in Yang–Mills theory in the Coulomb gauge, both in the continuum approach [1,2,3,4,5,6,7,8,9,10,11,12,13,14,15,16] and on the lattice [17,18,19,20,21,22,23]. Being non-covariant, Coulomb gauge is more cumbersome for perturbative calculations and, in fact, it has not yet been proved that Yang–Mills theory in the Coulomb gauge is perturbatively renormalisable. However, Coulomb gauge is superior to covariant gauges such as Landau gauge when it comes to nonperturbative investigations of the infrared sector of the theory. The reason is that in Coulomb gauge, Gauss' law can be explicitly resolved (and thus the separation of gauge dependent and gauge invariant degrees of freedom accomplished) [1]. This is a particular advantage in the Hamiltonian approach where the resolution of Gauss' law leads to a confining static potential between colour charges. A perturbative calculation of this potential allows the extraction of the running coupling constant [24,25]. Furthermore, in the so-called first order formalism of the functional integral approach, the resolution of Gauss' law in the Coulomb gauge leads to a cancellation of the Faddeev–Popov determinant and thus avoids in principle the introduction of ghost fields [13,14]. The Yang–Mills Hamiltonian in the Coulomb gauge is the starting point of a variational solution of the Yang–Mills Schrödinger equation in Refs. [6,7,8,10]. Using Gaussian types of ansätze for the wave functional, minimisation of the vacuum energy density gives rise to a set of equations (similar to the Dyson–Schwinger equations) for various propagators and vertices. Imposing certain approximations, these equations have been solved analytically in the infrared [26] and numerically in the whole momentum regime [8,27,12]. If the curvature of the space of gauge orbits expressed by the Faddeev–Popov determinant is properly included one indeed finds a linearly rising static potential and an infrared diverging gluon energy, both phenomena signalising confinement.

In the derivation of the Dyson–Schwinger equations from the variational principle [6,8], a couple of assumptions and approximations are involved which are difficult to control in $D = 3 + 1$ dimensions. For this reason, we apply in the present paper the variational approach of Ref. [8] to Yang–Mills theory in $D = 1 + 1$, which can be solved exactly in the Coulomb gauge. With the exact solution at hand we then test various assumptions and approximations involved in the $D = 3 + 1$ dimensional case.

Yang–Mills theory in $1 + 1$ dimensions is trivial in flat Minkowski space but becomes non-trivial on a compact manifold. We shall consider Yang–Mills theory on the space-time manifold $S^1 \times \mathbb{R}$ which is convenient for the Hamiltonian approach. On this manifold the Yang–Mills Schrödinger equation has been solved exactly with a (almost) complete gauge fixing [28]. This gauge fixing consists of the *pure Coulomb gauge*, which leaves in $D = 1+1$ a constant spatial gauge field, and an additional gauge condition, which exploits the residual global gauge invariance left in the *pure Coulomb gauge* to diagonalise the algebra-valued gauge field. We will refer to this (almost complete) gauge as the *diagonal Coulomb gauge*. The additional global gauge fixing is not implemented in the variational

approach in $D = 3 + 1$ dimensions. In $D = 1 + 1$, the *pure* and *diagonal Coulomb gauges* are here directly compared by identifying their Gribov regions and (previously unknown) boundary conditions on the wave functionals. The latter boundary conditions arise by paying proper attention to those zero modes of the respective Faddeev–Popov kernels that are not related to the field configurations on the Gribov horizon but to the incomplete gauge fixing. Thus, the exact vacuum wave functionals are derived in both gauges, and the propagators and vertices are calculated within the corresponding Gribov regions. These results for the Green functions are shown to be a particular solution of the exact Dyson–Schwinger equations defined on the *first* Gribov region. Other solutions to the Dyson–Schwinger equations are shown to exist and to be defined on a union of several Gribov regions, including many Gribov copies. We investigate which kind of approximation of the Dyson–Schwinger equations leads to which one of these solutions, for the sake of comparison to $D = 3 + 1$ where a truncation of the Dyson–Schwinger equations in mandatory.

The calculation of the static colour Coulomb potential within a variational approach to $D = 3 + 1$ yields linear quark confinement [27] but includes certain approximations. We here calculate the static colour Coulomb potential in both the *pure Coulomb gauge* and the *diagonal Coulomb gauge* and compare the results for the Coulomb string tension to the gauge invariant string tension extracted from the Wilson loop. Along these lines, the quality of approximations in the $D = 3 + 1$ calculations can be estimated by comparison to the $D = 1 + 1$ case.

The organisation of this paper is as follows: In section 2, we briefly review the Hamiltonian formulation of Yang–Mills theory in $1 + 1$ dimensions on the space-time manifold $S^1 \times \mathbb{R}$, extract the physical configuration space from the Wilson loop and identify the gauge invariant and gauge degrees of freedom. In section 3, we discuss incomplete gauge fixing in the Hamiltonian approach by the Faddeev–Popov method and calculate explicitly the Faddeev–Popov determinant of the *pure Coulomb gauge*, which differs from the one in the *diagonal Coulomb gauge*. In section 4, we discuss the gauge fixing on S^1 in detail and determine the Gribov regions and the so-called fundamental modular region. The restriction of the configuration space to the fundamental modular region imposes boundary conditions on the wave functionals, which are also extracted in this section. In section 5, Gauss' law is explicitly resolved for both the *pure* and *diagonal Coulomb gauges*. The exact solution of the Yang–Mills Schrödinger equation in the *pure Coulomb gauge* is given in section 6. With the exact vacuum wave functional at hand, the exact propagators and vertices are calculated in section 7. In section 8, the potential between static colour charges is determined and the Coulomb string tension is extracted. In section 9, the Dyson–Schwinger equations are derived. Gribov copy effects on the Green functions are discussed in section 10. The quality of a common truncation of Dyson–Schwinger equations is assessed in section 11. In section 12, we apply the variational approach of Ref. [8] to Yang–Mills theory in $D = 1 + 1$ on $S^1 \times \mathbb{R}$ using the same variational wave functional in order to check the approximations made in $D = 3 + 1$. A short summary and some concluding remarks are given in section 13. Some mathematical derivations are presented in appendices.

2 Hamiltonian formulation of 1+1 dimensional Yang–Mills theory on $S^1 \times \mathbb{R}$

We consider $SU(N_c)$ Yang–Mills theory in $1+1$ dimensions. In $D = 1+1$, the gauge field $A_\mu(x)$ is dimensionless while the gauge coupling constant g has dimension of inverse length. It is, however, convenient to absorb the gauge coupling g into the gauge field $gA_\mu \to A_\mu$, so that $A_\mu \equiv A_\mu^a T^a$ has dimension of inverse length. We will use antihermitian generators $T_a, a = 1, \ldots, N_c^2 - 1$ of the gauge group, satisfying

$$[T_a, T_b] = f_{abc} T_c \,, \tag{2.1}$$

where f_{abc} is the structure constant. For $SU(2)$, the generators are related to the Pauli matrices $\tau_{a=1,2,3}$ by $T_a = -\frac{i}{2}\tau_a$.

In 1+1 dimensional (flat) Minkowski space Yang–Mills theory is trivial but becomes non-trivial on a compact manifold. The only compact space-time manifold with a canonical time is the cylinder

$$S^1 \,(\text{space}) \,\times\, \mathbb{R}\,(\text{time}) \,. \tag{2.2}$$

On $S^1 \times \mathbb{R}$, the gauge invariant degrees of freedom are the spatial Wilson loops winding around S^1,

$$\overline{W}[A] = \frac{1}{N_c} \,\mathrm{tr}\,\mathrm{P}\, \exp\left(- \oint\limits_{S^1} dx^1 A_1(x^0, x^1) \right) \,, \tag{2.3}$$

which represent closed electric flux lines. The spatial S^1 can be realized by considering a finite interval on the x^1-axis of length L and imposing the periodic boundary condition [1]

$$A_\mu(x^0, x^1 = L) = A_\mu(x^0, x^1 = 0) \,. \tag{2.4}$$

In the absence of fermions in the fundamental representation this boundary condition remains intact under gauge transformations

$$A_\mu^U = U A_\mu U^\dagger + U \partial_\mu U^\dagger \tag{2.5}$$

satisfying the boundary condition

$$U(x^0, x^1 = L) = Z_n(x^0) U(x^0, x^1 = 0) \,, \tag{2.6}$$

where $Z_n, n = 0, 1, \ldots, N_c - 1$ is an element of the centre $Z(N_c)$ of the gauge group.

Throughout the paper we will work in the canonical Hamiltonian approach [30] and impose the Weyl gauge

$$A_0 = 0 \,. \tag{2.7}$$

[1] The periodic boundary condition can be taken without loss of generality since the $SU(N_c)$ bundle over S^1 is trivial as noticed in Ref. [29].

The gauge transformation required to bring a periodic gauge field $A_0(x^0, x^1 = L) = A_0(x^0, x^1 = 0)$ into the Weyl gauge,

$$U^\dagger(x^0, x^1) = \mathrm{P} \exp\left(- \int_0^{x^0} dt A_0(t, x^1) \right) , \tag{2.8}$$

is also periodic and thus within the class (2.6). On the flat space $\mathbb{R}$, an analogous gauge transformation

$$V^\dagger(x^0, x^1) = \mathrm{P} \exp\left(- \int_0^{x^1} ds A_1(x^0, s) \right) \tag{2.9}$$

could also gauge away the field A_1, i.e. $A_1^V = 0$. However, the gauge transformation V (2.9) is not within the class (2.6) and therefore not allowed on S^1. It is the compactification of space $\mathbb{R} \to S^1$ which makes the theory non-trivial.

The canonical quantisation is carried out at a fixed time x^0, so that $A_1(x^0 - \text{fixed}, x^1)$ is the only field "coordinate" left. To simplify the notation, we will omit henceforth the spatial index $i = 1$ and write $x^1 \to x$, $\partial_1 \to \partial$, $A_1^a(x^1) \to A^a(x)$ etc. The Hamiltonian of $1 + 1$ dimensional Yang–Mills theory then reads

$$H = \frac{g^2}{2} \int dx \, \Pi^a(x) \Pi^a(x) , \tag{2.10}$$

where

$$\Pi^a(x) = \frac{1}{i} \frac{\delta}{\delta A^a(x)} \tag{2.11}$$

is the momentum operator, which represents the electric field. Note in 1+1 dimensions, there is no magnetic field and hence no potential term in the Hamiltonian.

Having quantised the theory in the Weyl gauge, the classical Gauss law $\hat{D}\Pi = \rho$ is lost from the quantum equations of motion. Enforcing Gauss' law as an operator identity contradicts the canonical commutation relations.[2] One therefore imposes Gauss' law as a constraint on the wave functional $\Psi(A)$

$$\hat{D}(x) \Pi(x) \Psi(A) = \rho(x) \Psi(A) . \tag{2.12}$$

Here,

$$\hat{D}(x) = \partial + \hat{A}(x), \qquad \hat{A}(x) = A^a(x) \hat{T}_a, \tag{2.13}$$

[2] Alternatively, the Dirac bracket formalism can be used to quantise the theory after fixing the gauge transformations generated by Gauss' law. The Gauss law can then be imposed as an operator identity. This was shown in 3+1 dimensional Minkowski space to lead to the same energy spectrum [31].

denotes the covariant derivative in the adjoint representation with

$$(\hat{T}_a)_{bc} = f_{bac} \tag{2.14}$$

being the generators in the adjoint representation. Furthermore, $\rho(x)$ denotes the colour density of matter fields (or external sources). The operator on the l.h.s. of Eq. (2.12), $\hat{D}\Pi$, is the generator of so-called "small" gauge transformations (see section 4) and in the absence of matter fields, $\rho(x) = 0$, Gauss' law forces the wave functionals $\Psi(A)$ to be invariant under the small gauge transformations U,

$$\Psi(A^U) = \Psi(A) \; . \tag{2.15}$$

Instead of working with gauge invariant wave functionals, it is more convenient to explicitly resolve Gauss law by fixing the gauge [1] and for this purpose the Coulomb gauge

$$\partial \, A(x) = 0 \tag{2.16}$$

is particularly convenient. In one spatial dimension, the Coulomb gauge constrains the gauge field to spatially constant modes and the field theory reduces to quantum mechanics in these constant modes. The gauge transformation Ω which brings a given gauge field A into the Coulomb gauge $\partial A^\Omega = 0$ can be chosen

$$\Omega^\dagger(x) = V^\dagger(x)(V(L))^{\frac{x}{L}} \; , \tag{2.17}$$

where $V(x)$ is defined by Eq. (2.9) with the x^0-dependence suppressed. Contrary to $V(x)$, $\Omega(x)$ is periodic for periodic $A(x)$, and thus within the class of allowed gauge transformations (2.6). The gauge-transformed field

$$A^\Omega = \frac{1}{L} \ln V(L) \tag{2.18}$$

is space-independent and thus obviously satisfies the Coulomb gauge condition.

The Coulomb gauge (2.16) (together with Weyl gauge (2.7)) still leaves invariance with respect to global (space and time independent) gauge transformations, which can be exploited to diagonalise the constant gauge field

$$A = A^a T_a \; \rightarrow \; A^{a_0} T_{a_0} = A_{diag} \; . \tag{2.19}$$

Here T_{a_0}, $a_0 = 1, \ldots, N_c - 1$ denotes the generators of the Cartan sub-algebra which can be chosen to be diagonal. Equation (2.19) fixes the global transformation U up to a constant element of the Cartan sub-group, i.e. even after implementing the gauge condition $A = \textit{diagonal}$ in addition to the *pure Coulomb gauge*, there still is a residual global abelian $U(1)^{N_c-1}$ gauge symmetry. Moreover, there still is a discrete symmetry left: The above gauge conditions (2.16) and (2.19) do not fix the so-called Weyl symmetry consisting of

the $N_c!$ permutations of the N_c eigenvalues of $A^a T_a$. In the case of $SU(2)$, where the two eigenvalues have the same modulus but opposite signs, the Weyl symmetry switches the signs of the eigenvalues.

Note that we can re-express the two gauge conditions (2.16) and (2.19) as

$$f^{\bar{a}}[A] = A^{\bar{a}}(x) = 0\,, \tag{2.20a}$$
$$f^{a_0}[A] = \partial A^{a_0}(x) = 0\,, \tag{2.20b}$$

i.e. the Coulomb gauge condition is imposed only on the abelian part A^{a_0} while the non-abelian components of the gauge field denoted by the index $\bar{a} \neq a_0$ vanish. In the following we will refer to this gauge as *diagonal Coulomb gauge*, while Eq. (2.16) will be called *pure Coulomb gauge*.

To simplify the explicit calculations, we will confine ourselves henceforth to the gauge group $SU(2)$ where the structure constants coincide with the totally anti-symmetric tensor $f^{abc} = \varepsilon^{abc}$, $a = 1, 2, 3$, and we will choose the generator of the Cartan sub-group to be given by $a_0 = 3$. For $SU(2)$, the A^a can be interpreted as the Cartesian components of a vector $\mathbf{A} = A^a \boldsymbol{e}_a$ in a 3-dimensional Euclidean space with Cartesian unit vectors $\boldsymbol{e}_{a=1,2,3}$. In the *diagonal Coulomb gauge* specified by Eq. (2.20) the colour vector $\mathbf{A}$ is rotated into the direction of the positive or negative 3-axis

$$\mathbf{A} = A^3 \boldsymbol{e}_3\,,\ A^3 = \pm|\mathbf{A}|\,. \tag{2.21}$$

The two signs differ by a Weyl reflection $\mathbf{A} \to -\mathbf{A}$. Thus the gauge transformation from the *pure Coulomb gauge* into the *diagonal Coulomb gauge* is given by rotating the colour vector $\mathbf{A}$ into the positive 3-direction $\boldsymbol{e}_3$, possibly followed by a Weyl reflection $A^3 \to -A^3$.

The modulus $|\mathbf{A}|$ of the constant Coulomb gauge field represents the only gauge invariant degree of freedom. In fact, the only physical observable of the theory, the spatial Wilson loop $\overline{W}$ winding (non-trivially) around the whole space manifold S^1, Eq. (2.3), is easily calculated in (both pure and diagonal) $SU(2)$ Coulomb gauge to be given by

$$\overline{W} = \frac{1}{2}\,\mathrm{tr}\,\exp(-AL) = \cos\vartheta\,, \tag{2.22}$$

where we have introduced the dimensionless variable

$$\vartheta = \frac{|\mathbf{A}|L}{2}\,, \tag{2.23}$$

for later convenience. $\overline{W}$ attains all possible values in $[-1, 1]$ when ϑ traverses the interval

$$0 \leq \vartheta \leq \pi\,. \tag{2.24}$$

Equation (2.24) defines the physical configuration space of the theory. We will later recover the interval (2.24) as the so-called fundamental modular region.

To separate the constant Coulomb gauge field $\mathbf{A}$ into (global) gauge invariant and gauge dependent parts, it is convenient to use the spherical coordinates $|\mathbf{A}|, \theta, \phi$ to write [3]

$$\mathbf{A} = |\mathbf{A}|\, \hat{\mathbf{A}}(\theta, \phi) \equiv \frac{2}{L}\, \vartheta\, \hat{\mathbf{A}}(\theta, \phi)\ , \tag{2.25}$$

where

$$\hat{\mathbf{A}}(\theta, \phi) = \sin\theta\, (\cos\phi\, \boldsymbol{e}_1 + \sin\phi\, \boldsymbol{e}_2) + \cos\theta\, \boldsymbol{e}_3 \tag{2.26}$$

is the radial unit vector.

The primary aim of the present paper is to use 1+1 dimensional Yang–Mills theory as testing ground for the variational approach developed in $3+1$ dimensions [8], assessing the approximations introduced there. In studies of Coulomb gauge Yang–Mills theory in higher dimensions, merely the *pure Coulomb gauge* is fixed. Therefore, we will here mainly focus on the *pure Coulomb gauge* as well. Moreover, the *diagonal Coulomb gauge* will be used to investigate the effect of a complete gauge fixing on the Green functions of the theory.

3 Gauge fixing in the Hamiltonian approach by the Faddeev–Popov method

In the Hamiltonian approach in Weyl gauge, there is no need to fix the residual time-independent gauge symmetry. In principal, one can work (in the absence of external colour charges) with gauge invariant wave functionals, which trivially satisfy Gauss law. It is only a matter of convenience that one prefers to fix the gauge. Furthermore, as will be explicitly shown in the context of the resolution of Gauss' law (see section 5), the gauge fixing needs not to be complete, i.e. any partial gauge fixing is allowed in the Hamiltonian approach. In any case, the wave functionals have to be invariant under the residual gauge symmetries unfixed by the gauge condition. In the *pure Coulomb gauge*, the wave functionals have to be invariant under global colour rotations $U = const$, which are not fixed by that gauge.

Gauge fixing is accomplished in the Hamiltonian approach by applying the Faddeev–Popov method to the functional integral over the spatial gauge fields defining the scalar product in the Hilbert space of wave functionals. Consider the matrix element of a gauge invariant observable $\mathcal{O}[A^U] = \mathcal{O}[A]$

$$\langle \Psi_1 | \mathcal{O}[A] | \Psi_2 \rangle = \int \mathcal{D}A\, \Psi_1^*[A]\, \mathcal{O}[A]\, \Psi_2[A]\ . \tag{3.1}$$

The Faddeev–Popov method amounts to inserting into the functional integral the identity

$$1 = \mathrm{Det}\, \mathcal{M}[A] \int D\mu(\Omega)\, \delta(f^a[A^\Omega]) \tag{3.2}$$

[3] For a 3-vector $\mathbf{A}$, the caret "$\hat{}$" denotes as usual the unit vector $\hat{\mathbf{A}} = \mathbf{A}/|\mathbf{A}|$, while for algebra- and group-valued quantities the caret means the adjoint representation.

where $\Omega = \mathrm{e}^{\Theta}, \Theta = \Theta^a T_a$, denotes a gauge transformation and

$$\mathcal{M}^{ab}(x,y) = \frac{\delta f^a[A^\Omega](x)}{\delta\,\Theta^b(y)} \tag{3.3}$$

is the Faddeev–Popov kernel. Furthermore, for a complete gauge fixing, $D\mu(\Omega)$ denotes the Haar measure of the gauge group. Inserting the identity (3.2) into Eq. (3.1) and exploiting the gauge invariance of both the wave functional and the observable, one finds after a change of the integration variable

$$\langle\Psi_1|\mathcal{O}[A]|\Psi_2\rangle = \int \mathcal{D}A \,\mathrm{Det}\,\mathcal{M}[A]\,\delta(f^a[A])\Psi_1{}^*[A]\,\mathcal{O}[A]\,\Psi_2[A]\int D\mu(\Omega) \tag{3.4}$$

where the integration of the gauge group is now explicitly separated, yielding a (infinite) constant which can be absorbed into the normalisation of the wave functional.

If the gauge condition $f^a[A^\Omega] = 0$ does not fix the gauge completely, there are directions in the space of gauge transformations, along which the gauge-fixing functional $f^a[A^\Omega]$ does not change, i.e. $\delta f^a[A^\Omega]/\delta\Theta^b = 0$, and the tangent vectors corresponding to these directions represent zero modes of the Faddeev–Popov kernel (3.3). In order that the identity (3.2) holds and thus the Faddeev–Popov method works one has to exclude these zero modes and integrate only over the subspace of gauge transformations which are fixed by the gauge condition $f^a[A^\Omega] = 0$. Furthermore, the gauge fixing is defined only in the region of gauge field configurations A where the Faddeev–Popov determinant $\mathrm{Det}\,\mathcal{M}[A]$ is non-zero. This will be important for the application of the Faddeev–Popov method given below.

The explicit calculation of the Faddeev–Popov kernel is most easily accomplished by noticing that the Gauss law operator $\hat{D}\Pi$ is the generator of (so-called small [4]) gauge transformations

$$\begin{aligned} f^a[A^\Omega] &= \mathcal{G}(\Theta) f^a[A]\mathcal{G}^{-1}(\Theta)\,, \\ \mathcal{G}(\Theta) &= \exp\left(-i\int dx\left(\hat{D}^{ab}(x)\Theta^b(x)\right)\Pi^a(x)\right). \end{aligned} \tag{3.5}$$

For infinitesimal gauge transformations $\mathcal{G}(\delta\Theta) = 1 + i\int dx\,\delta\Theta^a(x)(\hat{D}\Pi)^a(x)$, we have accordingly

$$f^a[A^\Omega](x) = f^a[A](x) + \int dy\,\delta\Theta^b(y)\left[i(\hat{D}\Pi)^b(y), f^a[A](x)\right] \tag{3.6}$$

and comparison with the Taylor expansion of $f^a[A^\Omega]$ in powers of $\delta\Theta^a(x)$ reveals that the Faddeev–Popov kernel (3.3) can be expressed as

$$\mathcal{M}^{ab}(x,y) = i\,\hat{D}^{bc}(y)\left[\Pi^c(y), f^a[A](x)\right]. \tag{3.7}$$

[4] See section 4.

Below, we use this relation to determine the Faddeev–Popov kernels for the two gauges considered above and calculate the corresponding Faddeev–Popov determinants.

3.1 Diagonal Coulomb gauge

Applying the relation (3.7) to the *diagonal Coulomb gauge* condition (2.20), we obtain the Faddeev–Popov kernel ($\bar{b} = 1, 2$)

$$\mathcal{M}^{a\bar{b}}(x,y) = -\hat{D}^{a\bar{b}}(x)\delta(x,y) \tag{3.8a}$$

$$\mathcal{M}^{a3}(x,y) = -\hat{D}^{a3}(x)\partial^x\delta(x,y) \tag{3.8b}$$

On the gauge shell (where the gauge condition is fulfilled), the Faddeev–Popov kernel becomes block diagonal and reads in the Cartesian basis

$$\mathcal{M}(x,y) = \begin{pmatrix} -\partial_x & A^3 & 0 \\ -A^3 & -\partial_x & 0 \\ 0 & 0 & -\partial^2 \end{pmatrix} \delta(x,y) = \begin{pmatrix} i & 0 & 0 \\ 0 & i & 0 \\ 0 & 0 & i\,\partial_x \end{pmatrix} i\hat{D}(x)\;\delta(x,y)\;. \tag{3.9}$$

The Faddeev–Popov determinant becomes

$$\mathrm{Det}\,\mathcal{M} = \mathrm{Det}_{(1)}\,(-i\partial)^{33}\,\mathrm{Det}\,(i\hat{D})\;. \tag{3.10}$$

The first factor is a (divergent) irrelevant constant, which drops out from the expectation values and can be absorbed into the functional integral measure, see below. Note, this determinant is defined in the (one-dimensional) abelian colour sub-space $a = a_0 = 3$ only, indicated by the sub-script (1). To evaluate the second factor $\mathrm{Det}\,(i\hat{D})$, we consider the eigenvalue equation

$$i\hat{D}^{ab}[A](x)\varphi^b(x) = \lambda\,\varphi^a(x) \tag{3.11}$$

From the representation (3.3), it is clear that the eigenfunctions of the Faddeev–Popov kernel have to satisfy the same boundary condition as the gauge angles $\Theta^a(x)$. Since the gauge transformations on the spatial S^1 have to satisfy periodic boundary conditions $\Theta(x+L) = \Theta(x)$, the eigenfunctions of the Faddeev–Popov kernel have to be periodic as well. Since ∂ and $\hat{D}$ commute on the gauge-fixed manifold, the operators $\partial, \hat{D}$ and $\mathcal{M}$ have common eigenfunctions and we can impose the periodic boundary condition also on the eigenfunctions of $i\hat{D}$,

$$\varphi^a(x+L) = \varphi^a(x)\;. \tag{3.12}$$

With this boundary condition, which does not mix the different colour components, and with the fact that the gauge field is spatially constant, the eigenfunctions of $i\hat{D}$ factorise in space and colour dependent parts. Using the results of appendix A and Eq. (2.21), the

eigenfunctions are given by

$$\varphi^a_{n,\sigma}(x) \equiv \langle x, a|n, \sigma\rangle = \langle x|n\rangle\langle a|\sigma\rangle \tag{3.13}$$

where $\langle a|\sigma\rangle = \mathrm{e}^a_\sigma$ are (the Cartesian components of) the polar unit vectors $\boldsymbol{e}_\sigma$ (A.15) and

$$\langle x|n\rangle = \frac{1}{\sqrt{L}}\,\mathrm{e}^{-ik_n x}\;, \quad k_n = \frac{2\pi n}{L}\;, \quad n \in \mathbb{Z} \tag{3.14}$$

are plane waves (periodic in L). The corresponding eigenvalues read

$$\lambda_{n,\sigma} = k_n + \sigma A^3\;. \tag{3.15}$$

The two eigenvalues $\lambda_{n,\sigma=\pm1}$ correspond to the non-abelian block ($\bar{a} = 1, 2$) in the upper left corner in the Faddeev–Popov matrix (3.9) while the eigenvalue $\lambda_{n,\sigma=0} = k_n$ corresponds to the abelian colour direction $a_0 = 3$ (see Eq. (A.15)). Furthermore, the zero mode $\varphi_{n=0,\sigma=0} = \boldsymbol{e}_{\sigma=0}/\sqrt{L} \equiv \boldsymbol{e}_3/\sqrt{L}$ ($\lambda_{n=0,\sigma=0} = 0$) represents the tangent vector (to the gauge orbit) corresponding to the infinitesimal global $U(1)$ colour rotation ($\Theta^3 = const$) which is not fixed by the gauge condition (2.20). As discussed above, this mode has to be excluded from the spectrum of the Faddeev–Popov kernel (3.9), whose eigenvalues are given by

$$\Lambda_{n,\sigma} = \begin{cases} i\lambda_{n,\sigma} & , \quad \sigma = \pm1 \\ k_n\lambda_{n,\sigma} = k_n^2\;, & \quad \sigma = 0 \end{cases}\;. \tag{3.16}$$

Note also that the eigenmodes $\varphi_{n=0,\sigma=\pm1}$ corresponding to the global $SU(2)/U(1)$ gauge transformations which are fixed by the gauge condition (2.20) do not give rise to zero eigenvalues, $\lambda_{n=0,\sigma=\pm1} = \pm A^3 \neq 0$.

Excluding the zero mode $n = \sigma = 0$ (indicated in the following by a prime), we obtain with $A^3 = \pm|\mathbf{A}|$ (see Eq. (2.21))

$$\begin{aligned} \mathrm{Det}'\,(i\hat{D}[A]) &= \prod_{n=-\infty}^{\infty}{}' \prod_{\sigma=0,\pm1} \lambda_{n,\sigma} = \Big(\prod_{m\neq0} k_m\Big) \prod_{n=-\infty}^{\infty} \lambda_{n,1}\lambda_{n,-1} \\ &= \Big(\prod_{m\neq0} k_m\Big)\,|\mathbf{A}|^2\Big(\prod_{n=1}^{\infty}(k_n^2 - |\mathbf{A}|^2)\Big)^2 \\ &= \Big(\prod_{m\neq0} k_m^3\Big)\,\Big(|\mathbf{A}|\prod_{n=1}^{\infty}\Big(1 - \frac{|\mathbf{A}|^2}{k_n^2}\Big)\Big)^2 \end{aligned} \tag{3.17}$$

The first factor represents $\mathrm{Det}(i\partial)$ with the zero mode $n = 0$ excluded. Using

$$\sin x = x\prod_{n=1}^{\infty}\Big(1 - \Big(\frac{x}{\pi n}\Big)^2\Big) \tag{3.18}$$

we obtain

$$\mathrm{Det}'\left(i\hat{D}[A]\right) = \mathrm{Det}\left(i\partial\right)\left(\frac{2}{L}\right)^2 \sin^2\left(\frac{|\mathbf{A}|L}{2}\right) \equiv \mathrm{Det}\left(i\partial\right)\left(\frac{2}{L}\right)^2 \sin^2\vartheta\ . \tag{3.19}$$

All field-independent factors in the Faddeev–Popov determinant (3.10) can be absorbed in the functional integral measure. We thus arrive at the Faddeev–Popov determinant $\mathcal{J}_D$ of the *diagonal Coulomb gauge* (2.20)

$$\mathcal{J}_D := \frac{\mathrm{Det}\mathcal{M}}{\mathrm{Det}_{(1)}\left(-i\partial\right)^{33}\mathrm{Det}(i\partial)\left(\frac{2}{L}\right)^2} = \sin^2\vartheta\ . \tag{3.20}$$

Let us stress that it was absolutely crucial to exclude the gauge modes which are not fixed by the gauge condition. Otherwise the Faddeev–Popov determinant would have vanished identically.

The Faddeev–Popov determinant $\mathcal{J}_D$ has zeros at (note that by definition $\vartheta \geq 0$)

$$\vartheta \equiv \frac{|\mathbf{A}|L}{2} = n\pi\ , \quad n = 0, 1, 2, \ldots \tag{3.21}$$

and thus divides up the gauge-fixed configuration space into regions where the Faddeev–Popov method of gauge fixing is defined. These so-called *Gribov regions* are given by

$$n\pi \leq \vartheta < (n+1)\pi\ . \tag{3.22}$$

Recall that in the *diagonal Coulomb gauge* $A^3 = \pm|\mathbf{A}|$, so that in this variable the Gribov regions are given by

$$\left\{A_3 \;\middle|\; \frac{2n\pi}{L} \leq |A_3| < \frac{2(n+1)\pi}{L}\right\}\ , \quad n = 0, 1, 2, \ldots\ . \tag{3.23}$$

The boundaries of the Gribov regions, the *Gribov horizons*, are given by the discrete momenta k_n (3.14). We will return to the discussion of the Gribov regions in section 4.

Note that the Faddeev–Popov determinant $\mathcal{J}_D$ (3.20) vanishes also at the (classical) perturbative vacuum $A = 0$. This is not surprising since the diagonalisation of the gauge field, and thus the *diagonal Coulomb gauge*, is ill-defined for $A = 0$. Therefore, this gauge is not suitable for perturbation theory.

3.2 Pure Coulomb gauge

Let us now consider the *pure Coulomb gauge* (2.16) which leaves the global gauge transformations unfixed. The Faddeev–Popov kernel (3.7) is then given by

$$\mathcal{M}^{ab}(x,y) = (-\hat{D}^{ab}[A](x)\partial_x)\,\delta(x,y)\;. \tag{3.24}$$

Since the gauge field in the *pure Coulomb gauge* is related to the one in the *diagonal Coulomb gauge* by a global gauge transformation, we can express the covariant derivative $\hat{D}^{ab}[A]$ in the *pure Coulomb gauge* by the one in the *diagonal Coulomb gauge*. Let $U^\dagger$ denote the global gauge transformation which rotates the colour vector $\mathbf{A}$ into the positive 3-direction, i.e.

$$A^a\hat{T}_a = |\mathbf{A}|\hat{U}\hat{T}_3\hat{U}^T\;. \tag{3.25}$$

Then we have (see appendix A)

$$i\hat{D}[A] = \hat{U}\,i\hat{D}[|\mathbf{A}|T_3]\,\hat{U}^T \tag{3.26}$$

where $\hat{U}$ is the adjoint representation of U. Here, $i\hat{D}[|\mathbf{A}|T_3]$ is the covariant derivative in the *diagonal Coulomb gauge* (with $A^3 = \pm|\boldsymbol{A}|$) whose eigenvalues and eigenfunctions were determined in the previous subsection. From Eq. (3.26), it follows that $i\hat{D}[A^aT_a]$ has the same eigenvalues $\lambda_{n,\sigma}$ (3.15) as $i\hat{D}[|\mathbf{A}|T_3]$, i.e.

$$\lambda_{n,\sigma} = k_n \,+\, \sigma|\mathbf{A}|\,, \tag{3.27}$$

and that the eigenfunctions $|\tilde{\varphi}\rangle$ of $i\hat{D}[A]$ are related to the eigenfunctions $|\varphi\rangle$ (3.13) of $i\hat{D}[|\mathbf{A}|T_3]$ by

$$\tilde{\varphi}^a_{n,\sigma}(x) = \hat{U}_{ab}\varphi^b_{n,\sigma}(x) = \langle x|n\rangle u^a_\sigma\,, \tag{3.28}$$

where $\langle x|n\rangle$ are the periodic plane waves (3.14) and we have defined (see appendix A)

$$\begin{aligned} u^a_\sigma &:= \langle a|\hat{U}|\sigma\rangle = \langle a|\hat{U}|b\rangle\langle b|\sigma\rangle = \hat{U}_{ab}\mathrm{e}^b_\sigma \\ &= \langle a|\tau\rangle\langle\tau|\hat{U}|\sigma\rangle = \mathrm{e}^a_\tau D^1_{\tau\sigma}(\phi,\theta,0)\;. \end{aligned} \tag{3.29}$$

Since $i\hat{D}[A]$ (3.26) has the same eigenvalues as $i\hat{D}[|\mathbf{A}|T_3]$, and since $\det\hat{U} = 1$, one would expect that the Faddeev–Popov determinant in the *pure Coulomb gauge* gauge is, up to an irrelevant constant factor $\mathrm{Det}\,(i\partial)/\mathrm{Det}_{(1)}\,(-i\partial)^{33}$, the same as in the *diagonal Coulomb gauge* (2.20) considered above. However, since the *pure Coulomb gauge* does not fix the global gauge transformation U, we have to exclude the constant eigenmodes from the Faddeev–Popov kernel. These are given by the eigenfunctions with $n = 0$ and all σ. In addition to the zero mode $n = 0, \sigma = 0$ excluded already from the Faddeev–Popov kernel of the *diagonal Coulomb gauge*, one has to exclude here also the gauge modes $n = 0, \sigma = \pm 1$, corresponding to the non-zero eigenvalues $\lambda_{n=0,\sigma=\pm1} = \pm|\mathbf{A}|$. Although these modes

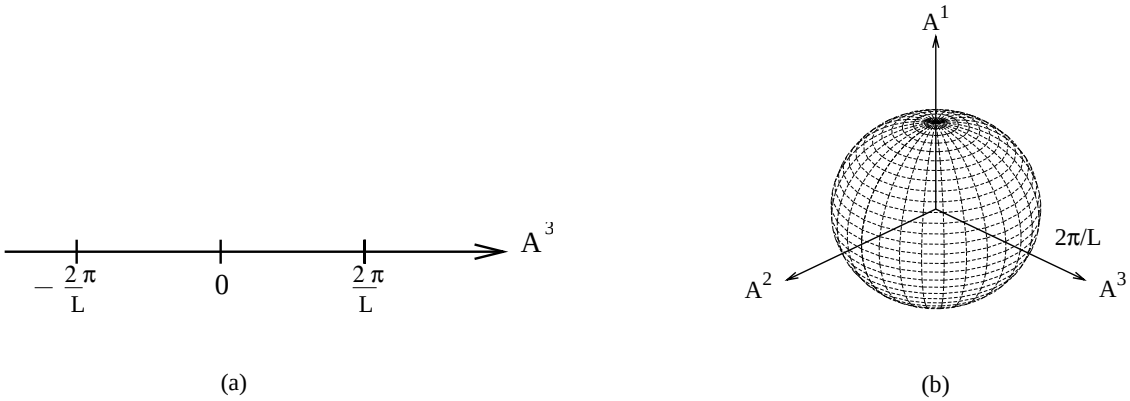

Fig. 1. The first Gribov region for (a) the *diagonal Coulomb gauge* and (b) the *pure Coulomb gauge*.

correspond to non-zero eigenvalues of $i\hat{D}[A]$ they give rise to zero modes of the full Faddeev–Popov kernel of the *pure Coulomb gauge*,

$$(-\hat{D}[A]\partial)\tilde{\varphi}_{n,\sigma} = \Lambda_{n,\sigma}\tilde{\varphi}_{n,\sigma}\ ,\ \Lambda_{n,\sigma} = \lambda_{n,\sigma}k_n \tag{3.30}$$

since $\Lambda_{n=0,\sigma} = 0$. Note that these zero modes form precisely the global gauge transformation $\hat{U}$ which diagonalises the constant Coulomb gauge field $\hat{A} = \hat{A}^a T_a$ (cf. Eqs. (3.26), (A.1)),

$$\tilde{\varphi}^a_{n=0,\sigma}(x) = \frac{1}{\sqrt{L}}\langle a|\hat{U}|\sigma\rangle\ . \tag{3.31}$$

Omitting these modes in calculating Det $(-\hat{D}\partial)$, equivalently to Eq. (3.17), we find for the Faddeev–Popov determinant $\mathcal{J}_P$ in the *pure Coulomb gauge*

$$\mathcal{J}_P = \frac{\mathrm{Det}\,(-\hat{D}\partial)}{\mathrm{Det}\,(-\partial^2)} = \frac{\sin^2\left(\frac{|\mathbf{A}|L}{2}\right)}{\left(\frac{|\mathbf{A}|L}{2}\right)^2} \equiv \frac{\sin^2\vartheta}{\vartheta^2}\ . \tag{3.32}$$

This determinant differs from the one of the *diagonal Coulomb gauge* (2.20) by the denominator (cf. Eq. (3.20)) and does not vanish at the perturbative vacuum $A = 0$. Furthermore, since $\lim_{|\mathbf{A}|\to 0} d\mathcal{J}_P/d|\mathbf{A}| = 0$ the space of gauge orbits is flat near the perturbative vacuum in this gauge. The first zero of the Faddeev–Popov determinant occurs at $\vartheta = |\mathbf{A}|L/2 = \pi$ which defines the first Gribov horizon to coincide (in the variable ϑ) with the one in the *diagonal Coulomb gauge* (3.22). However, in the *pure Coulomb gauge* the direction of the gauge field $\mathbf{A}$ is not fixed, so the Gribov regions Ω_n are given here by the spherical shells

$$\Omega_n := \left\{\mathbf{A}\ \middle|\ (n-1)\,\frac{2\pi}{L} \le |\mathbf{A}| < n\,\frac{2\pi}{L}\right\}\ ,\quad n = 1, 2, 3, \ldots . \tag{3.33}$$

In particular, the first Gribov region Ω_1 is given by the sphere $|\mathbf{A}| < \frac{2\pi}{L}$. The first Gribov regions of both the diagonal and the pure Coulomb gauge are illustrated in Fig. 1. The Gribov regions will be discussed in more detail in the upcoming section.

4 Gribov regions and boundary conditions on the wave functionals

In this section, the configuration spaces of both the *pure* and *diagonal Coulomb gauges* are examined. (For valuable discussions on this topic, also see, e.g., Ref. [32] and references therein.) The topology of gauge transformations relating the various Gribov regions of the *pure Coulomb gauge* and the *diagonal Coulomb gauge* is discussed here, the fundamental modular region is specified, and boundary conditions on the wave functionals are given.

4.1 Topology of gauge transformations on S^1

Since the first homotopy group $\Pi_1(SU(N_c))$ is trivial, there are no "large" gauge transformations in one (compact) spatial dimension, i.e. on S^1. However, in the absence of matter fields in the fundamental representation, the gauge group is in fact $SU(N_c)/Z(N_c)$. This is because the gauge field, living in the adjoint representation, is invariant under centre gauge transformations [5] $Z(x) \in Z(N_c)$. Since $\Pi_1(SU(N_c)/Z(N_c)) = Z(N_c)$, there are topological non-trivial gauge transformations falling in N_c different topological classes and consequently there are N_c distinct classical vacuum configurations $A_{(n)} = U_{(n)}\partial U^\dagger_{(n)}$ between which quantum tunnelling occurs. In the fundamental representation, the $U_{(n)}$ satisfy the boundary condition (2.6), with x^0 fixed, and are specified by the N_c centre elements $Z_n \in Z(N_c)$. The $U_{(n=0)}$, belonging to the trivial centre element $Z_0 = \mathbb{1}$ are periodic and form the "small" gauge transformations. The remaining ones are "large" transformations. Since $(Z_n)^{N_c} = \mathbb{1}, N_c$ successive large gauge transformations $U_{(n)}$ belonging to the same Z_n yield a small gauge transformation. The fundamental representation of $SU(N_c)/Z(N_c)$ is the adjoint representation of $SU(N_c)$, which we will denote in the following by a caret. The adjoint representation $\hat{U} = \exp(\Theta_a \hat{T}_a)$ is related to the fundamental representation $U = \exp(\Theta_a T_a)$ (with the same Θ_a !) by

$$U^\dagger T_a U = \hat{U}_{ab} T_b \ , \quad \hat{U}_{ab} = -2\,\mathrm{tr}\left(U^\dagger T_a U T_b\right) \ . \tag{4.1}$$

From this representation it is explicitly seen that the adjoint representation $\hat{U}$ is centre blind. Accordingly, the allowed gauge transformations satisfying (in the fundamental

[5] Since the centre $Z(N_c)$ is a discrete set, centre gauge transformations $Z(x)$ have to be piecewise constant. At the jumps of $Z(x)$ (from one centre element to another) the inhomogeneous term of the gauge transformation, $Z(x)\partial Z^\dagger(x)$, represents so-called ideal centre vortices [33,34]. The centre vortices of the fundamental representation, $Z(x)\partial Z^\dagger(x) = C^a(x)T_a$, become invisible Dirac sheets (strings) in the adjoint representation $\hat{Z}(x)\partial\hat{Z}^\dagger(x)$. In fact, a centre element $Z(x) = \exp(-\mu^a(x)T_a) \in Z(N_c)$ (in the fundamental representation, with $\mu^a(x)$ being a co-weight vector) becomes the unit matrix in the adjoint representation, $\hat{Z}(x) = \exp(-\mu^a(x)\hat{T}_a) = \mathbb{1}$, so that the inhomogeneous term $\hat{Z}(x)\partial\hat{Z}^\dagger(x)$ disappears in the adjoint representation.

representation of $SU(N_c)$) the boundary condition (2.6) are periodic in the adjoint representation

$$\hat{U}(x+L) = \hat{U}(x)\,. \tag{4.2}$$

To be more specific consider the gauge group $SU(2)$ whose centre is $Z(2) = \{\mathbb{1}, -\mathbb{1}\}$. The allowed gauge transformations satisfying Eq. (2.6) are either periodic (belonging to $Z_0 = \mathbb{1}$) or anti-periodic (belonging to $Z_1 = -\mathbb{1}$). In the absence of matter fields in the fundamental representation, the true gauge group is $SU(2)/Z(2) = SO(3)$. Since $\Pi_1(SO(3)) = Z(2)$, there are two inequivalent sets of gauge transformations allowed by Eq. (2.6). The periodic ones $U_{(0)}(L) = U_0(0)$ belonging to the trivial centre element $Z_0 = \mathbb{1}$, form the *small* gauge transformations, which can be smoothly deformed to unity. The anti-periodic gauge transformations, corresponding to the non-trivial centre element $Z_1 = -\mathbb{1}$, cannot be smoothly deformed to unity and are called *large*. To provide some explicit examples consider the gauge transformation

$$U(x) = \exp\left(\omega(x)\hat{\mathbf{n}}\cdot\mathbf{T}\right) \equiv \exp\left(-i\,\frac{\omega}{2}\,\hat{\mathbf{n}}\cdot\boldsymbol{\tau}\right) = \cos\frac{\omega}{2} - i\,\hat{\mathbf{n}}\cdot\boldsymbol{\tau}\sin\frac{\omega}{2} \tag{4.3}$$

with some constant unit vector $\hat{\mathbf{n}}$. A small (periodic) gauge transformation is obtained when $\omega(x)$ satisfies the boundary condition

$$\omega(x+L) = \omega(x) + 4n\pi\,, \tag{4.4}$$

while a large (anti-periodic) gauge transformation follows for

$$\omega(x+L) = \omega(x) + (2n+1)2\pi\,. \tag{4.5}$$

The corresponding adjoint representations $\left((\hat{T}_a)_{bc} = \epsilon_{bac}\right)$

$$(\hat{U}(x))_{ab} = \left(\mathrm{e}^{\omega\hat{\mathbf{n}}\cdot\mathbf{T}}\right)_{ab} = \delta_{ab}\cos\omega + \hat{n}_a\hat{n}_b(1-\cos\omega) + \epsilon_{acb}\hat{n}_c\sin\omega \tag{4.6}$$

are periodic in both cases.

4.2 Gribov and fundamental modular regions

In section 3, we found that in the *pure Coulomb gauge* the Faddeev–Popov determinant has zeros at $\vartheta = \frac{|\mathbf{A}|L}{2} = n\pi$. Hence, in the 3-dimensional space of constant gauge orbits the *Gribov horizons* $\partial\Omega_n$ are given by the surfaces of spheres around the origin with radius $|\mathbf{A}| = \frac{2\pi n}{L}(\vartheta = n\pi)$, see Eq. (3.33). Note also that in the limit $L \to \infty$ the first Gribov region Ω_1 shrinks to the point $A = 0$, in agreement with the fact that $1+1$ dimensional Yang–Mills theory becomes trivial on a flat space-time manifold.

The *pure Coulomb gauge* is not a complete gauge fixing since it leaves invariance with respect to global gauge transformations, which form the zero modes of the Faddeev–Popov

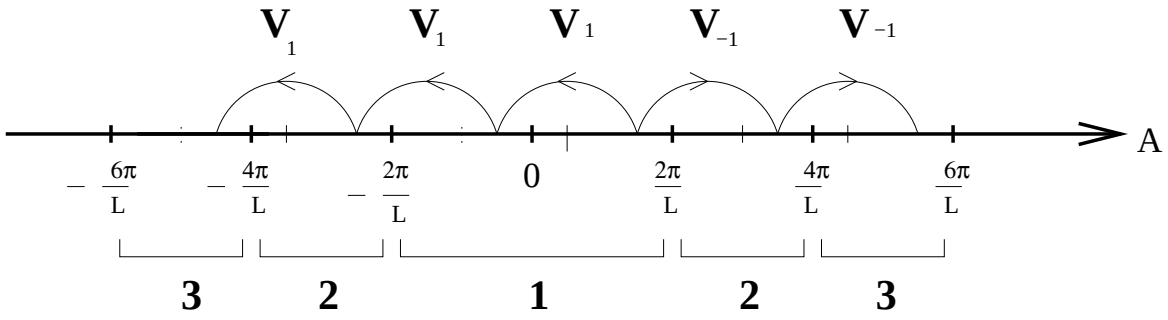

Fig. 2. Illustration of the displacements of a field configuration $\mathbf{A}$ from inside the first Gribov region to Gribov copies in the neighbouring Gribov regions by the large gauge transformations $V_{\pm 1} = (V(\hat{\mathbf{A}}))^{\pm 1}$.

kernel. However, the global gauge transformations are not the only symmetries left. In the following we will carefully examine the residual symmetries left after *pure Coulomb gauge* fixing. Due to the existence of these residual symmetries, the first Gribov region Ω_1 cannot yet be the *fundamental modular region* which, by definition, contains only a single copy of each gauge orbit. Since the *pure Coulomb gauge* is contained in the *diagonal Coulomb gauge*, the fundamental modular region is the same in both gauges, while the Gribov regions are, of course, different. The determination of the fundamental modular region is necessary in order to identify the symmetry relations (i.e. boundary conditions) to be fulfilled by the wave functionals.

Consider the large (i.e. anti-periodic) gauge transformation, cf. Eqs. (4.3) and (4.5),

$$V(\hat{\mathbf{A}}) = \exp\left(\frac{2\pi}{L} x\, \hat{\mathbf{A}} \cdot \mathbf{T}\right) \,,\; \hat{\mathbf{A}} = \frac{\mathbf{A}}{|\mathbf{A}|} \tag{4.7}$$

which shifts a constant gauge field $\mathbf{A} = |\mathbf{A}|\hat{\mathbf{n}}$ along its direction $\hat{\mathbf{n}}$ in colour space by multiples of $\frac{2\pi}{L}$,

$$\mathbf{A} \to \mathbf{A}^V = \mathbf{A} - \frac{2\pi}{L}\hat{\mathbf{A}} = \left(|\mathbf{A}| - \frac{2\pi}{L}\right)\hat{\mathbf{A}} \,. \tag{4.8}$$

Obviously, the transformed configuration A^V still satisfies the (pure or diagonal) Coulomb gauge condition if the original does.

The large gauge transformation (4.8) maps a configuration from the n^{th} Gribov region Ω_n to a configuration (on the same ray through the origin in colour space but) within Ω_{n-1}.[6] In this way, any gauge configuration in one Gribov region has a unique copy in every other Gribov region and all Gribov regions are homeomorphic to each other. Fig. 2 illustrates the shifting of a particular gauge configuration from the first Gribov region to the neighbouring ones. Furthermore, the large gauge transformation (4.8) maps a configuration of the n^{th} Gribov *horizon* $\partial\Omega_n$ to the configuration on the same ray through the origin on $\partial\Omega_{n-1}$.

[6] For a peculiarity of $n = 1$, see below.

In particular, the configurations on the first Gribov horizon $\partial\Omega_1$, where $|\mathbf{A}| = \frac{2\pi}{L}$, are mapped to the vacuum $A = 0$. This shows that all configurations of (all) Gribov horizons are equivalent under large gauge transformation to the vacuum $A = 0$. In particular, since two successive large gauge transformations form a small one, all configurations on a given Gribov horizon are related by small gauge transformations and are thus gauge copies of each other. Let us stress, however, that the configurations on the first Gribov horizon $\partial\Omega_1$ (and on all $\partial\Omega_n$ with odd n) are not equivalent to the vacuum $A = 0$ with respect to *small* gauge transformations, they are related to $A = 0$ by a non-trivial (large) gauge transformation. In the quantum theory tunnelling between these vacua will occur. This tunnelling will be entirely accounted for by solving the Schrödinger equation.

By a large gauge transformation (4.7), a configuration A inside the first Gribov region with $|\mathbf{A}| \leq \frac{\pi}{L}$ is also mapped to a copy A^V with $\frac{\pi}{L} \leq |\mathbf{A}^V| \leq \frac{2\pi}{L}$, $\hat{\mathbf{A}}^V = -\hat{\mathbf{A}}$ and vice versa. One could eliminate the large gauge transformation by restricting the modulus of the gauge field to

$$0 \leq |\mathbf{A}| < \frac{\pi}{L} \,. \tag{4.9}$$

However, Gauss' law only enforces the wave functionals to be invariant under small gauge transformations while they can transform according to an arbitrary representation of the symmetry group under large gauge transformations. For example, in the colour singlet sector under a large gauge transformation the wave functional can acquire a non-trivial phase $e^{i\alpha}$, which is well-known from the Θ-vacuum in $D = 3 + 1$. Therefore we will not remove the large gauge symmetry. [7]

The first Gribov region in the *pure Coulomb gauge*, Ω_1, is a ball B_3 around the origin with radius $|\mathbf{A}| = \frac{2\pi}{L}$, bounded by the first Gribov horizon $\partial\Omega_1$, which is the S_2. Since all configurations on this Gribov horizon are equivalent with respect to small gauge transformations, we have to identify all points of the first Gribov horizon, S_2, which compactifies the first Gribov region to S_3, which is the manifold of the $SU(2)$ group. This shows that the configuration space of Yang–Mills theory on $S^1 \times \mathbb{R}$ is the gauge group manifold itself. The mapping from the configuration space into the gauge group is provided by the (untraced) spatial Wilson loop winding around S^1. In the fundamental representation we have

$$W[A] = \mathrm{P} \exp\left(\oint_{S^1} dx A \right) = \exp(L\mathbf{A} \cdot \mathbf{T}) = \mathbb{1} \cos\vartheta + 2\hat{\mathbf{A}} \cdot \mathbf{T} \sin\vartheta \,, \tag{4.10}$$

$$\vartheta = \frac{|\mathbf{A}|L}{2} \,, \quad 0 \leq |\mathbf{A}| \leq \frac{2\pi}{L} \,.$$

[7] If one restricted the configuration space to $|\mathbf{A}| \leq \frac{\pi}{L}$, from the large gauge transformations only a residual discrete symmetry on the new Gribov horizon $|\mathbf{A}| = \frac{\pi}{L}$ would be left, which is given by the displacement transformations $V(\hat{\mathbf{A}})$ (4.7) and which relates the antipodal points $\pm\frac{\pi}{L}\hat{\mathbf{A}}$. Identifying these antipodal points, which are equivalent by the displacement transformation (4.8) the Gribov region, the ball B_3 with radius $\frac{\pi}{L}$, becomes the group manifold of $SO(3)$, which is the gauge group in the absence of fundamental charges.

The Gribov horizons $\partial\Omega_n$ with odd n (and in particular $\partial\Omega_1$) are mapped onto the non-trivial centre element

$$W\left[|\mathbf{A}| = (2n+1)\frac{2\pi}{L}\right] = -\mathbb{1}\ . \tag{4.11}$$

In higher dimensions, field configurations A, non-trivially linked to a closed loop C for which the corresponding Wilson loop $W[A](C)$ equals a non-trivial centre element, are referred to as centre vortices. In this spirit, the field configurations on the Gribov horizons $\partial\Omega_n$ with odd n represent centre vortices, in agreement with the general observation that centre vortices are on the Gribov horizon [18], due to their larger symmetry.

The first Gribov region Ω_1 of the *pure Coulomb gauge* can be restricted further by implementing the *diagonal Coulomb gauge* (2.21). In the *diagonal Coulomb gauge*, the first Gribov region is given by

$$-\pi \leq \frac{A^3 L}{2} < \pi\ , \tag{4.12}$$

see Eq. (3.23), and is obviously a subset of Ω_1. There are still gauge copies within the first Gribov region of the *diagonal Coulomb gauge*, due to the fact that there remains a residual discrete gauge symmetry, the Weyl reflection

$$A^3 \to -A^3\ . \tag{4.13}$$

Removing this symmetry by identifying configurations of opposite sign,

$$A^3 = |\mathbf{A}| = \frac{2\vartheta}{L}\ , \tag{4.14}$$

reduces the configuration space (4.12) to the *fundamental modular region*

$$A^3 \in \left[0, \frac{2\pi}{L}\right]\ , \quad \vartheta \in [0,\pi]\ . \tag{4.15}$$

This physical configuration space was already found from the gauge-invariant spatial Wilson loop, see Eq. (2.24), and reduces the configuration space to the genuinely gauge invariant degree of freedom $\vartheta = |\mathbf{A}|L/2$. The Faddeev–Popov determinant $\mathcal{J}_D(\vartheta)$, see Eq. (3.20), is gauge invariant as well, since it corresponds to the Faddeev–Popov determinant of a completely fixed gauge. Such a Faddeev–Popov determinant is gauge invariant due to the invariance of the Haar measure $\mathcal{D}\mu(U)$.

The gauge condition that immediately rotates the constant colour vector $\mathbf{A}$ of the *pure Coulomb gauge* into the positive 3-direction is accomplished by the gauge transformation $\hat{U}$ given by Eq. (A.9). In this gauge the Faddeev–Popov determinant has zeros (Gribov horizons) at $\vartheta = n\pi$, $n \in \mathbb{N}$ and the Gribov regions are given by the one-dimensional intervals

$$n\pi \leq \vartheta < (n+1)\pi\ ,\ n = 0, 1, 2, \ldots\ . \tag{4.16}$$

For such a gauge, the first Gribov region, $n = 0$, coincides with the fundamental modular region (4.15).

4.3 Boundary condition on the wave functionals

Let us now discuss the implications of the residual gauge symmetries on the wave functionals. In general, by Gauss' law the residual gauge symmetries which correspond to small gauge transformations that are not fixed by the gauge considered have to be respected by the wave functional. In the *pure Coulomb gauge* global gauge invariance is left unfixed and consequently the wave functional has to respect this symmetry, i.e.

$$\Psi(A^U) = \Psi(A)\,, \quad U = const\,. \tag{4.17}$$

Since the global gauge transformations are just rotations in colour space, the wave functionals have to be colour singlet states satisfying

$$\mathbf{L}\,\Psi(A) = 0 \tag{4.18}$$

where

$$L^a = \epsilon^{abc} A^b \frac{d}{idA^c} \tag{4.19}$$

is the "orbital" angular momentum in colour space, which is nothing but the colour spin of the gauge field. In the next section, we will obtain this constraint in the resolution of Gauss' law in the *pure Coulomb gauge* as a consequence of the zero modes of the Faddeev–Popov kernel belonging to the global gauge symmetry. Equation (4.18) implies that the wave functional is rotationally invariant,

$$\Psi(\mathbf{A}) = \Psi(|\mathbf{A}|) \tag{4.20}$$

and thus depends only on the gauge invariant modulus $|\mathbf{A}|$ of $\mathbf{A}$.

The global gauge transformations do not exhaust the set of small gauge transformations remaining unfixed in the *pure Coulomb gauge*. An even number of large gauge transformations (4.7) forms a space-dependent small one

$$V^{2n}(\hat{\mathbf{A}}) = \exp\left(2xk_n\,\hat{\mathbf{A}}\cdot\mathbf{T}\right)\,,\; k_n = \frac{2\pi n}{L}\,, \tag{4.21}$$

which shifts the gauge field by

$$\mathbf{A} \to \mathbf{A}^{V^{2n}(\hat{A})} = \left(\mathbf{A} - 2k_n\hat{\mathbf{A}}\right)\,. \tag{4.22}$$

Note that the gauge transform $A^{V^{2n}}$ still satisfies the *pure Coulomb gauge* if the original configuration A does so. Since the wave functional has to be invariant under small gauge transformations, it has to satisfy the condition

$$\Psi\left(\mathbf{A} - 2k_n\hat{\mathbf{A}}\right) = \Psi(\mathbf{A}) \tag{4.23}$$

and by Eq. (4.20)

$$\Psi\left(|2k_n - |\mathbf{A}||\right) = \Psi(|\mathbf{A}|)\,. \tag{4.24}$$

Restricting A to the first Gribov region

$$0 \leq |\mathbf{A}| < k_1 \equiv \frac{2\pi}{L}\,, \tag{4.25}$$

the above condition becomes

$$\Psi\left(\frac{4\pi}{L} - |\mathbf{A}|\right) = \Psi\left(|\mathbf{A}|\right) \tag{4.26}$$

or when expressed in terms of the dimensionless variable $\vartheta = \frac{|\mathbf{A}|L}{2}$

$$\Psi(2\pi - \vartheta) = \Psi(\vartheta)\,. \tag{4.27}$$

Under large gauge transformations $V(\hat{\mathbf{A}})$ (4.7) the wave functional needs only to be invariant up to a phase

$$\Psi\left(A^{V(\hat{\mathbf{A}})}\right) = \mathrm{e}^{i\alpha}\Psi(A) \tag{4.28}$$

and since $(V(\hat{\mathbf{A}}))^2$ is a small gauge transformation this phase has to be $e^{i\alpha} = \pm 1$. Using Eq. (4.8) and proceeding as above we find from the effect of the large gauge transformation the boundary condition

$$\Psi(\pi - \vartheta) = \pm\Psi(\vartheta)\,. \tag{4.29}$$

The two signs correspond to two superselection sectors of the theory, which are the discrete analog of the Θ-vacuum in $D = 3{+}1$. In section 6, we will find that the ground state belongs to the sector with the plus sign.

The global gauge symmetry left in the *pure Coulomb gauge* is used in the *diagonal Coulomb gauge* to diagonalise the (algebra-valued) gauge field

$$A^a = \delta^{a3}A^3\,, \quad A^3 = \pm|\mathbf{A}|\,. \tag{4.30}$$

After implementing this gauge there is still the residual $SO(2) \simeq U(1)$ global symmetry of rotations around the 3-axis. This abelian symmetry cannot be fixed since the gauge-fixed configurations (4.30) are invariant under these rotations. This implies that also the wave functional defined on the gauge-fixed manifold automatically respects this symmetry. Therefore, the residual global $U(1)$ symmetry can be left out in further considerations.

A small gauge transformation consisting of two successive displacement transformations $V(\boldsymbol{e}_3)$ (4.8) shifts A^3 to $A^3 - \frac{4\pi}{L}$. By the identification of $\pm A^3$ this configuration is equivalent to $\frac{4\pi}{L} - A^3$. Thus A^3 and $\frac{4\pi}{L} - A^3$ (or ϑ and $2\pi - \vartheta$) represent the same configuration. This residual invariance under the small gauge transformations $(V(\boldsymbol{e}_3))^2$ left by the *diagonal*

Coulomb gauge has to be respected by the wave functional, which therefore has to satisfy the boundary condition

$$\Psi(2\pi - \vartheta) = \Psi(\vartheta) \; . \tag{4.31}$$

This condition (4.31) was already obtained above in the *pure Coulomb gauge*, see Eq. (4.27). This is not surprising: Since the *diagonal Coulomb gauge* contains the *pure Coulomb gauge* the boundary conditions following from the residual gauge invariance in the *diagonal Coulomb gauge* apply also to the *pure Coulomb gauge*. In section 6 we will solve the Schrödinger equation thereby imposing the boundary conditions (4.31) in the *diagonal Coulomb gauge* and the conditions (4.18) and (4.31) in the *pure Coulomb gauge*.

5 Resolution of Gauss' law

As already discussed in section 2, in the Hamiltonian approach in Weyl gauge ($A_0 = 0$) Gauss' law (2.12) does not follow from the Heisenberg equation of motion and has to be imposed as a constraint on the wave functional. In the following, we explicitly resolve Gauss' law in both the *pure* and *diagonal Coulomb gauges*, thereby paying proper attention to the zero modes of the Faddeev–Popov kernel. We will find that the modes $n = 0, \sigma = 0, \pm 1$ are excluded from the Coulomb propagator in the *pure Coulomb gauge* (although the modes $n = 0, \sigma = \pm 1$ are not zero modes of the Coulomb kernel $\lambda_{n=0,\sigma\pm1} = \sigma A \neq 0$!). In the *diagonal Coulomb gauge* only the true zero mode $n = \sigma = 0$ is excluded from the Coulomb propagator. This is in accord with our discussion of the Faddeev–Popov method in section 3. We will first outline the general strategy of resolving Gauss' law and afterwards apply it separately to the *pure* and *diagonal Coulomb gauges*.

First note, that even in the *pure Coulomb gauge* where only constant gauge "fields" are left, the momentum operator has space-dependent components. We denote the part of the momentum operator conjugate to the modes of the gauge field left after gauge fixing by $\Pi_\perp$ and the remaining part by $\Pi_{||}(x)$,

$$\Pi(x) = \Pi_\perp + \Pi_{||}(x) \; . \tag{5.1}$$

These components are orthogonal to each other in the sense that

$$\int dx \, \Pi_\perp \Pi_{||}(x) = \int dx \, \Pi_{||}(x) \Pi_\perp = 0 \tag{5.2}$$

and we refer to them here as the "transversal" and "longitudinal" components of the momentum operator, respectively, although this notation is somewhat misleading in the case of the *diagonal Coulomb gauge* (see Appendix B). With Eq. (5.2), the Yang–Mills Hamiltonian (2.10) becomes

$$H = \frac{g^2}{2} \int dx \, \Pi^2(x) = \frac{g^2}{2} \int dx \, \left(\Pi_\perp^2 + \Pi_{||}^2(x) \right) \; . \tag{5.3}$$

As usual, we will solve Gauss' law for the longitudinal part $\Pi_{||}(x)$. Since $\partial\Pi_\perp = 0$ (in both gauges) we can rewrite Gauss' law (2.12) as

$$\hat{D}^{ab}(x)\Pi^b_{||}(x)\Psi(A) = \rho^a_{tot}(x)\Psi(A)\,, \tag{5.4}$$

where

$$\rho^a_{tot}(x) = \rho^a(x) + \rho^a_g \tag{5.5}$$

is the total colour charge, including the external charge $\rho^a(x)$ and the charge of the gauge bosons

$$\rho^a_g(x) = -\hat{A}^{ab}(x)\Pi^b_\perp\,. \tag{5.6}$$

Since Gauss' law is a constraint on the wave functional and not an operator identity, one can extract from Gauss' law only $\Pi_{||}\Psi(A)$ but cannot obtain $\Pi_{||}$ itself. For this reason, we consider the expectation value of the Hamiltonian and perform a partial integration with respect to the gauge field to obtain

$$\langle\Psi|H|\Psi\rangle = \frac{g^2}{2}\int\mathcal{D}A\int dx\,(\Pi(x)\Psi(A))^*\,\Pi(x)\Psi(A)\,. \tag{5.7}$$

Implementing here the (pure or diagonal) Coulomb gauge by the Faddeev–Popov method, splitting the momentum operator into longitudinal and transversal parts $\Pi = \Pi_{||} + \Pi_\perp$, expressing $\Pi_{||}\Psi$ by Gauss' law and performing a partial integration with respect to the gauge-fixed field, the Hamiltonian becomes

$$H = \frac{g^2}{2}\int dx\,\mathcal{J}^{-1}_{FP}\,\Pi_\perp\,\mathcal{J}_{FP}\,\Pi_\perp + H_C\,, \tag{5.8}$$

where $\mathcal{J}_{FP}$ is the Faddeev–Popov determinant and H_C is the so-called Coulomb Hamiltonian, defined by

$$\int\mathcal{D}A\,\mathcal{J}_{FP}(A)\frac{g^2}{2}\int dx\left(\Pi^a_{||}(x)\Psi(A)\right)^*\Pi^a_{||}(x)\Psi(A) =: \int\mathcal{D}A\,\mathcal{J}_{FP}(A)\Psi^*(A)H_C\Psi(A)\,. \tag{5.9}$$

Formally, from Eq. (5.4) follows

$$\Pi^a_{||}(x)\Psi(A) = \int dy\,\langle x|\left(\hat{D}^{-1}\right)^{ab}|y\rangle\,\rho^b_{tot}(y)\,\Psi(A) \tag{5.10}$$

and the Coulomb Hamiltonian becomes

$$H_C = \frac{g^2}{2}\int dxdy\,\mathcal{J}^{-1}_{FP}\,\rho^a_{tot}(x)\,F^{ab}(x,y)\,\mathcal{J}_{FP}\,\rho^b_{tot}(y)\,, \tag{5.11}$$

where

$$F^{ab}(x,y) = \langle x|(-\hat{D}^{-2})^{ab}|y\rangle = \langle x|\left[\left(-\hat{D}\partial\right)^{-1}(-\partial^2)\left(-\hat{D}\partial\right)^{-1}\right]^{ab}|y\rangle \tag{5.12}$$

is the so-called Coulomb kernel. However, the operator $\hat{D}$ has zero modes, which forbid a naive inversion. In Appendix B, we explicitly solve Eq. (5.4) for $\Pi^a_{||}(x)\Psi(A)$ and extract H_C

for both the *pure Coulomb gauge* and the *diagonal Coulomb gauge*, thereby paying proper attention to the zero modes. The upshot of these considerations is that the zero modes of the Faddeev–Popov kernel, which are a consequence of incomplete gauge fixing, give rise to additional constraints on the wave functionals. These constraints basically arise from the projection of Gauss' law onto the zero modes of the Faddeev–Popov kernel. In the *pure Coulomb gauge* these constraints read (B.31)

$$Q^a_{tot}\Psi = 0\,, \tag{5.13}$$

where

$$Q^a_{tot} = \int_0^L dx\, \rho^a_{tot}(x) = \int_0^L dx\, \Big(\rho^a(x) + \rho^a_g(x)\Big) \equiv Q^a + Q^a_g \tag{5.14}$$

is the total colour charge. In this gauge the transverse momentum operator (A.7) reads

$$\Pi^a_\perp = \frac{1}{L}\frac{d}{idA^a} \tag{5.15}$$

and the dynamical charge of the gauge bosons Q^a_g (5.6) becomes (up to a sign) the colour angular momentum operator (more precisely the colour spin) of the gauge field, L^a (4.19). The residual constraint (B.13) from Gauss' law becomes

$$L^a\Psi = Q^a\Psi\,, \tag{5.16}$$

where Q^a is the external charge. In the absence of external colour charges $Q^a = 0$ this constraint simplifies to

$$\boldsymbol{L}\Psi = 0\,, \tag{5.17}$$

i.e. the physical wave functionals do not depend on the angle degrees of freedom $\hat{\mathbf{A}}(\theta,\phi)$, which, in fact, are unphysical since they represent the residual global colour gauge degrees of freedom, which are not fixed by the *pure Coulomb gauge* condition. Thus, the physical vacuum wave functionals depend only on the "radial" coordinate $|\mathbf{A}|$ which is the physical degree of freedom of the gauge field. The constraint (5.17) was already found in the previous section, see Eq. (4.18), and reflects the invariance of the wave functional under global gauge transformations.

In the *diagonal Coulomb gauge*, where

$$A^a = \delta^{a3}A^3\,, \quad \Pi^a_\perp = \delta^{a3}\Pi^3_\perp\,, \tag{5.18}$$

the dynamical charge of the gauge bosons ρ^a_g (5.6) vanishes and the residual constraint from Gauss' law implies the vanishing of the Cartan component of the external charge in the physical state (see Eq. (B.32))

$$Q^3\Psi = 0\,. \tag{5.19}$$

In absence of external charges $Q^3 = 0$, in this gauge there is no residual constraint on the wave functional from Gauss' law.

The *diagonal Coulomb gauge* rotates the constant gauge mode in the 3-direction, i.e. $A^3 = \pm|\mathbf{A}|$ and with the restriction to the fundamental modular region (4.15), in this gauge A^3 equals the modulus of $\mathbf{A}$. Thus, in both gauges the physical wave functional depends only on the modulus of the constant gauge mode A^a, which is the only physical degree of freedom. Both gauges leave a residual *global* gauge invariance: Global $SU(2)$ symmetry in the case of the *pure Coulomb gauge* and global $U(1)$ symmetry in the case of the *diagonal Coulomb gauge*. By Noether's theorem, these global symmetries imply the existence of conserved charges: $Q_{tot}^{a=1,2,3}$ in the case of the *pure Coulomb gauge* and Q^3 in the *diagonal Coulomb gauge*. The residual constraints on the wave functionals obtained above from Gauss' law are nothing but the quantum version of Noether's theorem for these global colour symmetries. Also in $3+1$ dimensions the *pure Coulomb gauge* fixing still leaves invariance with respect to global colour gauge transformations and by Noether's theorem the total colour charge has to be conserved [35].

After resolution of Gauss' law (see Appendix B) one finds the following gauge-fixed Hamiltonian in the *pure Coulomb gauge*

$$H = -\frac{g^2}{2L}\,\frac{1}{\mathcal{J}_P}\frac{d}{dA^a}\,\mathcal{J}_P\,\frac{d}{dA^a} + H_C\,, \tag{5.20}$$

where $\mathcal{J}_P$ is defined by Eq. (3.32) and the Coulomb Hamiltonian (cf. Eq. (5.11)) is given by

$$H_C = \frac{g^2}{2}\int dxdy\,\rho^a(x)F^{ab}(x,y)\rho^b(y) \tag{5.21}$$

with Coulomb kernel

$$F^{ab}(x,y) = F^{ab}[A = A^aT_a](x,y) = \sum_{n\neq 0}\langle x|n\rangle\sum_{\sigma}\langle a|\hat{U}|\sigma\rangle\lambda_{n,\sigma}^{-2}\langle\sigma|\hat{U}^T|b\rangle\langle n|y\rangle\,, \tag{5.22}$$

from which all zero modes $n = 0$ of the Faddeev–Popov operator (3.24) are excluded, although $n = 0, \sigma = \pm 1$ are *not* zero modes of the operator $(-\hat{D}^2)$ in Eq. (5.12)! Note also that the dynamical charge ρ_g (5.6), although being here non-zero, has dropped out from the Coulomb Hamiltonian (5.21). This is a special feature of $1+1$ dimensions (see Appendix B) and is a consequence of ρ_g being space-independent in the Coulomb gauge. Similarly, the Faddeev–Popov determinant also drops out from the Coulomb Hamiltonian.

The first term in Eq. (5.20) arises from the "transversal" momentum operators $\Pi_\perp^a$ corresponding to the physical mode ($A^a = const$). This term has the form of a Laplacian in a curved space with the Faddeev–Popov determinant acting as the determinant of the metric. The second term of Eq. (5.20) arises from the "longitudinal" (here x-dependent) part $\Pi_\parallel^a(x)$ of the momentum operator. This term gives the static potential of external static colour charges, and it is considered an advantage of the *pure Coulomb gauge* that this term is explicitly isolated. Note, the Hamiltonian in the *pure Coulomb gauge* (5.20) is still invariant under global colour rotations, which are not fixed in this gauge.

Resolving Gauss' law in the *diagonal Coulomb gauge* (2.20) (which does fix the global colour rotations) yields the gauge-fixed Hamiltonian

$$H = -\frac{g^2}{2L}\frac{1}{\mathcal{J}_D}\frac{d}{dA^3}\mathcal{J}_D\frac{d}{dA^3} + H_C \,, \tag{5.23}$$

where $\mathcal{J}_D$ is defined in Eq. (3.20). Here the Coulomb Hamiltonian H_C is still given by Eq. (5.21), however, with the Coulomb kernel $F^{ab}[A](x,y)$ (5.22) replaced by

$$F^{ab}(x,y) = F^{ab}[A = |\mathbf{A}|T_3](x,y) = \sum_{n,\sigma}{}' \langle x|n\rangle\langle a|\sigma\rangle\lambda_{n,\sigma}^{-2}\langle\sigma|b\rangle\langle n|y\rangle \,, \tag{5.24}$$

where the prime indicates that the mode $n = \sigma = 0$ is excluded, which is the only zero mode of the Faddeev–Popov operator in this gauge.

Note, since the *pure Coulomb gauge* field A is related to the field in the *diagonal Coulomb gauge* by a global gauge transformation, see Eq. (3.25), one would expect that in view of Eq. (3.26), the Coulomb kernels (5.12) in these two gauges are related by

$$F^{ab}[A = UA^3T_3U^\dagger](x,y) = \hat{U}_{ac}F^{cd}[A^3T_3](x,y)\hat{U}^T_{db} \,. \tag{5.25}$$

This is almost the case (cf. Eqs. (5.22) and (5.24)) except for the additional zero modes $n = 0, \sigma = \pm 1$ to be excluded from the kernel (5.22) in the *pure Coulomb gauge*. The zero modes $n = 0, \sigma = 0, \pm 1$ are precisely given by the constant gauge transformation (3.29) $u^a_\sigma = \langle a|\hat{U}|\sigma\rangle(\langle x|n = 0\rangle = const)$ not fixed in the *pure Coulomb gauge*.

By fixing the *pure Coulomb gauge*, one switches from Cartesian to curvilinear coordinates and accordingly the gauge-fixed Hamiltonian acquires the form of the Hamiltonian in curved space [1]. The gauge-fixed Hamiltonian is, of course, no longer gauge invariant. In particular, the Hamiltonian (5.23) is not even invariant under global colour rotation since the *diagonal Coulomb gauge* (2.20) fixes also the global gauge transformations. Nevertheless, the *diagonal Coulomb gauge* still leaves invariance under global abelian gauge transformations (colour rotations around the 3-axis).

In the absence of external charges ($\rho^a(x) = 0$), the Coulomb term H_C (5.21) obviously vanishes in both gauges, however, for different reasons, see appendix B. In the *pure Coulomb gauge* it vanishes because all constant modes $n = 0, \sigma = 0, \pm 1$ are excluded from the Coulomb kernel $F^{ab}(x,y)$, while in the *diagonal Coulomb gauge* it vanishes because the physical modes live all in the Cartan algebra, resulting in a vanishing colour charge (5.6) of the gauge bosons.

6 The physical state space

The spectrum of the Yang–Mills Hamiltonian in $1+1$ dimensions can be obtained in a gauge invariant way [36]. We choose here the *diagonal Coulomb gauge*, with all unphysical degrees of freedom eliminated and the physical degree of freedom ϑ within the fundamental modular region $0 \leq \vartheta \leq \pi$, see section 4. Thus, one can regain the gauge invariant spectrum and simultaneously find the physical state space. From the vacuum wave functional $\Psi[A]$ in the *diagonal Coulomb gauge*, the one in the *pure Coulomb gauge* can be derived which will be very useful in the subsequent sections.

6.1 Diagonal Coulomb gauge

In the *diagonal Coulomb gauge* (2.20), the Yang–Mills Schrödinger equation of the $1+1$ dimensional theory

$$H\Psi_k = E_k\Psi_k \tag{6.1}$$

can be solved exactly [28]. In the absence of external colour charges the Yang–Mills Hamiltonian (5.23) reads in the compact variable $\vartheta = \frac{|\mathbf{A}|L}{2}$

$$H = -\frac{1}{2L}\left(\frac{gL}{2}\right)^2 \frac{1}{\mathcal{J}_D(\vartheta)}\,\frac{d}{d\vartheta}\,\mathcal{J}_D(\vartheta)\,\frac{d}{d\vartheta}\,. \tag{6.2}$$

To solve the Schrödinger equation, we introduce the "radial" wave functional $\phi(\vartheta)$ by

$$\Psi(\vartheta) = \frac{1}{\sqrt{\mathcal{J}_D(\vartheta)}}\,\phi(\vartheta)\,. \tag{6.3}$$

This eliminates the Faddeev–Popov determinant $\mathcal{J}_D(\vartheta) = \sin^2\vartheta$ in the scalar product

$$\langle\Psi_1|\Psi_2\rangle = \int_0^\pi d\vartheta\,\mathcal{J}_D(\vartheta)\Psi_1^*(\vartheta)\Psi_2(\vartheta) = \int_0^\pi d\vartheta\,\phi_1^*(\vartheta)\phi_2(\vartheta) \tag{6.4}$$

and reduces the Schrödinger equation (6.1) to

$$\frac{d^2\phi}{d\vartheta^2} = -k^2\phi\,, \quad k^2 = 1 + \frac{8E}{g^2L}\,. \tag{6.5}$$

The boundary condition (4.31) on the total wave functionals $\psi(\vartheta)$ requires the radial wave functional $\phi(\vartheta)$ to satisfy

$$\phi(2\pi - \vartheta) = -\phi(\vartheta)\,. \tag{6.6}$$

Thus, the solutions to Eq. (6.5) read

$$\phi_k(\vartheta) = \sqrt{\frac{2}{\pi}}\,\sin(k\vartheta)\;, \quad k \in \mathbb{N}\;. \tag{6.7}$$

These are normalised with respect to the scalar product (6.4). The corresponding energy eigenvalues are given by

$$E_k = \frac{g^2 L}{8}(k^2-1) = \frac{g^2 L}{2}\,j(j+1) = \frac{g^2 L}{8}\,l(l+2)\;. \tag{6.8}$$

Here, we have defined

$$j = \frac{k-1}{2} = 0,\,\frac{1}{2},\,1,\,\ldots \tag{6.9}$$

to identify the spectrum (6.8) as a rigid rotor in colour space where the integer and half-integer j correspond to the two superselection sectors defined by the boundary condition (4.29). Alternatively, one can use the definition

$$l = k - 1 = 2j \tag{6.10}$$

to recognise in Eq. (6.8) the energy eigenvalues of a point particle with mass $4/(g^2L)$ and angular momentum l on a unit sphere S_3 in $D = 4$, which is the group manifold of $SU(2)$. (In fact, H (6.2) is (up to the constant factor) the polar angle part of the Laplacian on S_3.) Either way, the eigenfunctions

$$\psi_j(\vartheta) = \sqrt{\frac{2}{\pi}}\,\frac{\sin((2j+1)\vartheta)}{\sin\vartheta} = \sqrt{\frac{2}{\pi}}\,\chi_j(2\vartheta) \tag{6.11}$$

are the characters of $SU(2)$ ($\hat{\mathbf{n}}$ – arbitrary unit vector)

$$\chi_j(\beta) = \sum_m \langle jm|\mathrm{e}^{i\frac{\beta}{2}\hat{\mathbf{n}}\cdot\boldsymbol{\tau}}|jm\rangle \tag{6.12}$$

and the eigenvalues (6.8) are seen to diverge in the thermodynamic limit $L \to \infty$ except for $j = 0$. Therefore, all states are frozen, except the one with $j = 0$, which has vanishing energy ($E_{k=1} = 0$) and the vacuum wave functional

$$\Psi(\vartheta) = \sqrt{\frac{2}{\pi}}\;. \tag{6.13}$$

The vacuum wave functional Ψ has no dependence on the gauge "field" $\vartheta = \frac{|\mathbf{A}|L}{2}$ and describes a stochastically distributed weight of gauge field configurations in the expectation values of the *diagonal Coulomb gauge*,

$$\langle\mathcal{O}(\vartheta)\rangle_{\text{diagonal gauge}} = \int_0^\pi d\vartheta\,\mathcal{J}_D(\vartheta)\mathcal{O}(\vartheta)|\Psi(\vartheta)|^2 = \frac{2}{\pi}\int_0^\pi d\vartheta\,\sin^2\vartheta\,\mathcal{O}(\vartheta)\;. \tag{6.14}$$

It is claimed that in $3+1$ dimensions the gauge field configurations that dominate the infrared physics are located on the common boundary of the Gribov region and the fundamental modular region [37]. In $1+1$ dimension, this is obviously not realized. The Faddeev–Popov determinant $\mathcal{J}_D = \sin^2\vartheta$ actually *suppresses* the contributions of $\vartheta = \pi$ which is the common boundary of Gribov and fundamental modular regions. This is due to the fact that in the fully gauge-fixed theory, i.e. in the *diagonal Coulomb gauge*, the configuration space is merely one-dimensional and entropy does not favour boundary contributions (although expected to do so in $D = 3+1$).

6.2 Pure Coulomb gauge

We are interested here in the vacuum wave functional in the *pure Coulomb gauge*. Although the *pure Coulomb gauge* Hamiltonian (5.20) apparently has a much more complicated structure than the Hamiltonian (6.2) in the *diagonal Coulomb gauge* both expressions are equivalent, due to gauge invariance. In the following, we will explicitly reduce the Hamiltonian in the *pure Coulomb gauge* to the *diagonal Coulomb gauge* Hamiltonian (6.2). This will provide us with the explicit form of the wave functional in the *pure Coulomb gauge*, which is needed for subsequent considerations.

In the absence of external charges, the Yang–Mills Hamiltonian (5.20) is proportional to the Laplacian Δ_C in the space of gauge orbits projected on the hyperplane defined by the *pure Coulomb gauge* condition

$$H = -\frac{g^2 L}{8}\Delta_C \;, \quad \Delta_C := \frac{1}{\mathcal{J}_P}\boldsymbol{\nabla}\cdot\mathcal{J}_P\boldsymbol{\nabla} \;, \quad \boldsymbol{\nabla} = \boldsymbol{e}_a\frac{\partial}{\partial A^a} \;. \tag{6.15}$$

Using spherical coordinates of the gauge "field", introduced already in Eq. (2.25),

$$\mathbf{A} = A\,\hat{\mathbf{A}}(\theta,\phi) \;, \quad A = |\mathbf{A}| = \sqrt{A^a A^a} \;, \tag{6.16}$$

and expressing the $\boldsymbol{\nabla}$ operators in Eq. (6.15) by the standard form

$$\boldsymbol{\nabla} = \hat{\mathbf{A}}\,\frac{d}{dA} - \frac{i}{A}\,\hat{\mathbf{A}}\times\mathbf{L} \;, \tag{6.17}$$

where $\mathbf{L}$ is the colour angular momentum operator (4.19), the Laplacian Δ_C reads

$$\begin{aligned}\Delta_C &= \left(A^2\mathcal{J}_P\right)^{-1}\frac{d}{dA}\left(A^2\mathcal{J}_P\right)\frac{d}{dA} - \frac{\mathbf{L}^2}{A^2} \\ &= \frac{1}{\mathcal{J}_D}\frac{d}{dA}\mathcal{J}_D\frac{d}{dA} - \frac{\mathbf{L}^2}{A^2} \;.\end{aligned} \tag{6.18}$$

Here, we have used the explicit forms of the Faddeev–Popov determinants $\mathcal{J}_P$ in the *pure Coulomb gauge* (3.32) and $\mathcal{J}_D$ in the *diagonal Coulomb gauge* (3.20). In the physical space

of colour singlet states where (see Eq. (5.17))

$$\mathbf{L}^2|\Psi\rangle = 0 \,, \tag{6.19}$$

the last term in Eq. (6.18) becomes irrelevant and the Hamiltonian H in Eq. (6.15) reduces precisely to the one in the *diagonal Coulomb gauge* (6.2). Its eigenfunctions in the colour singlet Hilbert space (6.19) are therefore the same as in the *diagonal Coulomb gauge*. However, in the *pure Coulomb gauge* the global gauge degrees of freedom θ, ϕ defining the orientation $\hat{\mathbf{A}}(\theta, \phi)$ of the colour vector $\mathbf{A}$ remain as coordinates, which enter the definition of the scalar product in the Hilbert space of the wave functionals,

$$\langle \Psi_1 | \Psi_2 \rangle = \frac{1}{4\pi} \int\limits_{S_2} d\Omega \int\limits_0^\pi d\vartheta \, \vartheta^2 \mathcal{J}_P(\vartheta) \Psi_1^*(\vartheta, \theta, \phi) \Psi_2(\vartheta, \theta, \phi) \,. \tag{6.20}$$

Here, $d\Omega(\theta, \phi)$ denotes the usual integration measure on S_2 and the Jacobian ϑ^2 comes from the transformation to spherical colour coordinates. Due to the factor $\frac{1}{4\pi}$ in the definition of the scalar product (6.20), the normalisation of the vacuum wave functional in the *pure Coulomb gauge* is identical to the one in the *diagonal Coulomb gauge* in Eq. (6.13),

$$\Psi(A) = \sqrt{\frac{2}{\pi}} \,. \tag{6.21}$$

The *pure Coulomb gauge* expectation values

$$\begin{aligned} \langle \mathcal{O}[A] \rangle &= \int \mathcal{D}A \, \mathcal{J}_P[A] \Psi^*[A] \mathcal{O}[A] \Psi[A] \\ &= \int\limits_0^\pi d\vartheta \, \vartheta^2 \, \mathcal{J}_P(\vartheta) \frac{1}{4\pi} \int\limits_{S_2} d\Omega \, \mathcal{O}[\vartheta, \theta, \phi] \, |\Psi|^2 \\ &= \frac{2}{\pi} \int\limits_0^\pi d\vartheta \, \sin^2 \vartheta \frac{1}{4\pi} \int\limits_{S_2} d\Omega \, \mathcal{O}[\vartheta, \theta, \phi] \end{aligned} \tag{6.22}$$

average the gauge degrees of freedom θ, ϕ. The gauge invariant variable ϑ is integrated with the same weight as in the *diagonal Coulomb gauge* expectation value (6.14). For operators $\mathcal{O}(\vartheta)$ in the *diagonal Coulomb gauge*, the expectation value (6.22) gives the same result as the one in the *diagonal Coulomb gauge* (6.14). Hence, we may use the definition (6.22) exclusively.

In subsequent sections we will use the exact wave functionals to calculate various propagators and vertices, the colour Coulomb potential and derive their Dyson–Schwinger equations.

7 Exact Propagators and Vertices

In $D = 3+1$, the study of Landau gauge Dyson–Schwinger equations (DSEs) has recently become quite popular (for a recent review, see Ref. [38] and references therein). The covariant Landau gauge is technically convenient and the structure of the DSEs is similar to the *pure Coulomb gauge*. In the *pure Coulomb gauge*, the variational approach to $D = 3+1$ Yang–Mills theory also results in a set of DSEs for the propagators and vertices [8]. In any case, a truncation of the non-linearly coupled DSEs is unavoidable. It is difficult to assess the validity of this approximation. In $1+1$ dimension, on the other hand, we can calculate the *exact* Green functions and compare them to the solution of approximated DSEs. In this section, we will use the exact vacuum state (6.21) to calculate the propagators and vertices in the *pure Coulomb gauge*. We begin with the gluon propagator. After the computation of the ghost and Coulomb propagators, the ghost-gluon vertex is calculated in the *pure Coulomb gauge*. Finally, we discuss the propagators in the *diagonal Coulomb gauge*.

7.1 Gluon propagator in pure Coulomb gauge

In $1+1$ dimensions, the *pure Coulomb gauge* fields are spatially independent. The gluon propagator is therefore a constant matrix, defined as the expectation value of two field operators,

$$D^{ab} = \langle A^a A^b \rangle \; . \tag{7.1}$$

Expressing the colour vector $A^a = \frac{2}{L}\vartheta \, \hat{\mathbf{A}}^a(\theta,\phi)$ in spherical coordinates, the *pure Coulomb gauge* expectation value (6.22) for the gluon propagator (7.1) yields

$$D^{ab} = \frac{2}{\pi}\left(\frac{2}{L}\right)^2 \int_0^\pi d\vartheta \, \vartheta^2 \sin^2\vartheta \, \frac{1}{4\pi} \int d\Omega \, \hat{\mathbf{A}}^a(\theta,\phi)\hat{\mathbf{A}}^b(\theta,\phi) \; . \tag{7.2}$$

By symmetry, the angular integration yields

$$\frac{1}{4\pi} \int d\Omega \, \hat{\mathbf{A}}^a(\theta,\phi)\hat{\mathbf{A}}^b(\theta,\phi) = \frac{1}{3}\,\delta^{ab} \tag{7.3}$$

and thus for Eq. (7.2)

$$D^{ab} = \delta^{ab}\frac{1}{L^2}\left(\frac{4}{9}\pi^2 - \frac{2}{3}\right) =: D_A\,\delta^{ab} \; , \quad D_A \approx 3.72\,\frac{1}{L^2} \; . \tag{7.4}$$

The *pure Coulomb gauge* gluon propagator has only diagonal components which all have the same value D_A. In the thermodynamic limit, $L \to \infty$, the gluon propagator is identically zero, in agreement with the fact that the theory becomes trivial for $L \to \infty$.

The ghost propagator occurs in the Dyson–Schwinger equations as a consequence of the projection on the hypersurface of Coulomb gauge (or Landau gauge). In the variational approach [8], this propagator is merely an auxiliary object to facilitate the computation of the energy density. It is defined as the expectation value of the inverse Faddeev–Popov kernel. The Faddeev–Popov kernel $\mathcal{M}$ of the *pure Coulomb gauge* is given in coordinate space by Eq. (3.24). In the momentum space, we have

$$\mathcal{M}_n^{ab} = \int_0^L dx\, \mathcal{M}^{ab}(x,y)\, \mathrm{e}^{-ik_n x} = \delta^{ab} k_n^2 - i\hat{A}^{ab} k_n =: \left(G_n^{-1}\right)^{ab} . \tag{7.5}$$

We refer to the inverse $\mathcal{M}_n^{-1}$ as the "ghost kernel" denoted by G_n. It is customary to consider the Cartesian colour components of the matrix-valued ghost propagator. Let us therefore invert $\mathcal{M}_n$ in the Cartesian basis. Using the $SU(2)$ identity

$$(\hat{A}\hat{A})^{ab} = A^a A^b - \delta^{ab}\mathbf{A}^2 , \tag{7.6}$$

one can verify that

$$G_n^{ab} = \frac{1}{k_n^2}\frac{1}{1-\frac{\mathbf{A}^2}{k_n^2}}\left(\delta^{ab} - \frac{A^a A^b}{k_n^2} + i\frac{\hat{A}^{ab}}{k_n}\right) \tag{7.7}$$

is indeed the inverse of $\mathcal{M}_n^{ab}$ (7.5). The expectation value (6.22) then defines the ghost propagator

$$\left\langle G_n^{ab}\right\rangle = \frac{d_n^{ab}}{k_n^2} \tag{7.8}$$

as well as the ghost form factor d_n^{ab}, which measures the deviation of $\langle G_n^{ab}\rangle$ from the tree-level behaviour δ^{ab}/k_n^2. The angular averages within the *pure Coulomb gauge* expectation value (7.8) can be taken with Eq. (7.3) and the identity

$$\frac{1}{4\pi}\int d\Omega\, \hat{A}^{ab} = 0 . \tag{7.9}$$

One thus finds a colour diagonal ghost form factor,

$$d_n^{ab} = \delta^{ab}\left\langle \frac{1}{1-\frac{\mathbf{A}^2}{k_n^2}}\left(1-\frac{1}{3}\frac{\mathbf{A}^2}{k_n^2}\right)\right\rangle =: \delta^{ab}\, d_n . \tag{7.10}$$

Its diagonal elements d_n can be rewritten as $\left(\frac{|\mathbf{A}|}{k_n} = \frac{\vartheta}{\pi n}\right)$

$$d_n = 1 + \frac{2}{3}\left\langle \frac{\vartheta^2}{(\pi n)^2 - \vartheta^2}\right\rangle = 1 + \frac{4}{3\pi}\int_0^\pi d\vartheta\, \sin^2\vartheta\, \frac{\vartheta^2}{(\pi n)^2-\vartheta^2} . \tag{7.11}$$

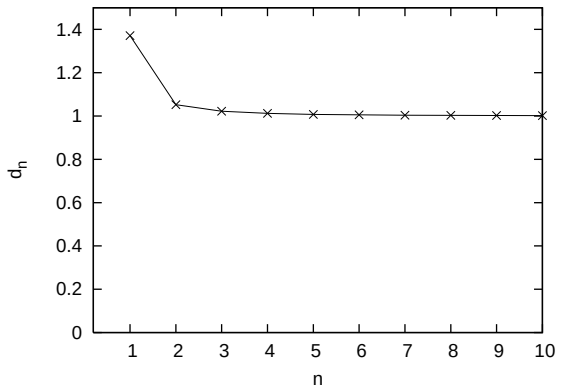

Fig. 3. The exact ghost form factor, given by Eq. (7.11).

The above integral may be expressed by integral sine functions. The allowed modes $n \in \mathbb{Z} \setminus \{0\}$ exclude the zero mode $n = 0$ of the Faddeev–Popov operator. In the ultraviolet limit, the ghost form factor (7.11) approaches tree-level,

$$\lim_{n\to\infty} d_n = 1 \ , \tag{7.12}$$

since the $D = 1+1$ theory is super-renormalisable and there are no anomalous dimensions. In the infrared, the ghost form factor is enhanced, as can be seen in Fig. 3. This enhancement is also found in $D = 3 + 1$ dimensions and is understood to come from near-zero eigenvalues of the Faddeev–Popov kernel in the vicinity of the Gribov horizon.

In the $3 + 1$ dimensional continuum theory, the inverse of the ghost form factor, d^{-1}, represents the generalised dielectric function ϵ of the Yang–Mills vacuum [39]. Fig. 3 shows that also in $D = 1 + 1$ the Yang–Mills vacuum behaves like a dia-electric medium ($\epsilon < 1$) in the infrared and becomes the ordinary vacuum ($\epsilon = 1$) in the ultraviolet.

7.3 Coulomb propagator in the pure Coulomb gauge

The *pure Coulomb gauge* Hamiltonian (5.20) comprises the so-called Coulomb term H_C, see Eq. (5.21), which accounts for the interaction energy between colour charges. By the calculation of the expectation value $\langle H_C \rangle$, the quark potential can be found, see section 8. The "Coulomb kernel" F, which mediates this interaction is defined in Eq. (5.22) and reads in momentum space

$$F_n^{ab} = G_n^{ac} k_n^2 G_n^{cb} \ . \tag{7.13}$$

Using the explicit form (7.7) of the ghost kernel G_n^{ab} and the identity (7.6), the Coulomb

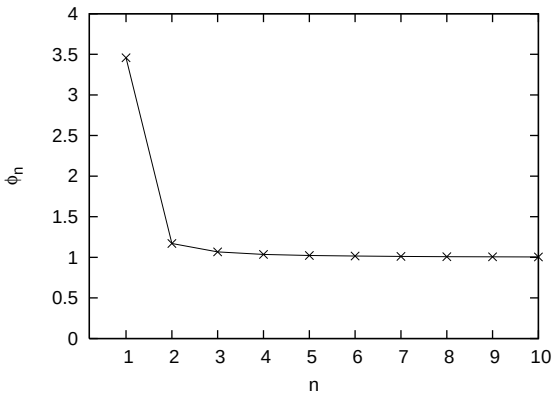

Fig. 4. Form factor ϕ_n of the Coulomb potential as given by Eq. (7.17).

kernel F_n^{ab} is cast into the form

$$F_n^{ab} = \frac{1}{k_n^2} \frac{1}{\left(1 - \frac{\mathbf{A}^2}{k_n^2}\right)^2} \left[\delta^{ab} \left(1 + \frac{\mathbf{A}^2}{k_n^2} \right) + \frac{A^a A^b}{k_n^2} \left(\frac{\mathbf{A}^2}{k_n^2} - 3 \right) + 2i \frac{\hat{A}^{ab}}{k_n} \right] . \tag{7.14}$$

The expectation value (6.22) of the operator F_n^{ab} in Eq. (7.14) defines the Coulomb propagator

$$\left\langle F_n^{ab} \right\rangle = \frac{\phi_n^{ab}}{k_n^2} \tag{7.15}$$

and the form factor ϕ_n^{ab} which measures the deviation of $\langle F_n^{ab} \rangle$ from tree-level, δ^{ab}/k_n^2 (being the abelian case). To evaluate the expectation value (7.15), let us first integrate the gauge degrees of freedom of $F_n^{ab}(A)$. Using the identities (7.3) and (7.9), one finds from F_n^{ab} in Eq. (7.14)

$$\begin{aligned} \frac{1}{4\pi} \int d\Omega \, F_n^{ab} &= \frac{\delta^{ab}}{k_n^2} \Big(1 - \Big(\frac{\vartheta}{\pi n} \Big)^2 \Big)^{-2} \left[1 + \Big(\frac{\vartheta}{\pi n} \Big)^2 + \frac{1}{3} \Big(\frac{\vartheta}{\pi n} \Big)^2 \Big(\Big(\frac{\vartheta}{\pi n} \Big)^2 - 3 \Big) \right] \\ &= \frac{\delta^{ab}}{k_n^2} \, \frac{1}{3} \left(1 + 2(\pi n)^2 \frac{(\pi n)^2 + \vartheta^2}{\left((\pi n)^2 - \vartheta^2\right)^2} \right) . \end{aligned} \tag{7.16}$$

The form factor ϕ_n^{ab} (7.15) of the Coulomb propagator is therefore strictly diagonal and its diagonal elements yield

$$\phi_n^{ab} =: \delta^{ab} \phi_n \, , \quad \phi_n = \frac{1}{3} \left(1 + 4\pi n^2 \int_0^\pi d\vartheta \, \sin^2 \vartheta \, \frac{(\pi n)^2 + \vartheta^2}{\left((\pi n)^2 - \vartheta^2\right)^2} \right) . \tag{7.17}$$

In the ultraviolet limit, the form factor ϕ_n approaches tree-level. As shown in Fig. 4, ϕ_n is infrared enhanced. In the $D = 3 + 1$ theory, the infrared enhancement of the Coulomb propagator is expected to come from the restriction of the configuration space to the Gribov

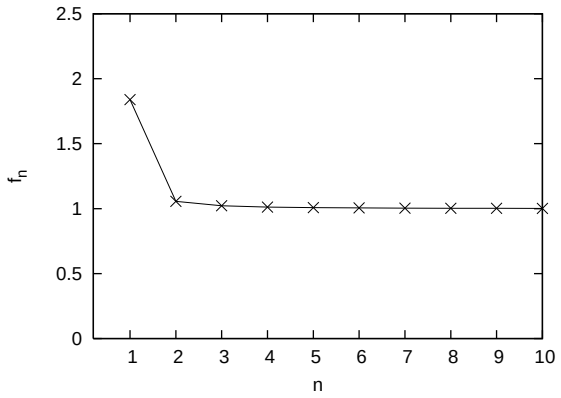

Fig. 5. Coulomb form factor f_n, as defined in Eq. (7.18).

region, as claimed by Gribov in his seminal paper [40], and to lead to a confining quark potential. This will be discussed further in section 8.

An issue in $D = 3 + 1$ dimensions is whether the expectation value of (7.13) can be factorised, i.e. can the connected part be neglected? In order to answer this question, a further form factor was introduced in Ref. [8]. It measures the deviation from the factorisation,

$$\left\langle G_n \, k_n^2 G_n \right\rangle =: \langle G_n \rangle \; k_n^2 \, f_n \; \langle G_n \rangle \;\; , \quad \Rightarrow \;\; f_n = \frac{\phi_n}{d_n^2} \; . \tag{7.18}$$

and can be expressed by the ratio of the form factor ϕ_n of the Coulomb propagator and the ghost form factor squared. Following Ref. [8], we refer to f_n as the "Coulomb form factor". In $1+1$ dimensions, where the exact solutions for d_n and ϕ_n are available, we can calculate f_n exactly. In Fig. 5, the result for f_n is depicted. It shows an infrared enhancement. A further discussion in the context of the $D = 3 + 1$ theory will follow in section 12.

7.4 Ghost-gluon vertex in pure Coulomb gauge

In the variational approach in the *pure Coulomb gauge* [8] and the Dyson–Schwinger approach in Landau gauge, the ghost-gluon vertex is of particular interest. In these approaches the proper ghost-gluon vertex is usually replaced by the bare one with the argument that this vertex is not renormalised [41]. In fact, recent lattice calculations performed in $D = 1+1$ Landau gauge provide little evidence for a dressing of this vertex [42]. However, although larger lattices are available in $D = 1 + 1$, there are significant statistical errors. The lattice results are also plagued by the existence of Gribov copies. The $1+1$ dimensional continuum theory, on the other hand, has full control of the Gribov problem, see section 4. In the following we will calculate the proper (one-particle irreducible) ghost-gluon vertex in the *pure Coulomb gauge*.

The bare ghost-gluon vertex is defined by [8]

$$\Gamma^{0,a}(x,x') = -\frac{dG^{-1}(x,x')}{dA^a} = \hat{T}^a \partial_x \delta(x,x') \,, \tag{7.19}$$

where $G^{-1} \equiv \mathcal{M}$ is the Faddeev–Popov kernel (3.24). Fourier expansion

$$\Gamma^{0,a}(x,x') = \frac{1}{L} \sum_n \mathrm{e}^{ik_n(x-x')} \Gamma^{0,a}_n \tag{7.20}$$

yields the momentum space representation

$$\Gamma^{0,a}_n = ik_n \hat{T}^a \,. \tag{7.21}$$

In the $D = 1{+}1$ Coulomb gauge the ghost-gluon vertex depends only on a single momentum for there is only the zero momentum mode of the gauge field. The proper ghost-gluon vertex Γ^a_n is defined via the expectation value for the connected ghost-gluon vertex [8]

$$\left\langle A^a G^{bc}_n \right\rangle = D^{aa'} \left\langle G^{bb'}_n \right\rangle (\Gamma^{a'}_n)^{b'c'} \left\langle G^{c'c}_n \right\rangle = D_A \frac{d_n}{k_n^2} (\Gamma^a_n)^{bc} \frac{d_n}{k_n^2} \tag{7.22}$$

which is the proper vertex with propagators attached on its legs. We have used the fact that the exact ghost and gluon propagators in the *pure Coulomb gauge* are colour diagonal. Using the explicit form (7.7) of the ghost kernel G^{ab}_n, we can write the expectation value (7.22) as

$$\left\langle A^a G^{bc}_n \right\rangle = \frac{1}{k_n^2} \left\langle \frac{1}{1 - \frac{\mathbf{A}^2}{k_n^2}} \left(A^a \delta^{bc} - A^a \frac{A^b A^c}{k_n^2} + i A^a \frac{\hat{A}^{bc}}{k_n} \right) \right\rangle \,. \tag{7.23}$$

In the *pure Coulomb gauge* expectation value (6.22), the angular integration renders the first two terms in Eq. (7.23) zero, while the last one yields

$$\begin{aligned} \left\langle A^a G^{bc}_n \right\rangle &= \frac{1}{k_n^2} \, ik_n (\hat{T}^d)^{bc} \left\langle \frac{A^a A^d}{k_n^2 - \mathbf{A}^2} \right\rangle \\ &= \frac{1}{k_n^2} \, (\Gamma^{0,d}_n)^{bc} \, \frac{1}{3} \, \delta^{ad} \left\langle \frac{\vartheta^2}{(\pi n)^2 - \vartheta^2} \right\rangle \\ &= \frac{1}{k_n^2} \, (\Gamma^{0,a}_n)^{bc} \, \frac{1}{2} \, (d_n - 1) \end{aligned} \tag{7.24}$$

where in the last line we have used the expression (7.11) for the ghost form factor d_n. It is helpful to define the form factor γ_n of the ghost-gluon vertex by

$$\Gamma^a_n =: \gamma_n \, \Gamma^{0,a}_n \,. \tag{7.25}$$

[8] For the wave functional chosen in Ref. [8], the definition (7.22) coincides with the one used there, $\left\langle G\Gamma^0 G \right\rangle =: \langle G \rangle \, \Gamma \, \langle G \rangle$.

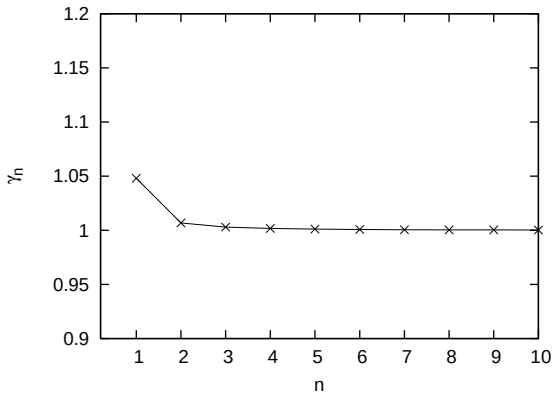

Fig. 6. Form factor γ_n of the proper ghost-gluon vertex, as given by Eq. (7.26).

This form factor can now be expressed by Eq. (7.24) using the definition (7.22) of Γ^a_n,

$$\gamma_n = \frac{k_n^2(d_n - 1)}{2\, D_A\, d_n^2} \,. \tag{7.26}$$

Let us check the ultraviolet limit, $n \to \infty$. From Eqs. (7.11), (7.2) and (7.3), one can see that

$$\lim_{n\to\infty} k_n^2(d_n - 1) = \frac{16}{3\pi L^2} \int_0^\pi d\vartheta\, \vartheta^2 \sin^2\vartheta \equiv 2D_A \tag{7.27}$$

where D_A is the gluon propagator defined in Eq. (7.4). It then follows immediately from Eqs. (7.26) and (7.12) that the ghost-gluon vertex approaches tree-level asymptotically,

$$\lim_{n\to\infty} \gamma_n = 1 \,. \tag{7.28}$$

In Fig. 6, one can see that the form factor γ_n, given by Eq. (7.26), hardly deviates from tree-level for the entire momentum range. Deviations are in the range of 5%. This strongly supports the popular approximation of truncating Dyson–Schwinger equations by choosing a tree-level ghost-gluon vertex. Further discussion will follow in section 11.

7.5 Propagators in diagonal Coulomb gauge

For a comparison to the *pure Coulomb gauge*, which does not completely eliminate the gauge degrees of freedom, we here calculate the propagators in the *diagonal Coulomb gauge* with restriction to the fundamental modular region. The gluon propagator D^{ab} in the *diagonal Coulomb gauge* is most easily found by letting $A^a \to \frac{2}{L}\vartheta\,\delta^{a3}$ before taking the expectation value (7.1). We can then express D^{aa} in the *diagonal Coulomb gauge* by the

pure Coulomb gauge result (7.4) for D_A,

$$D^{33} = \frac{2}{\pi}\left(\frac{2}{L}\right)^2 \int_0^\pi d\vartheta\, \vartheta^2 \sin^2\vartheta = 3D_A\,, \quad D^{11} = D^{22} = 0 \tag{7.29}$$

The colour trace of the gluon propagator is evidently the same in both gauges. From the observation that the *diagonal Coulomb gauge* can be reached from the *pure Coulomb gauge* by the unitary transformation (see appendix A)

$$A \to U\,A\,U^\dagger \tag{7.30}$$

of the matrix-valued variable $A = A^a T^a$, the invariance of the colour trace of the gluon propagator is seen to be an immediate consequence.

The Faddeev–Popov kernel $\mathcal{M}_n$ in the *diagonal Coulomb gauge* is substantially different from the one in the *pure Coulomb gauge*, see Eq. (3.9) (cf. Eq. (3.24)). It is convenient to expand $\mathcal{M}_n$ in the spherical basis (A.13) where $\mathcal{M}_n$ is diagonal,

$$\langle\sigma'|\mathcal{M}_n|\sigma\rangle = \Lambda_{n,\sigma}\delta_{\sigma'\sigma} =: \left(G_n^{-1}\right)^\sigma \delta_{\sigma'\sigma} \tag{7.31}$$

and the eigenvalues $\Lambda_{n,\sigma}$ are given by Eq. (3.16). We use the vacuum expectation value of the ghost kernel G_n^σ in the *diagonal Coulomb gauge* (7.31) to define the ghost form factor components d_n^σ,[9]

$$\langle G_n^\sigma\rangle =: \begin{cases} \frac{id_n^\sigma}{k_n}\,, & \sigma = \pm 1 \\ \frac{d_n^\sigma}{k_n^2}\,, & \sigma = 0 \end{cases}\,. \tag{7.32}$$

The vacuum expectation values (6.22) then yield for $n \neq 0$

$$d_n^{\sigma=\pm1} = \left\langle \frac{1}{1+\sigma\frac{\vartheta}{\pi n}} \right\rangle\,, \quad d_n^{\sigma=0} = 1\,. \tag{7.33}$$

Taking the colour trace $\sum_\sigma d_n^\sigma$ of the ghost form factor in the *diagonal Coulomb gauge* gives the same result as summing the diagonal elements d_n^{aa} of the ghost form factor in the *pure Coulomb gauge* (see Eq. (7.11)),

$$\sum_\sigma d_n^\sigma = 1 + 2\left\langle \frac{1}{1-(\frac{\vartheta}{\pi n})^2} \right\rangle = \sum_a d_n^{aa}\,. \tag{7.34}$$

[9] For the components $\sigma = \pm 1$, we related the form factor to the propagator differently from the $\sigma = 0$ component, in order for all d_n^σ to have the same dimension and complex phase. This circumstance which does not occur in the *pure Coulomb gauge* can here be traced back to the structure of the gauge condition (2.20) of the *diagonal Coulomb gauge*.

While the abelian component $\sigma = 0$ of the *diagonal Coulomb gauge* ghost form factor is at tree-level, see Eq. (7.33), the other diagonal components are larger than the *pure Coulomb gauge* result (7.11) for d_n, such that the colour trace is invariant.

The same scenario occurs for the Coulomb propagator $\langle F_n \rangle$. With the the definition (5.24) of F_n and $\lambda_{n,\sigma}$ given by Eq. (3.15), we have with $F_n|\sigma\rangle = F_n^\sigma|\sigma\rangle$

$$\langle F_n^\sigma \rangle = \left\langle \frac{1}{\lambda_{n,\sigma}^2} \right\rangle = \left\langle \frac{1}{(k_n + \sigma A^3)^2} \right\rangle = \frac{\phi_n^\sigma}{k_n^2} \tag{7.35}$$

and find for the form factor ϕ_n^σ of the Coulomb propagator for $n \neq 0$

$$\phi_n^{\sigma=\pm 1} = \left\langle \frac{1}{(1 + \sigma \frac{\vartheta}{\pi n})^2} \right\rangle \ , \quad \phi_n^{\sigma=0} = 1 \ . \tag{7.36}$$

Noting that the Coulomb kernel F_n in the *diagonal Coulomb gauge* actually follows from a rotation in colour space from the one in the *pure Coulomb gauge*, see Eq. (5.25), the invariance of the colour trace is clear.

The above results exclude the $n = 0$ modes which are the zero modes of the Faddeev–Popov operator in the *pure Coulomb gauge*. In the *diagonal Coulomb gauge*, however, the constant $n = 0$ modes with $\sigma = \pm 1$ are allowed. These give the results

$$\left\langle G_{n=0}^{\sigma=\pm 1} \right\rangle = i\sigma \frac{L}{2} \left\langle \frac{1}{\vartheta} \right\rangle \approx 0.39\, i\sigma L \tag{7.37}$$

$$\left\langle F_{n=0}^{\sigma=\pm 1} \right\rangle = \frac{L^2}{4} \left\langle \frac{1}{\vartheta^2} \right\rangle \approx 0.23\, L^2 \tag{7.38}$$

It turns out that these values are of no importance for the considerations below and are just given here for completeness.

8 The static quark potential

The gauge invariant potential energy of a quark-antiquark pair in $D = 1+1$ is well-known from the calculation of the temporal Wilson loop. A linearly rising potential emerges and the corresponding string tension σ_j shows strict Casimir scaling [43],

$$\sigma_j = \frac{g^2}{2} j(j+1) \ . \tag{8.1}$$

In the fundamental representation we have with $j = \frac{1}{2}$ the string tension

$$\sigma := \sigma_{\frac{1}{2}} = \frac{3}{8}\, g^2 \ . \tag{8.2}$$

In the Hamiltonian approach, the static colour potential can be obtained by taking the expectation value of the Hamiltonian if the charge distribution $\rho^a(x')$ is chosen to be a pair of opposite point charges of strength q^a and $-q^a$, localised at the positions x and y, respectively,

$$\rho^a(x') = q^a \left(\delta(x'-x) - \delta(x'-y)\right) \ . \tag{8.3}$$

This calculation is shown here to also give rise to a linear potential which is, however, a gauge dependent quantity. Therefore, the string tension σ_C defined by this linear potential gives only an upper bound [37,44] on the gauge invariant string tension σ in Eq. (8.2). Nevertheless, the Coulomb potential is calculated here for comparison to the potential calculated in the $D = 3+1$ theory.

8.1 Pure Coulomb gauge

We first fix only the *pure Coulomb gauge*. For the colour charge density (8.3), the Coulomb Hamiltonian (5.21) reduces to

$$H_C = \frac{g^2}{2} q^a q^b \left[F^{ab}(x,x) + F^{ab}(y,y) - F^{ab}(x,y) - F^{ab}(y,x)\right] \ , \tag{8.4}$$

with the Coulomb kernel $F^{ab}(x,y)$ (5.22) in the *pure Coulomb gauge*. The first two terms of Eq. (8.4) represent the self-energy of the static point charges. Only the charges belonging to the generators of the Cartan subalgebra can be specified and the expectation value of (8.4) in the Yang–Mills vacuum state for abelian (Cartan) unit charges defines the static quark potential. With $q^a = \delta^{a3}$ for $SU(2)$, the static quark potential $V_C(r)$ with $r = |x-y|$ becomes

$$V_C(r) = \langle H_C \rangle|_{q^a=\delta^{a3}} = g^2 \left\langle F^{33}(x,x) - F^{33}(x,y) \right\rangle \tag{8.5}$$

To obtain the above expectation value, we first take the angular average of the momentum space Coulomb kernel F_n^{ab}, see Eq. (7.16),

$$\begin{aligned}
&\frac{1}{4\pi} \int\limits_{S_2} d\Omega \, \Big(F^{33}(x,x) - F^{33}(x,y)\Big) \\
&\qquad = \frac{1}{L} \sum_{n\neq 0} \frac{1}{4\pi} \int\limits_{S_2} d\Omega \, F_n^{33} \, \Big(1 - \mathrm{e}^{-ik_n r}\Big) \\
&\qquad = \frac{2}{L} \sum_{n=1}^{\infty} \frac{1}{3} \left(\frac{L}{2\pi n}\right)^2 \left(1 + 2(\pi n)^2 \frac{(\pi n)^2 + \vartheta^2}{\left((\pi n)^2 - \vartheta^2\right)^2}\right) \Big(1 - \cos\Big(\tfrac{2\pi r}{L}\, n\Big)\Big) \ .
\end{aligned} \tag{8.6}$$

With $1-\cos(2\alpha) = 2\sin^2(\alpha)$, the Fourier transformation yields

$$\begin{aligned}
&\frac{1}{4\pi}\int\limits_{S_2} d\Omega\, \Big(F^{33}(x,x) - F^{33}(x,y)\Big) \\
&\qquad = \frac{1}{3}\,\frac{L}{\pi^2}\sum_{n=1}^{\infty}\left(\frac{1}{n^2} + 2\,\frac{\partial}{\partial\vartheta}\,\frac{\vartheta}{n^2-(\vartheta/\pi)^2}\right)\sin^2\left(\tfrac{\pi r}{L}\,n\right) \\
&\qquad = \frac{1}{3}\,\left(\frac{1}{2}r - \frac{1}{2}\frac{r^2}{L} + \frac{1}{2\sin^2\vartheta}\Big(L - r\cos\Big(2\,\tfrac{L-r}{L}\,\vartheta\Big) - (L-r)\cos\Big(2\,\tfrac{r}{L}\,\vartheta\Big)\Big)\right) \qquad (8.7)
\end{aligned}$$

Here, we have used the formulae in Ref. [45] to obtain for the above sums

$$\sum_{n=1}^{\infty}\frac{\sin^2\left(\frac{\pi r}{L}\,n\right)}{n^2-(\vartheta/\pi)^2} = \frac{\pi^2}{2}\,\frac{\sin(\frac{L-r}{L}\vartheta)\,\sin(\frac{r}{L}\vartheta)}{\vartheta\,\sin\vartheta} \;\stackrel{\vartheta\to 0}{\longrightarrow}\; \frac{\pi^2}{2}\,\left(\frac{r}{L} - \Big(\frac{r}{L}\Big)^2\right)\,. \qquad (8.8)$$

The (elementary) ϑ-integration of the expression (8.7) as defined in the expectation value (6.22) yields the static quark potential (8.5)

$$V_C(r) = \frac{g^2}{3}\,\left(L + \frac{1}{2}r - \frac{r^2}{2L} + L\,\frac{2r-L}{L-r}\,\frac{\sin(2\pi\frac{r}{L})}{2\pi\frac{r}{L}}\right) = \frac{g^2}{2}\,r\,\left(1 + \mathcal{O}\Big(\frac{r}{L}\Big)\right)\,. \qquad (8.9)$$

In the thermodynamic limit, the string tension σ_C is defined by

$$\lim_{L\to\infty} V_C(r) = \sigma_C\, r\,, \quad \Rightarrow\; \sigma_C = \frac{g^2}{2} > \sigma \qquad (8.10)$$

and is found to be larger than the gauge invariant string tension σ (8.2), as expected.

8.2 Diagonal Coulomb gauge

Let us now apply the global gauge transformation from the pure to the diagonal Coulomb gauge and recalculate the string tension of the potential. The 33-component of the Coulomb kernel F_n^{ab} can be found by setting $A^a = \frac{2}{L}\vartheta\,\delta^{a3}$ in Eq. (7.14),

$$F_n^{33} = \frac{1}{k_n^2}\,. \qquad (8.11)$$

It apparently mediates only the tree-level (abelian) part of the Coulomb interaction. Since F_n^{33} is thus field independent, the vacuum expectation value needs not to be taken and we

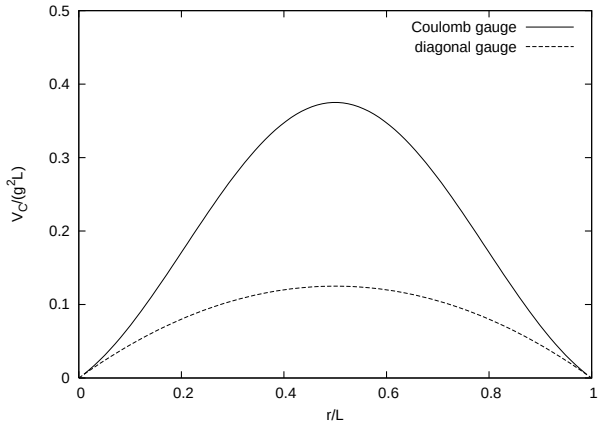

Fig. 7. Coulomb potential $V_C(r)$ for the *pure* and the *diagonal Coulomb gauge*.

directly arrive at the Coulomb potential (8.5) by Fourier transformation,[10]

$$V_C(r) = g^2 \frac{1}{L} \sum_{n\neq 0} F_n^{33} \left(1 - \mathrm{e}^{-ik_n r}\right) = g^2 \frac{L}{\pi^2} \sum_{n=1}^{\infty} \frac{\sin^2\left(\frac{\pi r}{L}\, n\right)}{n^2}$$
$$= \frac{g^2}{2}\left(r - \frac{r^2}{L}\right) = \frac{g^2}{2}\, r\, \left(1 + \mathcal{O}\Big(\frac{r}{L}\Big)\right) . \tag{8.12}$$

The string tension of the *diagonal Coulomb gauge* is obviously identical to the one in the *pure Coulomb gauge*, see Eq. (8.10). It can actually be seen by taking the limit $L \to \infty$ in the *pure Coulomb gauge* expression (8.7) that there Coulomb kernel also turns out field independent (i.e. ϑ independent) and coincides with the Fourier transform of the *diagonal Coulomb gauge* kernel (8.11).

The potential $V_C(r)$ is shown in Fig. 7 for the result in the *pure Coulomb gauge* (8.9) and in the *diagonal Coulomb gauge* (8.12). It is clear that in either gauge the function $V_C(r)$ must be symmetric about the axis $r = \frac{L}{2}$, since a separation of charges by r is identified with a separation by $L - r$ on the spatial manifold S^1. For $\frac{r}{L} \ll 1$, the potentials $V_C(r)$ are seen in Fig. 7 to have the same slope in both gauges, i.e. the string tensions have the same value σ_C given by Eq. (8.10).

[10] Strictly speaking, the sum of momentum modes n must be changed to $\sum_n{}'$ which excludes the zero mode $n = \sigma = 0$ of the Faddeev–Popov operator in the *diagonal Coulomb gauge*, but includes the modes $n = 0$ and $\sigma = \pm 1$, see section 3. The result for these zero modes is given in Eq. (7.38). However, in the subtraction of eigenenergies in the potential $V_C(r)$, see Eq. (8.5), all modes with $n = 0$ cancel and it makes no difference whether $\sum_{n\neq 0}$ or $\sum_n{}'$ is used.

9 Dyson–Schwinger equations

In this paper, it is intended to test the approximations made in the study of Dyson–Schwinger equations (DSEs) in higher dimensions by considering the $D = 1 + 1$ case. The exact DSEs for the ghost and gluon propagators are usually derived from the partition function of Yang–Mills theory. In the present case, we can simply use the definition (6.22) of vacuum expectation values to come by this set of equations. We restrict ourselves to the exact ground state of the *pure Coulomb gauge*, leaving aside the global rotation to the *diagonal Coulomb gauge*. It will be shown how Gribov copies affect the Dyson–Schwinger equations and their solution.

Let us start with the derivation of the DSE for the gluon propagator. It follows directly from the expectation value (6.22) that ($\Psi(A) = const$)

$$0 = \int\limits_{\Omega_1} \mathcal{D}A \, \frac{\delta}{\delta A^a} \mathcal{J}_P(A) \, |\Psi(A)|^2 \, \mathrm{e}^{j^c A^c} = \left\langle \left(\frac{\delta \ln \mathcal{J}_P}{\delta A^a} + j^a \right) \mathrm{e}^{j^c A^c} \right\rangle \tag{9.1}$$

holds, since the integral of the total derivative in Eq. (9.1) is proportional to the Faddeev–Popov determinant $\mathcal{J}_P$ evaluated at the first Gribov horizon $\partial\Omega_1$, where it vanishes. Applying a derivative $\delta/\delta j^b$ and setting the sources j^c to zero gives

$$0 = \left\langle A^b \, \frac{\delta \ln \mathcal{J}_P}{\delta A^a} + \delta^{ab} \right\rangle = - \left\langle A^b \, \mathrm{Tr}\, G \, \Gamma^{0,a} \right\rangle + \delta^{ab} \, . \tag{9.2}$$

The trace "Tr" in Eq. (9.2) sums up the diagonal elements in colour space as well as all modes k_n with $n = \pm 1, \pm 2 \ldots$, excluding the zero mode $n = 0$ of the Faddeev–Popov determinant

$$\mathcal{J}_P = \exp \mathrm{Tr} \ln G^{-1} \tag{9.3}$$

in the *pure Coulomb gauge*. We recognise in Eq. (9.2) the connected ghost-gluon vertex $\langle A^b G \rangle$. With its decomposition (7.22) into the proper vertex Γ^a_n and the attached propagators in momentum space, Eq. (9.2) can be written after contracting with δ^{ab} as

$$D_A^{-1} = \sum_{n \neq 0} \left(\frac{\mathrm{tr}\, \Gamma^{0,a}_n \Gamma^a_n}{(N_c^2 - 1) k_n^2} \right) \frac{d_n^2}{k_n^2} \tag{9.4}$$

This Dyson–Schwinger equation holds for any $SU(N_c)$ but we eventually set $N_c = 2$ for comparison with the exact $SU(2)$ results in chapter 7. Using the definition (7.25) of the form factor γ_n for the ghost-gluon vertex and $\mathrm{tr}\, \hat{T}^a \hat{T}^a = -N_c(N_c^2 - 1)$, the DSE for the gluon propagator (9.4) can be written more concisely,

$$D_A^{-1} = N_c \sum_{n \neq 0} \gamma_n \, \frac{d_n^2}{k_n^2} \, . \tag{9.5}$$

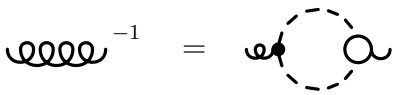

Fig. 8. DSE for the gluon propagator. Curly lines represent the gluon propagator, dashed lines the ghost propagator. The empty blob represents a proper ghost-gluon vertex, the dot a tree-level ghost-gluon vertex.

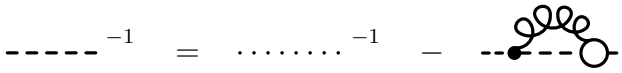

Fig. 9. DSE for the ghost propagator. The dotted line is the tree-level propagator.

Diagrammatically, the inverse gluon propagator is given by a ghost loop as shown in Fig. 8.[11] Inserting into the right-hand side of Eq. (9.5) the exact expressions for the ghost form factor d_n (7.11) and the ghost-gluon vertex γ_n (7.26), one can explicitly show that the ghost loop (r.h.s. of Eq. (9.5)) equals the expression for D_A^{-1} obtained in Eq. (7.4). In Ref. [8], the ghost loop is referred to as the "curvature" since it incorporates the curvature of the space of gauge-fixed variables. It is found that the curvature governs the infrared behaviour of the gluon propagator such that the exact DSE of $1+1$ dimensions in Fig. 8 is the infrared limit of the corresponding DSE in $3+1$ dimensions.

The DSE for the ghost propagator can be derived from the following operator identity [12] for the ghost kernel G:

$$G_n^{ab} = k_n^{-2}\delta^{ab} + k_n^{-2}(\Gamma_n^{0,d})^{ac}A^d G_n^{cb} \tag{9.6}$$

which follows from definition (7.5) and Eq. (7.21). Taking the expectation value of Eq. (9.6), we find with the decomposition (7.22) of the connected ghost-gluon vertex

$$d_n\delta^{ab} = \delta^{ab} + (\Gamma_n^{0,d})^{ac}D_A\frac{d_n}{k_n^2}(\Gamma_n^d)^{cb}\frac{d_n}{k_n^2}\,. \tag{9.7}$$

After contraction with δ^{ab} and using the definition (7.25) for the form factor γ_n of the ghost-gluon vertex, Eq. (9.7) turns into

$$d_n = 1 + \left(\frac{\mathrm{tr}\,\Gamma_n^{0,a}\Gamma_n^a}{(N_c^2-1)k_n^2}\right)D_A\frac{d_n^2}{k_n^2} = 1 + N_c\gamma_n D_A\frac{d_n^2}{k_n^2} \tag{9.8}$$

In Fig. 9, the ghost Dyson–Schwinger equation (9.8) is depicted. It is equivalent to the exact ghost DSE in $3+1$ dimensions. This is due to the fact that Eq. (9.8) follows from the

[11] Since in $D = 1+1$ *pure Coulomb gauge* the gauge field is constant, the convolution integral of the loop breaks down into a simple product in momentum space, see Eq. (9.5).
[12] Alternatively, one can introduce ghost fields and proceed similarly as for the gluon propagator.

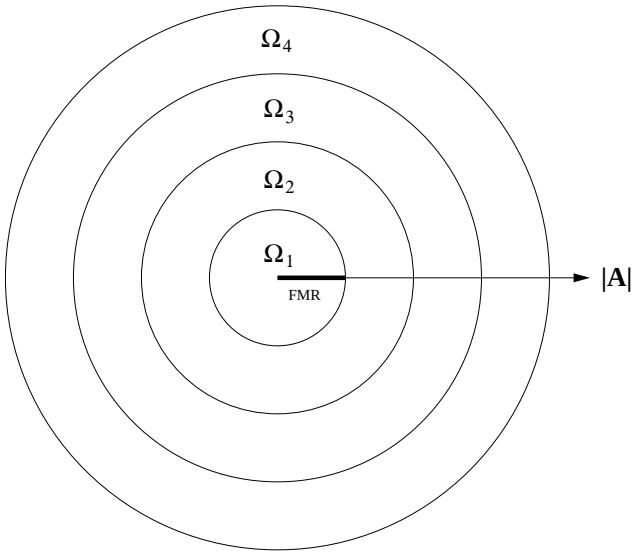

Fig. 10. Gribov regions of the *pure Coulomb gauge*, sketched as spherical shells defined by the magnitude of $|\mathbf{A}| = k_1, k_2, k_3, k_4, \ldots$. The location of the fundamental modular region (FMR) is indicated by a fat line.

operator identity (9.6) and not from the details of the wave functional.[13] The ghost DSE (9.8) can be solved for γ_n which confirms the relation (7.26) found in section 7 for $N_c = 2$.

In the derivation of the DSEs (9.5) and (9.8) the integrated configuration space was set to be the first Gribov region Ω_1 of the *pure Coulomb gauge*, given by $|\mathbf{A}| < \frac{2\pi}{L} \equiv k_1$ (see section 4). We now point at an important property of the Dyson–Schwinger equations. If the configuration space, here being the first Gribov regions Ω_1, is replaced by the union of the first two Gribov regions, $\Omega_1 \cup \Omega_2$, the DSEs (9.5) and (9.8) do not change. This is most readily seen for the ghost DSE (9.8) which follows from the operator identity (9.6) and therefore is not affected by the choice of the configuration space. The gluon DSE (9.5) is derived from the path integral identity (9.1) which makes use of the fact that the Faddeev–Popov determinant $\mathcal{J}_P$ vanishes at the first Gribov horizon $\partial\Omega_1$. Changing the configuration space to $\Omega_1 \cup \Omega_2$, the path integral identity (9.1) still holds true since by definition, the Gribov horizon is where the Faddeev–Popov determinant vanishes,

$$\mathcal{J}_P[A \in \partial\Omega_n] = 0 \quad \forall n \; . \tag{9.9}$$

We are therefore led in $\Omega_1 \cup \Omega_2$ to the same gluon DSE as in Eq. (9.5). More generally speaking: Regardless of the configuration space, so long as it is a union of Gribov regions, $\bigcup_n \Omega_n$, the Dyson–Schwinger equations stay form invariant. This form invariance also applies to the DSEs in $3+1$ dimensions.

In Fig. 10, the various Gribov regions Ω_n of the *pure Coulomb gauge* are sketched. For

[13] On the other hand, the gluon DSE as it stands in (9.4) is only true for the actual constant wave functional.

definiteness, we put to our disposal the union

$$\Gamma_{N_G} := \Omega_1 \cup \Omega_2 \cup \ldots \Omega_{N_G} \,, \quad N_G \in \mathbb{N} \tag{9.10}$$

of N_G Gribov regions. By the choice of N_G the configuration space is restricted to $|\mathbf{A}| < \frac{2\pi}{L} N_G \equiv k_{N_G}$. Despite the form invariance of the DSEs with respect to Γ_{N_G}, their solution cannot be expected to be the same for all N_G. As a matter of fact, the gluon and ghost propagators strongly depend on N_G, as shown in the upcoming section. Thus, the set of DSEs does not have a unique solution, but for every N_G there exists (at least) one separate solution. The information on the configuration space (9.10) is missing in the set of DSEs and must be provided by subsidiary conditions, i.e. put in by hand. In this sense, the DSEs alone do not provide the full non-abelian quantum gauge theory. In the $D = 3 + 1$ dimensional case, some approximation is used to solve the DSEs. Having obtained an approximative solution, there is no means of deciding on the value of N_G, i.e. whether this solution approximates the exact solution in the first Gribov region $\Gamma_1 \equiv \Omega_1$, or rather in Γ_2, or any other Γ_{N_G}, remains unknown. The effect of truncating the set of DSEs in $D = 1+1$ will be studied in section 11.

10 Many Gribov copies

In this section, the configuration space is extended from the first Gribov region to a union Γ_{N_G} (9.10) of several Gribov regions, thus including many Gribov copies. Using the exact constant wave functional, the propagators, vertices and the colour Coulomb potential are calculated in Γ_{N_G}. Moreover, we extend the configuration space to $N_G = \infty$, damping large N_G contributions with a Gaussian wave functional. This will illustrate the effect of insufficient gauge fixing on the infrared features of the theory.

10.1 Exact Green functions

The calculation of the Green functions in the extended configuration space Γ_{N_G}, defined in Eq. (9.10), is identical to the one in section 7 with the exception that the constant wave functional (6.21) needs to be normalised differently. This can be accounted for by letting

$$\int_0^{\pi} d\vartheta \ \ldots \quad \to \frac{1}{N_G} \int_0^{\pi N_G} d\vartheta \ \ldots \tag{10.1}$$

in the expectation values (6.22).

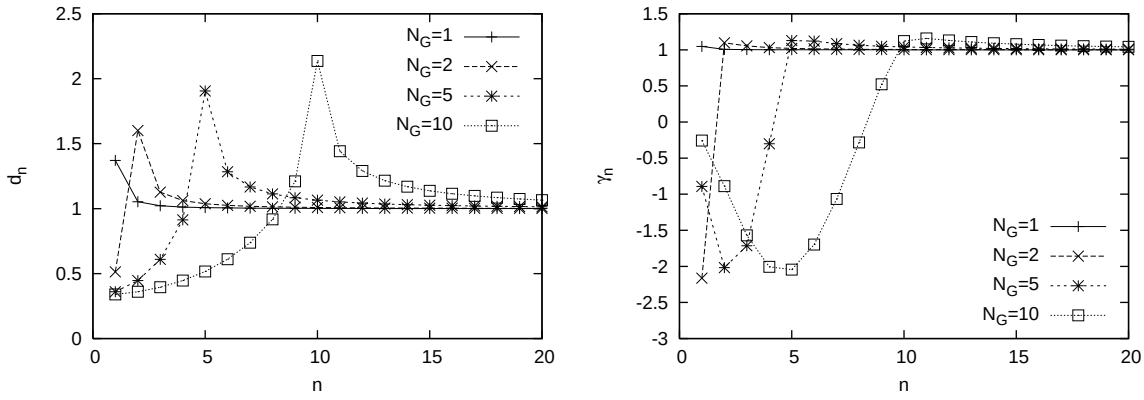

Fig. 11. *Left:* Exact ghost form factor, including N_G Gribov regions. *Right:* The form factor γ_n of the ghost-gluon vertex for various choices of N_G.

For the gluon propagator in the *pure Coulomb gauge* we thus find from Eq. (7.2)

$$D_A(N_G) = \frac{1}{L^2}\left(\frac{4}{9}N_G^2\pi^2 - \frac{2}{3}\right) \tag{10.2}$$

and it reduces to the result (7.4) for $N_G = 1$. Note that there is a strong dependence on the parameter N_G, i.e. a strong Gribov copy effect.

The result for the ghost form factor d_n in the *pure Coulomb gauge* follows from making the replacement (10.1) in the expectation value (7.11),

$$d_n(N_G) = 1 + \frac{4}{3\pi}\frac{1}{N_G}\int_0^{\pi N_G} d\vartheta\, \frac{\vartheta^2 \sin^2\vartheta}{(n\pi)^2 - \vartheta^2}\ . \tag{10.3}$$

Obviously, the ghost form factor still approaches tree-level for the ultraviolet limit $n \to \infty$. There are, however, substantial changes in the infrared. The result (10.3) for the exact ghost form factor d_n can be seen in Fig. 11. In the first Gribov region, $N_G = 1$, the ghost form factor shows an infrared enhancement, as already shown in section 7. Including further gauge copies makes d_n peak for intermediate momenta. This peak resembling a resonance appears at $n = N_G$ where the momentum k_n equals the radius of the configurations space. [14] For $n < N_G$, the ghost form factor drops below tree-level, due to negative eigenvalues of the Faddeev–Popov operator. In the limit $N_G \to \infty$, the lowest momentum mode $d_{n=1}$ approaches a definite value,

$$\lim_{N_G\to\infty} d_1(N_G) = \frac{1}{3}\ . \tag{10.4}$$

It is interesting to note that the deviation of the ghost form factor d_n from tree-level, when

[14] In the thermodynamic limit, $L \to \infty$, the peak of the ghost form factor in the first Gribov region is asymptotically at $k = 0$. This corresponds to the "horizon condition" in $D = 3 + 1$ dimensions.

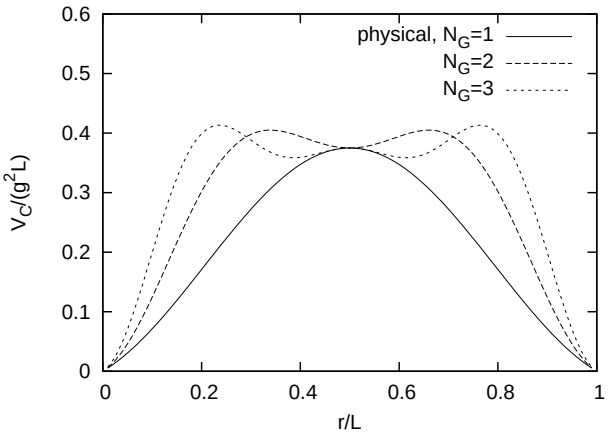

Fig. 12. Coulomb potential $V_C(r)$.

summed over all modes, gives a constant independent of N_G,

$$\sum_{n\neq 0}(d_n-1)=\frac{4}{3\pi}\frac{1}{N_G}\int\limits_0^{\pi N_G}d\vartheta\,\sum_{n\neq 0}\frac{\vartheta^2\sin^2\vartheta}{(n\pi)^2-\vartheta^2}=\frac{4}{3\pi}\frac{1}{N_G}\int\limits_0^{\pi N_G}d\vartheta\,\sin\vartheta(\sin\vartheta-\vartheta\cos\vartheta)=1\;. \tag{10.5}$$

This is illustrated in Fig. 11 and can be understood as being a consequence of the gluon propagator DSE. Solving the ghost DSE (9.8) for the ghost-gluon vertex γ_n,

$$\gamma_n=\frac{k_n^2\,(d_n-1)}{N_c\,D_A\,d_n^2}\;, \tag{10.6}$$

and plugging it into the gluon DSE (9.5) directly leads to Eq. (10.5).

Relation (10.6) holds for any $SU(N_c)$ gauge group and, more importantly, for any choice Γ_{N_G} of the configuration space. Having calculated the gluon propagator D_A and the ghost form factor d_n as functions of N_G, Eq. (10.6) gives the solution for the form factor γ_n of the ghost-gluon vertex. The result is shown in Fig. 11. While within the first Gribov region, $N_G=1$, there is hardly any deviation from tree-level, this deviation is quite pronounced for $N_G>1$. Let us note here that an approximation of the proper ghost-gluon vertex by the tree-level vertex is good if and only if the configuration space is restricted to the first Gribov region Ω_1. Working with this approximation in solving the Dyson–Schwinger equations has an important effect on the propagators. This will be discussed in the next section.

The form factor ϕ_n for the Coulomb propagator with the result (7.17) for $N_G=1$ is found for general N_G by making the replacement (10.1) in Eq. (7.17). By Fourier transformation, the Coulomb potential $V_C(N_G,r)$ for external charges separated by r can be obtained in

the same manner as presented for $N_G = 1$ in section 8. The result is

$$V_C(N_G, r) = \frac{g^2}{3}\left(\frac{1}{2}r - \frac{r^2}{2L} + L - L\,\frac{L-2r}{L-r}\,\frac{\sin\left(2\pi N_G \frac{r}{L}\right)}{2\pi N_G \frac{r}{L}}\right) \tag{10.7}$$

$$\stackrel{L\to\infty}{\longrightarrow} \quad \frac{g^2}{2}\,r \quad \forall N_G \tag{10.8}$$

and can be seen in Fig. 12. While the string tension remains the same for all values of N_G (cf. Eqs. (8.9) and (10.8)), visible effects occur for large ratios $\frac{r}{L}$. For $N_G > 1$, there are locally stable minima of the potential near $r = \frac{L}{2}$, an unphysical gauge copy effect.

10.2 Insufficient gauge fixing

If lattice calculations use a gauge fixing, the common technique is to minimise a suitable functional along the gauge orbit. The restriction to the fundamental modular region is achieved only at the absolute minimum of this functional. If this absolute minimum cannot be reached exactly, extra gauge copies will alter the result. In order to mimic the situation that the influence of gauge copies cannot be strictly excluded but only suppressed, we choose here a Gaussian damping of the gauge field configurations,

$$\psi[A] = \mathcal{N}\sqrt{\frac{2}{\pi}}\,\exp\left(-\frac{\vartheta^2}{4\alpha^2}\right)\,, \quad \mathcal{N}^2 = \tfrac{\sqrt{2\pi}}{\alpha}\left(1+\coth(\alpha^2)\right)\,, \tag{10.9}$$

extending the configuration space, see Eq. (9.10), to Γ_∞. Expectation values in the state (10.9) are most readily obtained by replacing

$$\int_0^\pi d\vartheta\ \ldots \quad \to\ \mathcal{N}^2 \int_0^\infty d\vartheta\, \mathrm{e}^{-\frac{\vartheta^2}{2\alpha^2}}\ \ldots \tag{10.10}$$

in the corresponding integrals. By adjustment of the (free) parameter $\alpha \in \mathbb{R}$, it can be controlled how many Gribov copies have a considerable weight in an expectation value. A large value α will take along many Gribov copies while a small value localises the weight of field configurations around $A = 0$, suppressing Gribov copies.

Let us calculate the constant gluon propagator D_A (7.1) in the Gaussian wave functional (10.9) as a function of α. Using the replacement (10.10) in the expectation value (7.2) gives

$$D_A(\alpha) = \frac{2}{3\pi}\mathcal{N}^2\left(\frac{2}{L}\right)^2 \int_0^\infty d\vartheta\, \sin^2\vartheta\,\vartheta^2\,\mathrm{e}^{-\vartheta^2/2\alpha^2} = \frac{1}{L^2}\,\frac{4}{3}\left(\alpha^2 + \frac{4\alpha^4}{\mathrm{e}^{2\alpha^2}-1}\right)\,. \tag{10.11}$$

Obviously, the larger the width α of the Gaussian (10.9), the larger $D_A(\alpha)$. This agrees with

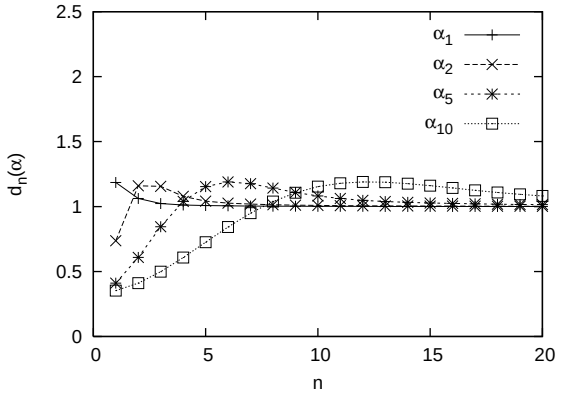

Fig. 13. Ghost form factor $d_n(\alpha)$ in the Gaussian wave functional (10.9) with those choices $\alpha_1, \alpha_2, \alpha_5, \alpha_{10}$ that yield the gluon propagator in the exact vacuum state with $N_G = 1, 2, 5, 10$.

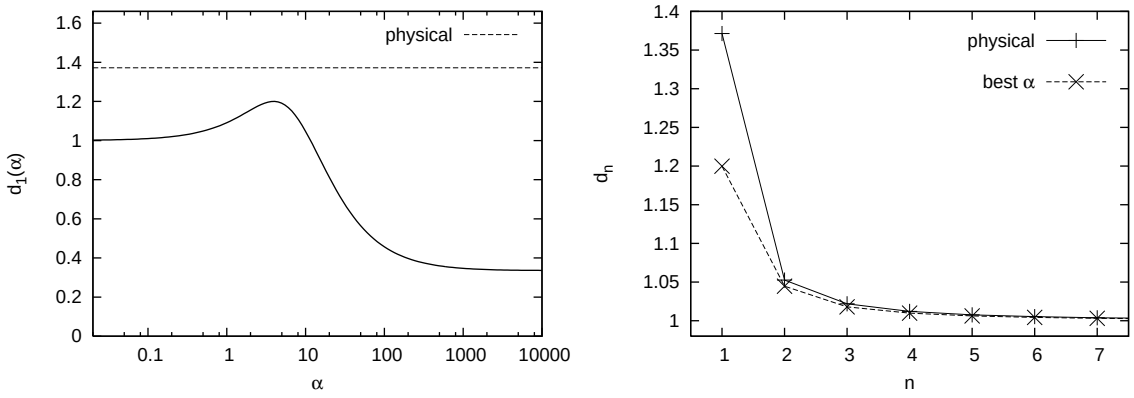

Fig. 14. *Left:* The infrared enhancement, $d_1(\alpha)$, is smaller than the physical value, $d_1 \approx 1.37$ for all values of α. *Right:* The ghost form factor in the state (10.9) for the value $\alpha \approx 1.40$ that gives the strongest infrared enhancement, compared to the exact physical result.

the result (10.2) of the exact wave functional where $D_A(N_G)$ rises quadratically with the number N_G of Gribov copies. One can now adjust α in Eq. (10.11) such that it equals the result (10.2) for the exact vacuum state, given a specific N_G. For the values $N_G = 1, 2, 5, 10$, respectively, the corresponding values for α are

$$\alpha_1 \approx 1.63 \,, \quad \alpha_2 \approx 3.56 \,, \quad \alpha_5 \approx 9.04 \,, \quad \alpha_{10} \approx 18.1 \,. \tag{10.12}$$

This procedure simulates the inclusion of N_G Gribov regions in the expectation values by a choice of the Gaussian wave functional (10.9).

We now proceed to calculate the ghost form factor $d_n(\alpha)$ in the state (10.9). The replacement (10.10) in the integral (7.11) yields

$$d_n(\alpha) = 1 + \frac{4}{3\pi}\mathcal{N}^2 \int\limits_0^\infty d\vartheta \, \sin^2\vartheta \frac{\vartheta^2}{(\pi n)^2 - \vartheta^2} \, \mathrm{e}^{-\vartheta^2/2\alpha^2} \,. \tag{10.13}$$

The limits of $\alpha \to 0$ and $\alpha \to \infty$ produce results that can be anticipated. As $\alpha \to 0$, the Gaussian picks out the point $A = 0$ from configuration space. Hence the tree-level behaviour of the ghost form factor appears:

$$\lim_{\alpha\to 0} d_n(\alpha) = 1 \,, \quad \forall n \,. \tag{10.14}$$

The other extreme, $\alpha \to \infty$, takes infinitely many Gribov copies into account and therefore must resemble the case $N_G \to \infty$ for the exact vacuum state. Indeed, for $d_1(\alpha)$, we find

$$\lim_{\alpha\to\infty} d_1(\alpha) = \frac{1}{3} \,, \tag{10.15}$$

in agreement with Eq. (10.4).

In Fig. 13, the result (10.13) for $d_n(\alpha)$ is shown for the four values of α in Eq. (10.12) which yield the exact gluon propagator for $N_G = 1, 2, 5, 10$. This should be compared to the ghost propagator in the exact wave functional for $N_G = 1, 2, 5, 10$ in Fig. 11. The effect visible in the exact wave functional, that taking more Gribov copies into account damps the infrared enhancement of d_n and produces a spurious peak (here weakened) at intermediate momenta, can indeed be mimicked by the wave functional (10.9) with the appropriate Gaussian damping α.

However, if one tries to quantitatively achieve the infrared enhancement of the *physical* solution, i.e. the exact d_n within the first Gribov region Ω_1, the wave functional (10.9) fails. There exists no value for α such that the infrared enhancement of the exact physical solution, d_n in Fig. 3, is realized. The value $d_{n=1} = 1.37$ of the exact form factor (7.11) is larger than any choice of α can produce for the mode $d_{n=1}(\alpha)$ in the Gaussian wave functional (10.9). In Fig. 14, it is shown how $d_1(\alpha)$ varies with α. For the value α_{max} where

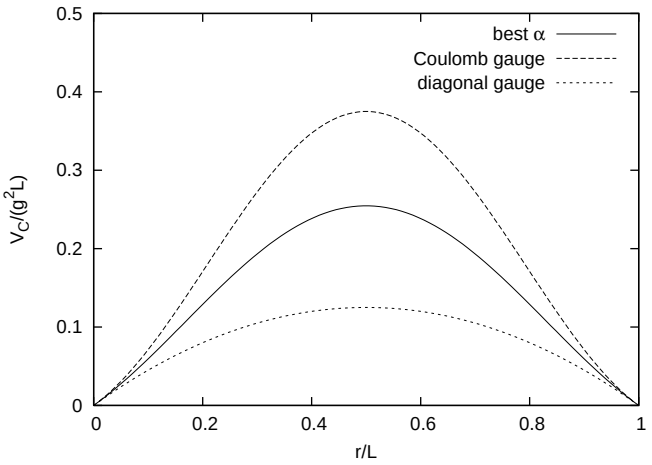

Fig. 15. Coulomb potential $V_C(\alpha, r)$ in the Gaussian wave functional (10.9) with the "best" value (10.16) for the width α. Also shown are the results in the exact ground state for the *pure Coulomb gauge* and the *diagonal Coulomb gauge* from Fig. 7.

the infrared enhancement of the ghost propagator in the Gaussian wave functional (10.9) is the strongest,

$$\alpha_{max} \approx 1.40 \,, \quad d_1(\alpha_{max}) \approx 1.20 \,, \tag{10.16}$$

it is seen how it still underestimates the physical result, $d_1(\alpha_{max}) < 1.37$. This indicates that if a lattice calculation is unable to exclude all Gribov copies, the genuine infrared physics cannot be described. In higher dimensions, this would mean that the infrared enhancement of the ghost form factor on the lattice is weaker than expected from continuum studies, an effect that is indeed observed [19,46].

Expecting that with the choice $\alpha = \alpha_{max}$, most (though not all) of the infrared features can be carried along, [15] we go on to compute other expectation values of interest. For instance, the Coulomb potential $V_C(\alpha, r)$ between two external static colour charges separated by r can be computed by taking the *pure Coulomb gauge* expectation value of the operator (8.7) in the Gaussian wave functional (10.9),

$$\begin{aligned} V_C(\alpha, r) &= g^2 \frac{2}{3\pi} \mathcal{N}^2 \int_0^\infty d\vartheta \, \sin^2\vartheta \, \mathrm{e}^{-\frac{\vartheta^2}{2\alpha^2}} \\ &\qquad \times \left(\frac{1}{2} r - \frac{1}{2} \frac{r^2}{L} + \frac{1}{2\sin^2\vartheta} \left(L - r\cos\left(2\,\tfrac{L-r}{L}\,\vartheta\right) - (L-r)\cos\left(2\,\tfrac{r}{L}\,\vartheta\right)\right)\right) \\ &= \frac{g^2}{6} \left(r - \frac{r^2}{L} + \left(1 + \coth(\alpha^2)\right) \left(L - r\,\mathrm{e}^{-2\alpha^2(1-\frac{r}{L})^2} - (L-r)\,\mathrm{e}^{-2\alpha^2(\frac{r}{L})^2}\right)\right) \\ &\stackrel{L\to\infty}{\longrightarrow} \quad \frac{g^2}{2} r \quad \forall\alpha \end{aligned} \tag{10.17}$$

[15] This choice is reminiscent of the "horizon condition" in higher dimensions.

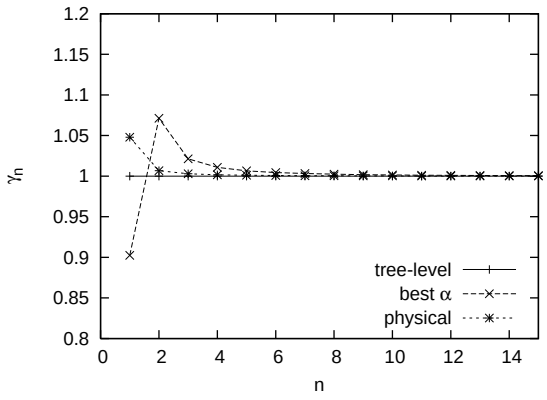

Fig. 16. Ghost-gluon vertex form factor γ_n in the Gaussian wave functional (10.9) with the "best" value (10.16) for the width α. Also shown is the physical solution, see Fig. 6, and the tree-level value.

In the thermodynamic limit $L \to \infty$, the potential (10.17) approaches the same behaviour as $V_C(r)$ in the exact ground state. It was already shown above that the Coulomb string tension σ_C, defined in the thermodynamic limit, turns out independent of the wave functional and the configuration space Γ_{N_G}. For the choice (10.16) of α, the potential $V_C(r)$ in Eq. (10.17) is shown in Fig. 15. Varying α, the potential is seen to vary between the exact solutions of the *pure Coulomb gauge* and the *diagonal Coulomb gauge*. As a matter of fact, the result (8.12) of the *diagonal Coulomb gauge* is reached in the limit $\alpha \to 0$,

$$\lim_{\alpha\to 0} V_C(\alpha, r) = \frac{g^2}{2}\left(r - \frac{r^2}{L}\right) \equiv V_C(r)|_{\text{diagonal gauge}} \ . \tag{10.18}$$

Recall that the limit $\alpha \to 0$ turns the Gaussian wave functional (10.9) into a delta distribution, peaked at $A = 0$. The limit (10.18) therefore emphasises that in $1+1$ dimensions, the Coulomb potential $V_C(r)$ is a quantity that is independent of quantum fluctuations, when properly evaluated in the fundamental modular region.

In the opposite limit, $\alpha \to \infty$, the potential $V_C(\alpha, r)$ coincides with $V_C(N_G, r)$ in the exact vacuum state, see Eq. (10.8), having taken the limit $N_G \to \infty$. This is intuitively clear since the Gaussian state (10.9) becomes constant for $\alpha \to \infty$ (and not normalisable). Note, however, that the limits $\alpha \to \infty$ and $L \to \infty$ are not interchangeable. In order to find the right string tension, one is to first evaluate the energy in a normalisable state ($\alpha < \infty$), take the thermodynamic limit $L \to \infty$, and then determine the string tension as a function of α. In the opposite order of limits, one finds a different result for σ_C.

Finally, we calculate the ghost-gluon vertex in the state (10.9). It can be found using the expression (10.6) which holds for any wave functional (and any Γ_{N_G}); in the evaluation we simply use the results (10.11) and (10.13) for the gluon and ghost propagators. The result is shown in Fig. 16. The deviation of γ_n from the exact physical result is small, although it

is enhanced for the infrared modes. Anyhow, the tree-level vertex is a better approximation of the exact ghost-gluon vertex than the one in the Gaussian wave functional (10.9).

11 Truncation effects

In higher dimensions, it is not possible to obtain exact nonperturbative expressions for the Green functions. A common approximation that enables us to find the infrared asymptotic solutions of the Dyson–Schwinger equations is to render the ghost-gluon vertex tree-level. We will make this approximation here in $1+1$ dimensional *pure Coulomb gauge* and investigate the effect on the propagators. To be explicit, we set

$$\Gamma^a_n \to \Gamma^{0,a}_n \ , \quad \Rightarrow \ \gamma_n = 1 \ . \tag{11.1}$$

Recall it was shown in the preceding sections that despite the form invariance of the exact DSEs with respect to the configuration space Γ_{N_G}, the true Green functions (calculated with the exact vacuum wave functional) do depend on Γ_{N_G}. With the approximation (11.1), the DSEs for the gluon and ghost propagators, Eqs. (9.5) and (9.8), turn into

$$d_n = 1 + N_c D_A \frac{d_n^2}{k_n^2} \ , \quad D_A^{-1} = N_c \sum_{n\neq 0} \frac{d_n^2}{k_n^2} \ . \tag{11.2}$$

Diagrammatically, these equations are depicted in Figs. 8 and 9, with the blobs replaced by dots. We note that due to the approximation (11.1), this set of equations is closed and can be solved. The crucial point is to realize that the solution will no longer depend on the choice of the configuration space Γ_{N_G}. Since the ghost-gluon vertex was chosen to be independent of Γ_{N_G}, see Eq. (11.1), the gluon and ghost propagators are now also independent of Γ_{N_G}. The original exact set of DSEs holds within any of the Gribov regions. However, solving the approximated set of DSEs, the information is lost in which Gribov region the Green functions are evaluated in. This problem also occurs in the infrared ghost dominance model of the $D = 3+1$ theory.

Let us now solve Eq. (11.2) explicitly. Since it is quadratic in d_n, we find two solutions,

$$d_n = \frac{1 \pm \sqrt{1 - 4\frac{N_c D_A}{k_n^2}}}{2\frac{N_c D_A}{k_n^2}} \ . \tag{11.3}$$

In order for the limit $d_n \to 1$ for $k_n = \frac{2\pi n}{L} \to \infty$ to be fulfilled, we need the lower sign.

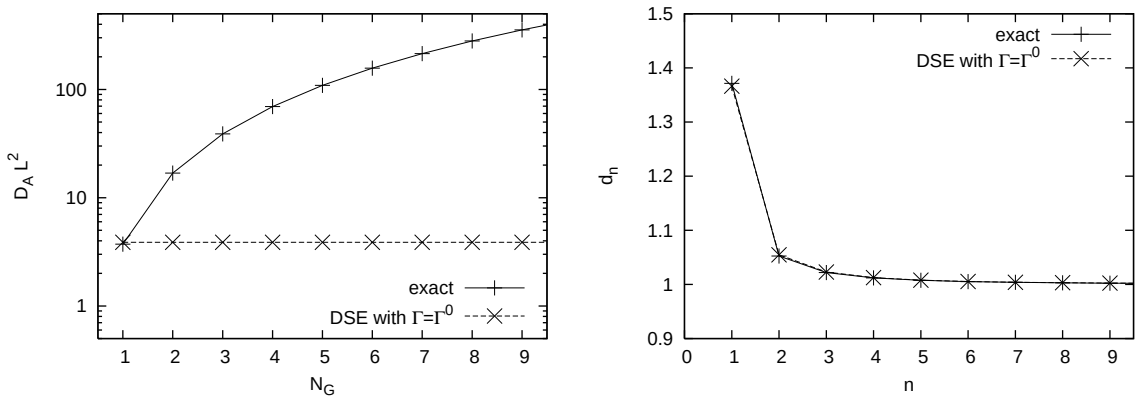

Fig. 17. *Left:* Comparison of the exact gluon propagator to the one from the DSEs with a tree-level ghost-gluon vertex, shown as a function of N_G. *Right:* Comparison of the exact ghost form factor d_n in the first Gribov region ($N_G = 1$) to one calculated from the truncated DSEs, both shown as functions of the momentum mode n.

Plugging this solution into the second DSE in Eq. (11.2), we find

$$D_A N_c L^2 = \sum_{n\neq 0} (\pi n)^2 \left(1 - \sqrt{1 - \frac{D_A N_c L^2}{(\pi n)^2}}\right)^2 \qquad \Rightarrow D_A N_c L^2 \approx 7.74 \tag{11.4}$$

The numerical solution yields with $N_c = 2$ for the gluon propagator

$$D_A \approx 3.87 \, \frac{1}{L^2} \, . \tag{11.5}$$

This value can be plugged into Eq. (11.3), with the lower sign, to immediately get the result for the ghost form factor.

The gluon propagator (11.5) is evidently independent of the Gribov region. One can choose Γ_{N_G} with any N_G, the approximation (11.1) will always yield the gluon propagator given by Eq. (11.5). On the other hand, we know the *exact* result for the gluon propagator with a given value of N_G, see Eq. (10.2). The latter can now be compared with the approximative result (11.5), for each N_G.

In Fig. 17, it is seen how for large N_G, the exact and approximative results differ dramatically. However, for $N_G = 1$, i.e. in the first Gribov region, there is a good agreement. The tree-level approximation for the ghost-gluon vertex yields a value for the gluon propagator that is very close to the exact result in the first Gribov region. The same occurs for the ghost propagator. As can be seen in on the right panel of Fig. 17, the approximative (with $\gamma_n = 1$) DSE result for the ghost form factor d_n hardly deviates from the exact result for $N_G = 1$. At the same time, the approximative and exact solutions of d_n for other values of N_G disagree both quantitatively and qualitatively, cf. Fig. 11. Also shown in Fig. 11 is the ghost-gluon vertex in the exact vacuum state for different values of N_G. One can realize that the tree-level approximation (11.1) is only for $N_G = 1$ a good one.

We infer that while the exact Dyson–Schwinger equations are form invariant with respect to the configuration space Γ_{N_G}, the approximation of the ghost-gluon vertex by its tree-level value effectively puts the approximative solution of the propagators into the first Gribov region $\Gamma_1 \equiv \Omega_1$. This supports the approach of solving DSEs in $D = 3+1$, truncated by means of a tree-level ghost-gluon vertex.

12 Variational approach

In order to test the variational approach to Yang–Mills theory in $3+1$ dimensions, the same ansatz for the wave functional as in Ref. [8] is here applied to solve the Yang–Mills Schrödinger equation in $D = 1+1$ in the *pure Coulomb gauge*. The variational calculation is performed using the same approximations as in Ref. [8].

The variational wave functional is given by

$$\Psi(A) = \frac{1}{\sqrt{\mathcal{J}_P(A)}}\,\widetilde{\Psi}(A)\,, \quad \widetilde{\Psi}(A) = \mathcal{N}\mathrm{e}^{-\frac{1}{2}A^a\omega A^a} := \langle A|\omega\rangle\,, \tag{12.1}$$

where ω is a variational parameter determined by minimising the vacuum energy density. The ansatz (12.1) is mainly motivated by simplicity. It removes the Faddeev–Popov determinant $\mathcal{J}_P$ from the integration measure in the expectation values of the *pure Coulomb gauge*,

$$\langle\Psi|\mathcal{O}(A)|\Psi\rangle = \int\limits_{\Gamma_\infty} \mathcal{D}A\,\mathcal{J}_P(A)\,\mathcal{O}(A)|\Psi(A)|^2 = \int\limits_{\Gamma_\infty} \mathcal{D}A\,\mathcal{O}(A)|\widetilde{\Psi}(A)|^2 =: \langle\mathcal{O}(A)\rangle_\omega\,. \tag{12.2}$$

and thus allows for an immediate application of Wick's theorem. Here and in the following, $\langle\ldots\rangle_\omega$ denotes the expectation value in the state $|\omega\rangle$ (12.1), for which the scalar product is defined with the flat integration measure $\mathcal{D}A \equiv \prod\limits_a dA^a$.

The configuration space in the expectation value (12.2) is not restricted to the first Gribov region Ω_1 but is extended to the union Γ_∞ of all Gribov regions, see Eq. (9.10). This is motivated from the $D = 3+1$ case where only little is known about the Gribov horizon and a restriction to Ω_1 is technically cumbersome.[16] In section 10.2, we have seen that within Γ_∞, any Gaussian damping of gauge copies will fail to recover the exact infrared behaviour of the ghost form factor. Note, however, that the wave functional in Eq. (12.1) is supplemented by a Faddeev–Popov determinant. We will show below that with appropriate approximations, the correct infrared behaviour of the ghost form factor can thus still be maintained.

[16] The so-called Gribov–Zwanziger action is used in a few studies [47] to realize a restriction to Ω_1.

The normalisation constant $\mathcal{N}$ in the ansatz (12.1) for the wave functional is chosen such that $\langle 1 \rangle_\omega = 1$ and is given by

$$\ln \mathcal{N} = \frac{N_c^2 - 1}{4} \ln \left(\frac{\omega}{\pi} \right) \ . \tag{12.3}$$

Thus, the static (equal-time) gluon propagator reads

$$D^{ab} = \langle \Psi | A^a A^b | \Psi \rangle = \langle A^a A^b \rangle_\omega = \delta^{ab} (2\omega)^{-1} =: \delta^{ab} \, D_A \ . \tag{12.4}$$

In $D = 3 + 1$ the kernel ω has the meaning of the gluon energy. In the present $1 + 1$ dimensional case ω has dimension $mass^{-2}$ and is required by normalisability of the wave functional to be positive, $\omega > 0$. Let us emphasise that whatever the variational principle yields for ω, it will determine the gluon propagator D_A by Eq. (12.4).

The vacuum energy $E(\omega)$ is calculated by taking the expectation value of the Yang–Mills Hamiltonian in the *pure Coulomb gauge* (5.20) in the absence of external charges. After a partial integration, $E(\omega)$ yields

$$\begin{aligned} E(\omega) = \langle \Psi | H | \Psi \rangle &= \int \mathcal{D}A \, \mathcal{J}_P(A) \Psi^*(A) H \Psi(A) \\ &= \frac{g^2 L}{2} \int \mathcal{D}A \, \left(\widetilde{\Pi}_\perp^a \widetilde{\Psi} \right)^* \left(\widetilde{\Pi}_\perp^a \widetilde{\Psi} \right) \ , \end{aligned} \tag{12.5}$$

where

$$\widetilde{\Pi}_\perp^a = \mathcal{J}_P^{1/2} \Pi_\perp^a \mathcal{J}_P^{-1/2} = \Pi_\perp^a - \frac{1}{2} \left(\Pi_\perp^a \ln \mathcal{J}_P \right) \ . \tag{12.6}$$

Using

$$\widetilde{\Pi}_\perp^a \widetilde{\Psi} = \frac{i}{L} \left[\omega A^a + \frac{1}{2} \left(\frac{d \ln \mathcal{J}_P}{d A^a} \right) \right] \widetilde{\Psi} \tag{12.7}$$

we find

$$\begin{aligned} E(\omega) &= \frac{g^2}{2L} \left\langle \left(\omega A^a + \frac{1}{2} \frac{d \ln \mathcal{J}_P}{d A^a} \right)^2 \right\rangle_\omega \\ &= \frac{g^2}{2L} \left[\omega^2 \left\langle A^a A^a \right\rangle_\omega + \omega \left\langle A^a \frac{d \ln \mathcal{J}_P}{d A^a} \right\rangle_\omega + \frac{1}{4} \left\langle \left(\frac{d \ln \mathcal{J}_P}{d A^a} \right)^2 \right\rangle_\omega \right] \ . \end{aligned} \tag{12.8}$$

Following Ref. [8] we will explicitly calculate the first two terms and then find the last term by completing the result to a total square, which is correct up to two loops. The first term in Eq. (12.8) can obviously be expressed by the gluon propagator (12.4). For the second term, we use the abbreviation

$$\chi^{ab} := - \omega \left\langle A^a \frac{d \ln \mathcal{J}_P}{d A^b} \right\rangle_\omega \ , \tag{12.9}$$

which was referred to as the "curvature" in Ref. [8]. Using the definition (7.22) of the proper ghost-gluon vertex and its form factor γ_n (7.25), the curvature χ^{ab} can be written as [17]

$$\begin{aligned}\chi^{ab} &= +\omega \left\langle A^a \operatorname{Tr} G\, \Gamma_n^{0,b} \right\rangle_\omega = \frac{1}{2} \sum_{n\neq 0} \gamma_n \frac{d_n^2}{k_n^4} \operatorname{tr}\left(\Gamma_n^{0,a} \Gamma_n^{0,b}\right) \\ &= \frac{N_c}{2} \sum_{n\neq 0} \gamma_n \frac{d_n^2}{k_n^2}\, \delta^{ab} =: \chi\, \delta^{ab} \end{aligned} \tag{12.10}$$

and its diagonal elements define the scalar curvature χ. Performing the quadratic completion, the expression (12.8) for the vacuum energy can be cast into the form

$$E(\omega) = g^2\, \frac{N_C^2 - 1}{4L} \frac{(\omega - \chi)^2}{\omega} \tag{12.11}$$

and it is obviously minimised for the choice

$$\omega = \chi \tag{12.12}$$

of the variational kernel ω. Equation (12.12) is called the gap equation and it gives rise to an infrared divergent gluon energy $\omega(k)$ in $3+1$ dimensions [8,27].

The gap equation (12.12) states that the gluon propagator (12.4) can be related to the curvature χ and we may use the definition (12.9) of χ^{ab} to calculate the gluon propagator exactly. However, approximations have been made and—more importantly—the configuration space was not properly restricted to Γ_1. Let us look at the task of determining the solution for the gluon and ghost propagators differently. We note that plugging the gap equation (12.12) into Eq. (12.4) yields with Eq. (12.10)

$$D_A^{-1} = N_c \sum_{n\neq 0} \gamma_n \frac{d_n^2}{k_n^2}\ . \tag{12.13}$$

Turning back to Eq. (9.5), we recognise that relation (12.13) is identical to the gluon propagator DSE in the exact vacuum state. Moreover, we can use the ghost propagator DSE (9.8) from the exact vacuum state since it follows from an operator identity, independent of the wave functional or configuration space. The set of equations the variational calculation above resulted in is equivalent to the set of Dyson–Schwinger equations derived in the exact vacuum state. The difference is that here the expectation values (i.e. d_n, D_A, γ_n) are evaluated in the state (12.1) and in the configuration space Γ_∞, yielding different results. It was shown in section 10 that choosing a set of several ($N_G > 1$) Gribov regions for Γ_{N_G} results in drastic changes for the Green functions. However, if we use the tree-level approximation for the ghost-gluon vertex, it is clear from the discussion in section

[17] The definition (12.9) of the curvature is equivalent to the one in Ref. [8] within the wave functional (12.1). The same holds for the proper ghost-gluon vertex.

11 that the solution to the DSEs so obtained is very close to the exact solution. With a conspiracy of approximations, namely the quadratic completion in Eq. (12.8) and the vertex approximation $\gamma_n = 1$, the variational state (12.1) in Γ_∞ yields the same propagators as the exact vacuum state (6.21) in the first Gribov region $\Gamma_1 \equiv \Omega_1$.

Identifying the variational wave functional (12.1) for the solution $\omega = \chi$ with the exact wave functional $\Psi = const$ implies that the Gaussian must cancel the Faddeev–Popov determinant $\mathcal{J}_P$,

$$\mathcal{J}_P \;\longrightarrow\; \exp\left(-A^a \chi^{ab} A^b\right) \,. \tag{12.14}$$

In Ref. [10] it was shown that up to two-loop order in the energy the replacement (12.14) is exact and thus results in the correct DSEs.

In $D = 3+1$ both ω and χ are momentum dependent and the cancellation of $\mathcal{J}_P^{-\frac{1}{2}}$ against the Gaussian in the wave functional is obtained in the infrared limit $k \to 0$ only. We thus observe that in the infrared limit the wave functional in $D = 3+1$ reduces to the exact wave functional in $D = 1+1$ dimensions. As discussed in Ref. [10] the constant wave functional does not constrain the infrared modes of the gauge field and thus describes a stochastic vacuum where the infrared modes can arbitrarily fluctuate.

As shown in Ref. [10], the cancellation of Gaussian and Faddeev–Popov determinant persists in $D = 3+1$ in the infrared even if the more general ansatz is used,

$$\Psi(A) = \mathcal{J}_P^{-\alpha}(A)\tilde{\Psi}(A) \,. \tag{12.15}$$

In this state with a arbitrary exponent α of the Faddeev–Popov determinant, the gluon propagator becomes

$$\langle A^a A^b \rangle = \delta^{ab}(2\widetilde{\omega})^{-1} \,, \tag{12.16}$$

where

$$\widetilde{\omega} = \omega - (2\alpha - 1)\chi \,. \tag{12.17}$$

The gap equation is the same as above, see Eq. (12.12), except that ω is replaced by $\widetilde{\omega}$,

$$\widetilde{\omega} = \chi \,. \tag{12.18}$$

We therefore find from (12.17)

$$\omega = 2\alpha\chi \,. \tag{12.19}$$

For $\alpha = \frac{1}{2}$ we recover, of course, the previous result (12.12), while $\alpha = 0$ yields $\omega = 0$ and the variational wave functional (12.15) becomes the exact one

$$\Psi(A) = \mathcal{N} = const. \tag{12.20}$$

and thus yields also the exact results for the propagators, provided the range of the field A is properly restricted to the first Gribov region.

Finally, let us turn to the Coulomb form factor f_n which measures the deviation of the Coulomb propagator $\langle G(-\partial^2)G\rangle$ from the factorised form $\langle G\rangle\,(-\partial^2)\,\langle G\rangle$ and was calculated in the exact wave functional at the end of section 7.5. In $3+1$ dimensions, the (momentum-dependent) form factor $f(k)$ is set to unity since it fails to satisfy the corresponding integral equation within the approximations made [48]. The form factor $f(k)$ requires a higher-order calculation (as pointed out in Ref. [8,31]), and for this reason it is investigated here in $1+1$ dimensions where approximations are not necessary.

The integral equation that is derived for the Coulomb form factor f_n follows from the identity [49]

$$F(A) = G(A)(-\partial^2)G(A) = \frac{\partial}{\partial g}(gG(g\bar{A}))\ . \tag{12.21}$$

Here, we have scaled the gauge field by the coupling constant g,

$$A = g\,\bar{A} \tag{12.22}$$

so that with

$$G^{-1}(g\,\bar{A}) = -\,\partial^2 - g\,\hat{\bar{A}}\,\partial \tag{12.23}$$

we can derive Eq. (12.21) by differentiation. Following Ref. [2], in the variational approach [8] the vacuum expectation value of the relation (12.21) was taken, thereby ignoring the implicit g-dependence of the wave functional to obtain the approximative relation

$$\langle F\rangle \approx \frac{\partial}{\partial g}\,(g\langle G\rangle) \tag{12.24}$$

which is the so-called Swift relation [2]. In the present $1+1$ dimensional case the exact vacuum wave functional is independent of g but the Faddeev–Popov determinant $\mathcal{J}_P(g\bar{A})$ in the integration measure is g-dependent and this g-dependence is ignored in Eq. (12.24). Expressing $\langle G\rangle$ and $\langle F\rangle$ in terms of the ghost and Coulomb form factors, d_n (7.8) and f_n (7.18), the Swift relation (12.24) becomes [18]

$$f_n \approx d_n^{-2}\frac{\partial}{\partial g}(g\,d_n) = d_n^{-1} - g\frac{\partial}{\partial g}d_n^{-1}\ . \tag{12.25}$$

Using the inverse form of the DSE (9.8) for the ghost form factor,

$$d_n^{-1} = 1 - N_c\,\gamma_n\,D_A\,\frac{d_n}{k_n^2}\ , \tag{12.26}$$

an integral equation for f_n can be found,

$$f_n \approx 1 + N_c\,\gamma_n\,D_A\,\frac{d_n^2 f_n}{k_n^2}\ . \tag{12.27}$$

[18] This relation differs from the one given in Ref. [8], where an extra factor of g was included in the ghost form factor.

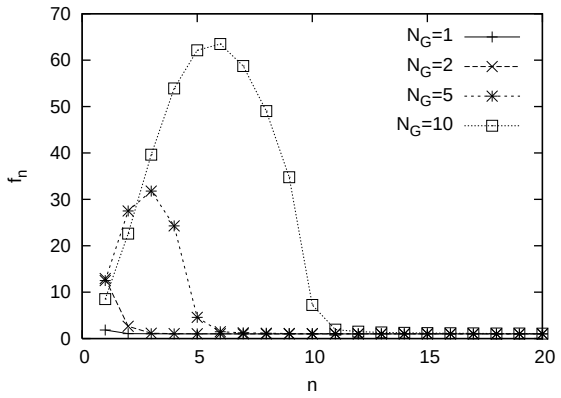

Fig. 18. Coulomb form factor f_n, defined by Eq. (7.18), in the exact vacuum state depending on the number N_G of included Gribov regions.

Note that this integral equation is not exact, due to the Swift approximation (12.24). In the exact wave functional of the $1+1$ dimensional *pure Coulomb gauge*, the ghost propagator is independent of g [31] [19]

$$\begin{aligned} \frac{\partial}{\partial g}\langle G\rangle &= \frac{\partial}{\partial g}\,\frac{\int_{\Omega_1}\mathcal{D}\bar{A}\,G(g\,\bar{A})\,\mathrm{Det}\,G^{-1}(g\,\bar{A})}{\int_{\Omega_1}\mathcal{D}\bar{A}\,\mathrm{Det}\,G^{-1}(g\,\bar{A})} \\ &= \frac{\partial}{\partial g}\,\frac{\int_{\Omega_1}\mathcal{D}\bar{A}\,G(\bar{A})\,\mathrm{Det}\,G^{-1}(\bar{A})}{\int_{\Omega_1}\mathcal{D}\bar{A}\,\mathrm{Det}\,G^{-1}(\bar{A})} \;=0 \end{aligned} \tag{12.28}$$

and hence the ghost form factor also is, $\partial d_n/\partial g = 0$. The Swift relation (12.25) thus simplifies to

$$f_n = d_n^{-1}\ . \tag{12.29}$$

This relation implies that f_n is infrared suppressed if d_n is infrared enhanced, which is in contradiction to the true behaviour of f_n and d_n, see Figs. 3 and 5. Even more directly, the contradiction can be seen by plugging Eq. (12.29) into the approximative integral equation (12.27) and comparing to the exact ghost form factor DSE (12.26).

The contradiction arises from the approximation made to arrive at the Swift relation (12.24). In the infrared limit of the $D = 3+1$ theory which is correctly described by the $D = 1+1$ wave functional [10], the Swift relation therefore must lead to inconsistencies [31,48].

Recent lattice calculations in $D = 3+1$ of the Coulomb form factor $f(k)$ seem to indicate that in the infrared $f(k)$ is enhanced. This enhancement gets weaker the better the Coulomb gauge is fixed. In $1+1$ dimensions, the form factor f_n can be calculated exactly, see section 7.5. The effect of including several Gribov regions, i.e. choosing $\Gamma_{N_G>1}$ as done in section

[19] The same is true for the ghost propagator in $3+1$ dimensions if we consider the stochastic vacuum $\Psi[A] = const$ of the Coulomb gauge Hamiltonian approach or the ghost dominance model $S_{YM} = 0$ in the Landau gauge to study the infrared asymptotics.

10.1, leads to an interesting observation. In Fig. 18, it is shown how the exact result for f_n varies with the number N_G of included Gribov regions. The larger N_G, the more pronounced a (spurious) infrared enhancement. This gauge copy effect is in agreement with the findings on the lattice in $3+1$ dimensions and indicates that in order to get the exact result for $f(k)$, gauge fixing on the lattice has to be performed very carefully.

13 Summary and Conclusions

In this paper, we have considered $1+1$ dimensional $SU(2)$ Yang–Mills theory in canonical quantisation in the *pure Coulomb gauge* as a testing ground for Yang–Mills theory studies in higher dimensions. The investigations were carried out in the *pure Coulomb gauge* and in the *diagonal Coulomb gauge*, where the residual global gauge invariance, left unfixed in the *pure Coulomb gauge*, is fixed by diagonalising the constant spatial gauge field. Although the two gauges differ only by a global $SU(2)/U(1)$ gauge-fixing constraint, they have different Faddeev–Popov determinants due to additional zero modes of the Faddeev–Popov kernel in the *pure Coulomb gauge*. While the *pure Coulomb gauge* is perfectly suitable for perturbation theory, the *diagonal Coulomb gauge* is ill-defined for the perturbative vacuum $A = 0$, for which the Faddeev–Popov determinant vanishes. The occurrence of such gauge-fixing defects is a characteristic feature of so-called abelian gauges the *diagonal Coulomb gauge* belongs to. In higher dimensions gauge-fixing defects of abelian gauges manifest themselves as magnetic monopoles in the corresponding abelian projection [50] (see also Ref. [51]).

We have explicitly demonstrated that the Faddeev–Popov method does not require complete gauge fixing but works for any partial gauge fixing, provided that the zero modes of the Faddeev–Popov kernel arising from the residual gauge symmetry (left unfixed by the partial gauge fixing) are properly treated. In the resolution of Gauss' law, these zero modes give rise to residual constraints on the wave functional, which express the invariance of the wave functional under the residual gauge symmetry: The Noether charges corresponding to these residual symmetries must vanish in physical states. The constraints on the wave functionals arising from the residual unfixed gauge symmetry exist also in higher dimensions but have not been explicitly identified so far, except for space-independent gauge transformations [35]. They also naturally emerge in the functional integral approach in the so-called first order formalism where the temporal gauge field can be explicitly integrated to leave a δ-functional, which enforces Gauss' law [14]. In the *pure Coulomb gauge*, the Gauss' law constraint can be worked out analogously to the Hamiltonian approach and the δ-functional can be used to integrate out the longitudinal components of the momentum field. When the resolution of Gauss' law is properly done, i.e. the zero modes of the Faddeev–Popov kernel properly treated, from the δ-functional some ordinary δ-function survives, which precisely enforces the vanishing of the Noether charges corresponding to the residual unfixed gauge symmetries [35].

The exact spectrum of the Yang–Mills Hamiltonian was obtained within both the *diagonal* and the *pure Coulomb gauge*, having implemented the constraints on the wave functional arising in the resolution of Gauss' law from the zero modes of the Faddeev–Popov kernel. In the thermodynamic limit, we recovered the well-known spectrum that leaves only the vacuum state at zero energy, freezing out all excited states. The exact vacuum state was used to calculate the ghost and gluon propagators, the ghost-gluon vertex and the static colour Coulomb potential. We compared the results in the *pure Coulomb gauge* restricted to the first Gribov region to those in the *diagonal Coulomb gauge* restricted to the fundamental modular region. For the propagators, the colour trace was found to be left invariant when transforming from the *pure Coulomb gauge* to the *diagonal Coulomb gauge*. We found that the ghost propagator is infrared enhanced, in agreement with the horizon condition widely used in Dyson–Schwinger studies of $D = 3+1$. This infrared enhancement is the strongest when the configuration space is properly restricted to the first Gribov region. We studied the effect of including several Gribov copies, either by extending the configuration space to a union of Gribov regions, or by using all Gribov regions with a Gaussian damping. It was seen that the quantitative infrared enhancement of the ghost propagator cannot be realized by any of these calculations that include gauge copies from outside the first Gribov region. This indicates that lattice calculations of the ghost propagator require a very accurate gauge fixing and explains the shortcomings of the infrared enhancement of the ghost propagator on the lattice when compared to continuum studies [19,46].

The Coulomb string tension yielded the same results for both gauges which is a fortunate result, considering that in $D = 3 + 1$ calculations the gauge is not completely fixed. The quantitative result of the static colour Coulomb potential, away from the thermodynamic limit, differs for both gauges. The result of the *pure Coulomb gauge* can be sort of artificially deformed into the result in the *diagonal Coulomb gauge* by suppressing Gribov copies with a Gaussian wave functional of width zero, as discussed in section 10. The investigations showed that on $S^1 \times \mathbb{R}$, the Coulomb string tension arises from the abelian part of the Coulomb interaction and actually is identical to the string tension of the abelian theory, thus providing an upper bound of the gauge invariant string tension [44]. The effect of gauge copies on the static colour Coulomb potential was studied by taking several Gribov regions into account, and resulted in spurious locally stable minima for large separations of external colour charges.

The Dyson–Schwinger equations for the propagators and vertices in the *pure Coulomb gauge* were derived. It was shown that the exact solution within the first Gribov region satisfies the Dyson–Schwinger equations, but that these solutions are not the only ones. Changing the configuration space from any union of Gribov regions to another leaves the Dyson–Schwinger equations form invariant. This persists in the $D = 3+1$ case. Therefore, it is legitimate to ask: In which union of Gribov regions are the Green functions given when the set of Dyson–Schwinger equations is solved by means of a truncation? We found in $D = 1 + 1$ that choosing the ghost-gluon vertex at tree-level, effectively puts the solutions for the propagators and vertices into the first Gribov region. As for the colour traces

of the propagators, even the result within the fundamental modular region is attained. The tree-level ghost-gluon vertex approximation for solving Dyson–Schwinger equations—which was advocated by several investigations before [8,52,53,54]—thus receives further strong support.

The variational approach to Coulomb gauge Yang–Mills theory in $D = 3 + 1$ dimensions [8] integrates over all Gribov regions for technical reasons. It was shown in section 12 by using the same ansatz for the vacuum wave functional in $D = 1 + 1$, that with the appropriate approximation (quadratic completion in kinetic energy expression) the variational principle yields a set of Dyson–Schwinger equations that is the exact one. With the tree-level ghost-gluon vertex, the exact solution within the first Gribov region is thus very well approximated. It can be expected that the infrared limit of the $D = 3 + 1$ theory, which is described by a stochastic wave functional as in $D = 1 + 1$, is thus also well-approximated. Furthermore, we found that the Coulomb form factor that is necessary for the calculation of the static colour Coulomb potential is not too far from tree-level in the exact $D = 1 + 1$ calculation and that the inclusion of many Gribov copies simulate a spurious infrared enhancement of the Coulomb form factor. We infer there are no indications that the choice of a trivial Coulomb form factor is worse than any other approximation made in the $D = 3+1$ calculations.

Acknowledgements

Useful discussions with D. Campagnari, M. Quandt, P. Watson are greatly acknowledged. This work was supported in part by DFG under contract no. DFG-Re856/6-1 and DFG-Re856/6-2.

Appendix A $SU(2)$ colour rotations

The unitary matrix U, which rotates the colour vector $\hat{\mathbf{n}}(\theta,\phi)$ into the 3-direction (and thus, in particular, diagonalises the gauge field (2.19)) is defined by

$$U^\dagger \hat{\mathbf{n}}(\theta,\phi)\cdot\mathbf{T}\,U = T_3\,. \tag{A.1}$$

This matrix is defined up to an abelian gauge transformation $U \to U\omega$, $\omega = \exp(\varphi T_3) \in U(1) \subset SU(2)$, i.e. it is defined on the coset $SU(2)/U(1)$. The adjoint representation $\hat{U}$, defined by

$$U^\dagger T_a U = \hat{U}^{ab} T_b \tag{A.2}$$

is related to the fundamental representation U by

$$\hat{U}_{ab} = -2\,\mathrm{tr}\left(U^\dagger T_a U T_b\right)\ , \quad \mathrm{tr}\,(T_a T_b) = -\frac{1}{2}\delta_{ab}\,. \tag{A.3}$$

Equation (A.3) is most easily proved by Taylor expanding U in terms of $\Theta = \Theta_a T_a$ and using

$$[T_a,\Theta] = \hat{\Theta}^{ab} T_b\,. \tag{A.4}$$

Furthermore, since (A.2) is based only on the algebra of the generators it is valid in any representation, in particular the adjoint representation (where $U^\dagger = U^T$),

$$\hat{U}^T \hat{T}_a \hat{U} = \hat{U}_{ab}\hat{T}_b\,. \tag{A.5}$$

The matrix U can be realized by

$$U(\theta,\phi) = \mathrm{e}^{\theta \boldsymbol{e}_\phi\cdot\mathbf{T}}\ , \quad \mathbf{T} = -\frac{i}{2}\boldsymbol{\tau}\,, \tag{A.6}$$

where

$$\boldsymbol{e}_\phi = -\sin\phi\,\boldsymbol{e}_1 + \cos\phi\,\boldsymbol{e}_2 \tag{A.7}$$

is the unit vector in the direction of the azimuthal angle ϕ. The matrix U (A.6) can be alternatively expressed in terms of Euler angles as

$$U(\theta,\phi) = \mathrm{e}^{\phi T_3}\mathrm{e}^{\theta T_2}\,. \tag{A.8}$$

Equations (A.1), (A.6), (A.7) are valid in any representation of $SU(2)$ and thus also in the adjoint representation

$$\hat{U}(\theta,\phi) := \mathrm{e}^{\theta\boldsymbol{e}_\phi\cdot\hat{\mathbf{T}}} = \mathrm{e}^{\phi\hat{T}_3}\mathrm{e}^{\theta\hat{T}_2}\,. \tag{A.9}$$

From the defining equations (A.1), (A.3) and $\hat{U}^T = \hat{U}^{-1}$ also follows that the components of the unit colour vector $\hat{\mathbf{n}}(\theta,\phi)$ are given by

$$\hat{\mathbf{n}}^a(\theta,\phi) = \hat{U}_{a3}(\theta,\phi)\,. \tag{A.10}$$

It is convenient to use the bracket notation

$$\hat{U}_{ab} \equiv \langle a|\hat{U}|b\rangle \tag{A.11}$$

and to express $\hat{U}$ in the basis of the eigenvectors $|\sigma = 0, \pm 1\rangle$ of the spin 1 operators

$$\hat{S}^a = i\hat{T}^a \ , \ (\hat{T}_a)^{bc} = \epsilon^{bac} \tag{A.12}$$

satisfying

$$\begin{aligned} \hat{S}^2|\sigma\rangle &= 1(1+1)|\sigma\rangle \\ \hat{S}_3|\sigma\rangle &= \sigma|\sigma\rangle \ . \end{aligned} \tag{A.13}$$

The transition elements

$$\langle a|\sigma\rangle =: \mathrm{e}^a_\sigma \tag{A.14}$$

are the Cartesian components of the spherical unit vectors (in colour space)

$$\boldsymbol{e}_{\sigma=1} = -\frac{1}{\sqrt{2}} \begin{pmatrix} 1 \\ i \\ 0 \end{pmatrix}, \qquad \boldsymbol{e}_{\sigma=-1} = \frac{1}{\sqrt{2}} \begin{pmatrix} 1 \\ -i \\ 0 \end{pmatrix}, \qquad \boldsymbol{e}_{\sigma=0} = \begin{pmatrix} 0 \\ 0 \\ 1 \end{pmatrix} \ . \tag{A.15}$$

Here, Greek letters $\sigma, \tau, \ldots$ denote spherical colour components $\{1, 0, -1\}$, while Latin letters $a, b, \ldots$ denote the Cartesian colour components $\{1, 2, 3\}$. The matrix elements of the adjoint representation $\hat{U}$ (A.9) in the spherical basis

$$\langle\sigma|\hat{U}(\theta,\phi)|\sigma'\rangle = \langle\sigma|a\rangle\langle a|\hat{U}|b\rangle\langle b|\sigma'\rangle = \mathrm{e}^{a^*}_\sigma \hat{U}_{ab}(\theta,\phi)\mathrm{e}^b_{\sigma'} \tag{A.16}$$

are related to the Wigner D-function by

$$\langle\sigma|\hat{U}(\theta,\phi)|\sigma'\rangle = D^{J=1}_{\sigma\sigma'}(\phi,\theta,0) \ . \tag{A.17}$$

Using $\langle\sigma|3\rangle = \mathrm{e}^{3^*}_\sigma = \delta_{\sigma 0}$, the colour unit vector (A.10) can be expressed as

$$\hat{n}^a(\theta,\phi) = \langle a|\sigma\rangle\langle\sigma|\hat{U}|\tau\rangle\langle\tau|3\rangle = \mathrm{e}^a_\sigma D^1_{\sigma 0}(\phi,\theta,0) \ . \tag{A.18}$$

Appendix B Explicit resolution of Gauss' law

To identify $\Pi^a_{||}(x)$ we Fourier expand the periodic gauge field $A(x+L) = A(x)$

$$A(x) = \frac{1}{L}\sum_n \mathrm{e}^{ik_n x} A(n) \ , \quad k_n = \frac{2\pi n}{L} \ , \quad n \in \mathbb{Z} \ . \tag{B.1}$$

The inverse transformation reads

$$A(n) = \int_0^L dx\, \mathrm{e}^{-ik_n x} A(x) \tag{B.2}$$

and the continuum limit $L \to \infty$ is obtained by the replacement

$$\frac{1}{L}\sum_n \to \int \frac{dk}{2\pi}\,. \tag{B.3}$$

For later use we also quote the completeness and orthogonality relations

$$\delta(x) = \frac{1}{L}\sum_n \mathrm{e}^{ik_n x}\,, \quad \delta_{m,n} = \frac{1}{L}\int_0^L dx\, \mathrm{e}^{i(k_m - k_n)x}\,, \tag{B.4}$$

where $\delta(x)$ denotes the periodic δ-function, satisfying

$$\delta(x+L) = \delta(x)\,. \tag{B.5}$$

From (B.1) we find for the momentum operator

$$\Pi^a(x) = \frac{\delta}{i\delta A^a(x)} = \frac{1}{L}\sum_n \mathrm{e}^{-ik_n x}\frac{d}{idA^a(n)}\,. \tag{B.6}$$

B.1 Pure Coulomb gauge

In momentum space the *pure Coulomb gauge* (2.16) reads

$$A(n) = \delta_{n,0} A(0)\,, \tag{B.7}$$

where

$$A(0) = \frac{1}{L}\int_0^L dx A(x) =: A \tag{B.8}$$

is the constant part of the gauge field, which is left after gauge fixing. From Eq. (B.6) we read off the transversal (x-independent) and longitudinal (x-dependent) parts of the momentum operator to be given by

$$\Pi^a_\perp = \frac{1}{L}\frac{d}{idA^a}\,, \quad \Pi^a_{||}(x) = \frac{1}{L}\sum_{n\neq 0} \mathrm{e}^{-ik_n x}\frac{d}{idA^a(n)}\,. \tag{B.9}$$

In the *pure Coulomb gauge*, where the degrees of freedom are $A^{a=1,2,3}$, the charge of the gauge bosons (5.6) is space independent but non-zero. Using (cf. Eq. (3.26))

$$i\hat{D}^{ab}\mathrm{e}^{-ik_n x} = \mathrm{e}^{-ik_n x}\langle a|\hat{U}|\sigma\rangle\lambda_{n,\sigma}\langle\sigma|\hat{U}^T|b\rangle\,, \tag{B.10}$$

we obtain

$$i\hat{D}^{ab}\Pi^b_{||}(x) = \frac{1}{L}\sum_{n\neq 0} \mathrm{e}^{-ik_n x}\langle a|\hat{U}|\sigma\rangle\lambda_{n,\sigma}\langle\sigma|\hat{U}^T|b\rangle\frac{d}{idA^b(n)} \,. \tag{B.11}$$

Inserting this relation into Gauss' law (5.4) and multiplying the resulting equation by $\mathrm{e}^{ik_m x}$, and integrating over x thereby using Eq. (B.4) we obtain

$$\sum_{n\neq 0}\delta_{n,m}\langle a|\hat{U}|\sigma\rangle\lambda_{n,\sigma}\langle\sigma|\hat{U}^T|b\rangle\frac{d}{idA^b(n)}\Psi(A) = i\int_0^L dx\mathrm{e}^{ik_m x}\rho^a_{tot}(x)\Psi(A) \,. \tag{B.12}$$

For $m = 0$ the l.h.s. of Eq. (B.12) vanishes and we find that the wave functional has to satisfy the following constraint

$$Q^a\,\Psi(A) \equiv \int_0^L dx\,\rho^a_{tot}(x)\,\Psi(A) = 0 \,. \tag{B.13}$$

For $m \neq 0$ the summation over n on the l.h.s. collapses to the term $m = n$ and Eq. (B.12) becomes after multiplying it by $\langle\sigma|\hat{U}^T|a\rangle$ and summing over a

$$\lambda_{m,\sigma}\langle\sigma|\hat{U}^T|b\rangle\frac{d}{idA^b(m)}\Psi(A) = i\langle\sigma|\hat{U}^T|a\rangle\int_0^L dx\,\mathrm{e}^{ik_m x}\rho^a_{tot}(x)\Psi(A) \,. \tag{B.14}$$

Multiplying Eq. (B.14) by $\frac{1}{L}\mathrm{e}^{-ik_m y}\langle c|\hat{U}|\sigma\rangle\lambda^{-1}_{m,\sigma}$ and summing over $m \neq 0$ and σ we get

$$\begin{aligned}
\Pi^c_{||}(y)\Psi(A) &= \frac{1}{L}\sum_{m\neq 0}\mathrm{e}^{-ik_m y}\frac{d}{idA^c(m)}\Psi(A) \\
&= i\frac{1}{L}\sum_{m\neq 0}\sum_{\sigma}\mathrm{e}^{-ik_m y}\int_0^L dx\,\mathrm{e}^{ik_m x}\langle c|\hat{U}|\sigma\rangle\lambda^{-1}_{m,\sigma}\langle\sigma|\hat{U}^T|a\rangle\rho^a_{tot}(x)\Psi(A) \qquad \text{(B.15)} \\
&= i\int_0^L dx\sum_{m\neq 0}\sum_{\sigma}\tilde{\varphi}^c_{m,\sigma}(y)\lambda^{-1}_{m,\sigma}\tilde{\varphi}^{a^*}_{m,\sigma}(x)\rho^a_{tot}(x)\Psi(A) \,, \qquad \text{(B.16)}
\end{aligned}$$

where we have used the explicit form of the eigenfunctions $\tilde{\varphi}^a_{n,\sigma}(x)$ (3.28) of the covariant derivative $i\hat{D}^{ab}$. Note if the modes $m = 0, \sigma = \pm 1$ were included in Eq. (B.16), the sum would produce the inverse kernel

$$\langle y, b|(i\hat{D})^{-1}|a, x\rangle = {\sum_{m,\sigma}}'\tilde{\varphi}^b_{m,\sigma}(y)\lambda^{-1}_{m,\sigma}\tilde{\varphi}^{a^*}_{m,\sigma}(x) \,, \tag{B.17}$$

where the prime indicates that the mode $m = \sigma = 0$ is excluded (while $m = 0, \sigma = \pm 1$ is included).

It is now straightforward to calculate the Coulomb Hamiltonian H_C defined by Eq. (5.9). With Eq. (B.16) we obtain after straightforward manipulations

$$H_C = \frac{g^2}{2} \int dxdy\, \rho^a_{tot}(x) F^{ab}(x,y) \rho^b_{tot}(y)\,, \tag{B.18}$$

where

$$F^{ab}(x,y) = \sum_{n\neq 0} \sum_{\sigma} \langle x,a|\hat{U}|n,\sigma\rangle \lambda^{-2}_{n,\sigma} \langle n,\sigma|\hat{U}^T|y,b\rangle = \sum_{n\neq 0} \sum_{\sigma} \tilde{\varphi}^a_{n,\sigma}(x) \lambda^{-2}_{n,\sigma} \tilde{\varphi}^{b^*}_{n,\sigma}(y) \tag{B.19}$$

is the so-called Coulomb kernel. Let us stress the mode $n=0, \sigma=\pm 1$ is here not included although it is not a zero mode $\lambda_{n=0,\sigma=\pm 1} \neq 0$. Since this mode is also excluded from the ghost kernel

$$\hat{G}^{ab}(x,y) = \langle x,a|\hat{G}^{-1}|y,b\rangle = \langle x,a|(-\hat{D}\partial)^{-1}|y,b\rangle = \sum_{n\neq 0} \sum_{\sigma} \tilde{\varphi}^a_{n,\sigma}(x)\, (k_n \lambda_{n,\sigma})^{-1}\, \tilde{\varphi}^{b^*}_{n,\sigma}(y) \tag{B.20}$$

the Coulomb kernel (B.19) can be represented as

$$F^{ab}(x,y) = \langle x,a|(-\hat{D}\partial)^{-1}(-\partial^2)(-\hat{D}\partial)^{-1}|y,b\rangle\,, \tag{B.21}$$

which is the usual representation. In the abelian case, this kernel reduces to the usual Coulomb potential. In the non-abelian theory, this is a dynamical object depending on the field variables via the covariant derivative.

The above derivation of H_C has shown that Gauss' law in the *pure Coulomb gauge* does not only give rise to the Coulomb Hamiltonian H_C (B.18) but in addition yields the constraint (B.13) on the wave functional. This constraint arises from the zero modes of the Faddeev-Popov kernel, which are a consequence of the incomplete gauge fixing. In a complete gauge fixing such residual constraints would not arise [20].

Due to the fact that constant modes $k_n = 0$ are excluded from the Coulomb kernel, the dynamical charge of the gauge bosons, ρ_g, being space-independent, drops out from the

[20] When the constraint (B.13) is obeyed by the wave functional the mode $m=0, \sigma=\pm 1$ can safely be included in the Coulomb kernel (B.19) since it does not contribute when the Coulomb Hamiltonian acts on the wave functional. Thus with the constraint (B.13) satisfied we can use the alternative kernel

$$F^{ab}(x,y) = {\sum_{n,\sigma}}' \langle x,a|\hat{U}|n,\sigma\rangle \lambda^{-2}_{n,\sigma} \langle n,\sigma|\hat{U}^T|y,b\rangle = \langle x,a|(i\hat{D})^{-2}|y,b\rangle \tag{B.22}$$

in the Coulomb Hamiltonian. It is precisely this kernel (but with A restricted to the hyperplane of the *diagonal Coulomb gauge*) which arises as "Coulomb kernel" in the *diagonal Coulomb gauge* derived in the next subsection.

Coulomb term (B.18). In fact, with the explicit form of eigenfunctions $\tilde{\varphi}^a_{n,\sigma}(x)$ (3.28) we have

$$\int dx F^{ab}(x,y) = \frac{1}{L}\int dx \sum_{n\neq 0} \mathrm{e}^{ik_n(x-y)} F^{ab}_n = \sum_{n\neq 0} \delta_{n,0} F^{ab}_n = 0\,. \tag{B.23}$$

Thus we can replace in H_C (B.18) the total charge ρ^a_{tot} by the external charge ρ^a,

$$H_C = \frac{g^2}{2}\int dxdy \rho^a(x) F^{ab}(x,y)\rho^b(y)\,, \tag{B.24}$$

and in the absence of external charges $\rho^a(x) = 0$ the Yang-Mills Hamiltonian reduces to the transversal part (6.15).

B.2 Diagonal Coulomb gauge

In the *diagonal Coulomb gauge* (2.20) the remaining physical degree of freedom of the gauge field is $A^3 \equiv A^3(n=0)$ and the corresponding physical momentum reads

$$\Pi^a_\perp = \delta^{a3}\Pi^3_\perp\,,\ \Pi^3_\perp = \frac{1}{L}\frac{d}{idA^3}\,. \tag{B.25}$$

We will keep here the same notation as in the *pure Coulomb gauge* and denote the remaining unphysical part of the momentum operator by

$$\Pi^a_{||} = \Pi^a - \Pi^a_\perp\,. \tag{B.26}$$

This part is given here by

$$\Pi^a_{||} = \frac{1}{L}{\sum_n}' \mathrm{e}^{-ik_n x}\frac{d}{idA^a(n)}\,, \tag{B.27}$$

where the prime indicates that the term $n=0$ is excluded for the generator of the Cartan algebra $a = a_0 = 3$ only. Note that contrary to the *pure Coulomb gauge*, the "transverse" components $d/dA^{a=\bar{a}}(0)$ belonging to the generators $a = \bar{a}$ of the coset $SU(N)/U(1)^{N-1}$ are here parts of $\Pi_{||}$.

With the explicit form of the gauge-fixed field (2.20) and the corresponding momentum $\Pi_\perp$ (B.25) one notices that the charge of gauge boson (5.6) vanishes in this case,

$$\rho^a_g = -\hat{A}^{ab}_\perp \Pi^b_\perp = -\hat{A}^{a3}_\perp \Pi^3_\perp = -f^{a33} A^3_\perp \Pi^3_\perp = 0\,. \tag{B.28}$$

Inserting the explicit form of $\Pi^a_{||}$, given by Eq. (B.27), into Gauss' law (5.4) and using furthermore

$$i\hat{D}^{ab}[A^3 T_3]\mathrm{e}^{-ik_n x} = \mathrm{e}^{-ik_n x}\sum_\sigma \langle a|\sigma\rangle \lambda_{n,\sigma}\langle\sigma|b\rangle\,, \tag{B.29}$$

Gauss' law becomes

$$\frac{1}{L}\sum_n{}' \mathrm{e}^{-ik_n x}\sum_\sigma \langle a|\sigma\rangle\lambda_{n,\sigma}\langle\sigma|b\rangle\frac{d}{idA^b(n)}\Psi(A) = i\rho^a(x)\Psi(A)\,. \tag{B.30}$$

Multiplying this equation by $\mathrm{e}^{ik_m x}\langle\sigma|a\rangle$, integrating over x and summing over a, we obtain

$$\sum_n{}' \delta_{n,m}\lambda_{n,\sigma}\langle\sigma|b\rangle\frac{d}{idA^b(n)}\Psi(A) = i\langle\sigma|a\rangle\int_0^L dx\mathrm{e}^{ik_m x}\rho^a(x)\Psi(A)\,. \tag{B.31}$$

Recall that the prime indicates that the term $n=0$ is excluded from the sum for $b=3$. Since $\langle\sigma|b=3\rangle = \mathrm{e}^{3^*}_\sigma \equiv \delta_{\sigma 0}$ on the l.h.s. the term $n=0$ is excluded for $\sigma=0$. Thus for $m=\sigma=0$ the l.h.s. vanishes and we find the following constraint on the wave functional

$$Q^3\Psi \equiv \int_0^L dx\rho^3(x)\Psi = 0\,, \tag{B.32}$$

which should be compared with the constraint (B.13) in the *pure Coulomb gauge*. Since in the present case the charge of the gauge bosons vanishes, Eq. (B.32) is the restriction of the constraint (B.13) to the charge of the Cartan subgroup. For $m=0, \sigma\neq 0$ and for $m\neq 0, \sigma$-arbitrary, Eq. (B.31) becomes

$$\lambda_{m,\sigma}\langle\sigma|b\rangle\frac{d}{idA^b(m)}\Psi(A) = i\langle\sigma|a\rangle\int_0^L dx\,\mathrm{e}^{ik_m x}\rho^a(x)\Psi(A)\,. \tag{B.33}$$

Note that since $\langle\sigma\neq 0|b=3\rangle = 0$ the summation over b is for $m=0, \sigma\neq 0$ restricted to $b=1,2$. Multiplying the last equation by $\langle c|\sigma\rangle\lambda^{-1}_{m,\sigma}$ and summing over σ we obtain

$$\frac{d}{idA^c(m)}\Psi(A) = i\sum_\sigma{}'\langle c|\sigma\rangle\lambda^{-1}_{m,\sigma}\langle\sigma|a\rangle\int_0^L dx\,\mathrm{e}^{ik_m x}\rho^a(x)\Psi(A)\,, \tag{B.34}$$

where the prime indicates again that the term $\sigma=0$ is excluded for $m=0$. Multiplying this equation by $\mathrm{e}^{-ik_m y}/L$ and summing over m and using (B.27) we obtain the desired representation

$$\Pi^c_{\|}(y)\Psi(A) = i\int_0^L dx\langle y,c|(i\hat{D}[A^3T_3])^{-1}|x,a\rangle\rho^a(x)\Psi(A)\,, \tag{B.35}$$

where

$$\langle y,c|(i\hat{D}[A^3T_3])^{-1}|x,a\rangle = \sum_{m,\sigma}{}'\varphi^c_{m,\sigma}(y)\lambda^{-1}_{m,\sigma}\varphi^{a^*}_{m,\sigma}(x)\,,\quad \varphi^a_{m,\sigma}(x) = \frac{1}{\sqrt{L}}\mathrm{e}^{-ik_m x}\mathrm{e}^a_\sigma\,. \tag{B.36}$$

With Eq. (B.35) one finds for the Coulomb Hamiltonian H_C defined by Eq. (5.9) in this gauge with $\mathcal{J}_{FP} = \mathcal{J}_D$ the following expression

$$H_C = \frac{g^2}{2} \int dxdy \rho^a(x) F^{ab}(x,y) \rho^b(y) \tag{B.37}$$

with the Coulomb kernel given by

$$F^{ab}(x,y) = \langle x,a|(i\hat{D}[A^3 T_3]))^{-2}|y,b\rangle = \sum_{n,\sigma}{}' \langle x|n\rangle\langle a|\sigma\rangle \lambda_{n,\sigma}^{-2} \langle\sigma|b\rangle\langle n|y\rangle \; . \tag{B.38}$$

Contrary to the Coulomb kernel in the *pure Coulomb gauge* (B.19) here only the zero mode $m = \sigma = 0$ is excluded, as indicated by the prime, while the mode $m = 0, \sigma = \pm 1$ is included. The above considerations show that the Coulomb Hamiltonian depends on the details of the gauge fixing and is thus a priori not a physical quantity.

References

[1] N. H. Christ and T. D. Lee, "Operator ordering and Feynman rules in gauge theories," *Phys. Rev.* **D22** (1980) 939.

[2] A. R. Swift, "Selfconsistent model of confinement," *Phys. Rev.* **D38** (1988) 668–691.

[3] D. Schutte, "Nonperturbative many body techniques applied to a Yang-Mills field theory," *Phys. Rev.* **D31** (1985) 810–821.

[4] R. E. Cutkosky and K. C. Wang, "Vacuum and excited states of Coulomb gauge SU(n) Yang-Mills fields," *Phys. Rev.* **D37** (1988) 3024.

[5] D. Zwanziger, "Non-perturbative Faddeev-Popov formula and infrared limit of QCD," *Phys. Rev.* **D69** (2004) 016002, `hep-ph/0303028`.

[6] A. P. Szczepaniak and E. S. Swanson, "Coulomb gauge QCD, confinement, and the constituent representation," *Phys. Rev.* **D65** (2002) 025012, `hep-ph/0107078`.

[7] A. P. Szczepaniak, "Confinement and gluon propagator in Coulomb gauge QCD," *Phys. Rev.* **D69** (2004) 074031, `hep-ph/0306030`.

[8] C. Feuchter and H. Reinhardt, "Variational solution of the Yang-Mills Schroedinger equation in Coulomb gauge," *Phys. Rev.* **D70** (2004) 105021, `hep-th/0408236`.

[9] C. Feuchter and H. Reinhardt, "Quark and gluon confinement in Coulomb gauge," `hep-th/0402106`.

[10] H. Reinhardt and C. Feuchter, "On the Yang-Mills wave functional in Coulomb gauge," *Phys. Rev.* **D71** (2005) 105002, `hep-th/0408237`.

[11] H. Reinhardt and D. Epple, "The 't Hooft loop in the Hamiltonian approach to Yang-Mills theory in Coulomb gauge," *Phys. Rev.* **D76** (2007) 065015, `arXiv:0706.0175 [hep-th]`.

[12] C. Feuchter and H. Reinhardt, "The Yang-Mills Vacuum in Coulomb Gauge in D=2+1 Dimensions," *Phys. Rev.* **D77** (2008) 085023, `0711.2452`.

[13] D. Zwanziger, "Renormalization in the Coulomb gauge and order parameter for confinement in QCD," *Nucl. Phys.* **B518** (1998) 237–272.

[14] P. Watson and H. Reinhardt, "Propagator Dyson-Schwinger equations of Coulomb gauge Yang-Mills theory within the first order formalism," *Phys. Rev.* **D75** (2007) 045021, `hep-th/0612114`.

[15] P. Watson and H. Reinhardt, "Two-Point Functions of Coulomb Gauge Yang-Mills Theory," *Phys. Rev.* **D77** (2008) 025030, `arXiv:0709.3963 [hep-th]`.

[16] P. Watson and H. Reinhardt, "Perturbation Theory of Coulomb Gauge Yang-Mills Theory Within the First Order Formalism," *Phys. Rev.* **D76** (2007) 125016, `arXiv:0709.0140 [hep-th]`.

[17] A. Cucchieri and D. Zwanziger, "Numerical study of gluon propagator and confinement scenario in minimal Coulomb gauge," *Phys. Rev.* **D65** (2002) 014001, hep-lat/0008026.

[18] J. Greensite, S. Olejnik, and D. Zwanziger, "Coulomb energy, remnant symmetry, and the phases of non- Abelian gauge theories," *Phys. Rev.* **D69** (2004) 074506, hep-lat/0401003.

[19] K. Langfeld and L. Moyaerts, "Propagators in Coulomb gauge from SU(2) lattice gauge theory," *Phys. Rev.* **D70** (2004) 074507, hep-lat/0406024.

[20] L. Moyaerts, *A numerical study of quantum forces*. PhD thesis, Univ. of Tübingen, Germany, 2004.

[21] A. Nakamura and T. Saito, "Color confinement in Coulomb gauge QCD," *Prog. Theor. Phys.* **115** (2006) 189–200, hep-lat/0512042.

[22] J. Greensite and S. Olejnik, "Dimensional Reduction and the Yang-Mills Vacuum State in 2+1 Dimensions," *Phys. Rev.* **D77** (2008) 065003, 0707.2860.

[23] M. Quandt, G. Burgio, S. Chimchinda, and H. Reinhardt, "Coulomb gauge Green functions and Gribov copies in SU(2) lattice gauge theory," *PoS* **LAT2007** (2007) 325, arXiv:0710.0549 [hep-lat].

[24] S. D. Drell, "Asymptotic freedom," *SLAC-PUB-2694* (1981).

[25] I. B. Khriplovich, "Green's functions in theories with non-abelian gauge group," *Yad. Fiz.* **10** (1969) 409–424.

[26] W. Schleifenbaum, M. Leder, and H. Reinhardt, "Infrared analysis of propagators and vertices of Yang-Mills theory in Landau and Coulomb gauge," *Phys. Rev.* **D73** (2006) 125019, hep-th/0605115.

[27] D. Epple, H. Reinhardt, and W. Schleifenbaum, "Confining Solution of the Dyson-Schwinger Equations in Coulomb Gauge," *Phys. Rev.* **D75** (2007) 045011, hep-th/0612241.

[28] J. E. Hetrick and Y. Hosotani, "Yang-Mills theory on a circle," *Phys. Lett.* **B230** (1989) 88.

[29] Y. Hosotani, "Dynamics of Nonintegrable Phases and Gauge Symmetry Breaking," *Ann. Phys.* **190** (1989) 233.

[30] R. Jackiw, "Introduction to the Yang-Mills Quantum Theory," *Rev. Mod. Phys.* **52** (1980) 661.

[31] W. Schleifenbaum, "Nonperturbative aspects of Yang-Mills theory," 0809.1339. PhD thesis, Tübingen.

[32] T. Pause and T. Heinzl, "The configuration space of low-dimensional Yang-Mills theories," *Nucl. Phys.* **B524** (1998) 695–741, hep-th/9801169.

[33] M. Engelhardt and H. Reinhardt, "Center projection vortices in continuum Yang-Mills theory," *Nucl. Phys.* **B567** (2000) 249, hep-th/9907139.

[34] H. Reinhardt, "On 't Hooft's loop operator," *Phys. Lett.* **B557** (2003) 317–323, hep-th/0212264.

[35] H. Reinhardt and P. Watson, "Resolving temporal Gribov copies in Coulomb gauge Yang-Mills theory," 0808.2436.

[36] S. G. Rajeev, "Yang-Mills theory on a cylinder," *Phys. Lett.* **B212** (1988) 203.

[37] D. Zwanziger, "Lattice Coulomb Hamiltonian and static color-Coulomb field," *Nucl. Phys.* **B485** (1997) 185–240, hep-th/9603203.

[38] C. S. Fischer, "Infrared properties of QCD from Dyson-Schwinger equations," *J. Phys.* **G32** (2006) R253–R291, hep-ph/0605173.

[39] H. Reinhardt, "The dielectric function of the QCD vacuum," *Phys. Rev. Lett.* **101** (2008) 0803.0504.

[40] V. N. Gribov, "Quantization of non-Abelian gauge theories," *Nucl. Phys.* **B139** (1978) 1.

[41] Taylor, J. C., "Ward identities and charge renormalization of the Yang-Mills field," *Nucl. Phys.* **B33** (1971) 436–444.

[42] A. Maas, "Two- and three-point Green's functions in two-dimensional Landau-gauge Yang-Mills theory," *Phys. Rev.* **D75** (2007) 116004, 0704.0722.

[43] M. Blau and G. Thompson, "Lectures on 2-d gauge theories: Topological aspects and path integral techniques," hep-th/9310144.

[44] D. Zwanziger, "No confinement without Coulomb confinement," *Phys. Rev. Lett.* **90** (2003) 102001, hep-lat/0209105.

[45] I. S. Gradshtein and I. Ryzhik, *Table of Integrals, Series, and Products*. Academic Press, New York, 5th edition ed., 1994.

[46] A. Cucchieri and T. Mendes, "What's up with IR gluon and ghost propagators in Landau gauge? A puzzling answer from huge lattices," *PoS* **LAT2007** (2007) 297, 0710.0412.

[47] D. Dudal, S. P. Sorella, N. Vandersickel, and H. Verschelde, "New features of the gluon and ghost propagator in the infrared region from the Gribov-Zwanziger approach," *Phys. Rev.* **D77** (2008) 071501, 0711.4496.

[48] D. Epple, H. Reinhardt, W. Schleifenbaum, and A. P. Szczepaniak, "Subcritical solution of the Yang-Mills Schroedinger equation in the Coulomb gauge," *Phys. Rev.* **D77** (2008) 085007, 0712.3694.

[49] J. L. Rodriguez Marrero and A. R. Swift, "Color confinement and the quantum chromodynamic vacuum. 2. Gluon propagation and the Coulomb interaction," *Phys. Rev.* **D31** (1985) 917.

[50] G. 't Hooft, "Topology of the Gauge Condition and New Confinement Phases in Nonabelian Gauge Theories," *Nucl. Phys.* **B190** (1981) 455.

[51] H. Reinhardt, "Resolution of Gauss' law in Yang-Mills theory by gauge- invariant projection: Topology and magnetic monopoles," *Nucl. Phys.* **B503** (1997) 505–529, hep-th/9702049.

[52] A. Cucchieri, T. Mendes, and A. Mihara, "Numerical study of the ghost-gluon vertex in Landau gauge," *JHEP* **12** (2004) 012, hep-lat/0408034.

[53] W. Schleifenbaum, A. Maas, J. Wambach, and R. Alkofer, "Infrared behaviour of the ghost gluon vertex in Landau gauge Yang-Mills theory," *Phys. Rev.* **D72** (2005) 014017, hep-ph/0411052.

[54] A. Sternbeck, E. M. Ilgenfritz, M. Muller-Preussker, and A. Schiller, "Studying the infrared region in Landau gauge QCD," *PoS* **LAT2005** (2006) 333, hep-lat/0509090.